

Specificity of molecular responses to ERK1/2 and MKK1/2 inhibitors in melanoma cells

By Joel M. Basken

B.S., University of Wisconsin-Madison, 2006

A thesis submitted to the Faculty
of the Graduate School in partial
fulfillment of the requirements
for the degree of Doctor of Philosophy

Department of Molecular, Cellular,
and Developmental Biology
2017

This thesis entitled:

Specificity of molecular responses to ERK1/2 and MKK1/2 inhibitors in melanoma cells

written by Joel M. Basken

has been approved for the Department of Molecular, Cellular, and Developmental
Biology by:

William Old, Ph.D.

Natalie Ahn, Ph.D.

Date: _____

The final copy of this thesis has been examined by the signatories, and we find that both the content and the form meet acceptable presentation standards of scholarly work in the above mentioned discipline.

Basken, Joel M. (Ph.D., Molecular, Cellular and Developmental Biology)

Specificity of molecular responses to ERK1/2 and MKK1/2 inhibitors in melanoma cells

Thesis directed by Natalie G. Ahn

Abstract

Skin cancer is the most commonly diagnosed cancer in the U.S. and 75% of skin cancer related deaths are due to malignant melanoma, a cancer originating in melanin producing melanocytes. The RAF/MKK/ERK signaling cascade is constitutively activated in over 90% of melanomas and 52% of tumors contain BRAF V600E/K oncogenic driver mutations. Although small molecule inhibitors specifically targeting mutant BRAF V600E/K and the downstream kinases MKK1/2 have been successful in clinical settings, resistance invariably develops. In preclinical studies, inhibitors of ERK1/2 can overcome resistance to BRAF V600E/K and MKK1/2 inhibitors, making them promising alternative pathway inhibitors for the treatment of melanoma. However, the specificity of molecular responses to ERK1/2 inhibitors remains unknown. In this thesis, I use SILAC-based phosphoproteomics to quantify molecular responses to the clinically available MKK1/2 inhibitor, trametinib, and the ERK1/2 inhibitors, SCH772984, GDC0994 and Vertex-11e in WM239a human metastatic melanoma cells. I observed significant responses in approximately 5% of all phosphosites identified. Significantly regulated phosphosites showed a high degree of overlap between all inhibitors, suggesting that the pathway functions linearly with relatively little evidence for branchpoints that lead to bifurcation upstream of ERK1/2. I also observe phosphosites responsive to only one of four MKK1/2 or ERK1/2 inhibitors. For example, trametinib shows an ability to block activating phosphorylation sites on p38 α MAPK, which are not shared by ERK1/2 inhibitors SCH772984 and GDC0994, the MKK1/2 inhibitor selumetinib, or the BRAF V600E/K inhibitor, vemurafenib. Trametinib

directly inhibits MKK6 in vitro, although with a IC_{50} 10-fold higher than its inhibition of p38 α MAPK in cells. This suggests the potential that the direct target of trametinib in cells is upstream of MKK6. Further analyses of phosphoproteomics responses to two MKK1/2 inhibitors and two ERK1/2 inhibitors identifies phosphorylation sites that can be classified as (i) known or novel targets of BRAF-MKK-ERK signaling, (ii) potential branchpoints at MKK1/2 upstream of ERK1/2, and (iii) off-targets of different inhibitors. My results show how information from phosphoproteomics comparisons of multiple MKK1/2 and ERK1/2 inhibitors can be combined to provide a deeper understanding of pathway specificity.

Acknowledgements

I would like to thank my advisor, Natalie Ahn for her mentoring and patience throughout my graduate school career. Her scientific passion and curiosity have been great motivation for me to pursue questions within my own project. She has also assembled an amazing group of lab members who have helped make this work possible. In particular, Dr. Scott Stuart has provided countless hours of training, scientific advice, troubleshooting, and friendship. A six pack of Milk Stout does not begin to express my appreciation, but it'll have to do. I would also like to thank Dr. Mary Katherine Tarrant for guidance on how to succeed as a graduate student and making our lab environment enjoyable. Jennifer Liddle has progressed through her Ph.D. alongside me and our conversations are always enlightening, although not always scientific.

Drs. Jeremy Balsbaugh and Thomas Lee of the JSCBB mass spectrometry facility taught me the fundamentals of proteomics, helped run my samples on the instruments, and tolerated my repeated questions. Drs. Will Old, Chris Ebmeier, and Zach Poss in the Old lab all helped maximize the quality of my phosphoproteomic data. Will explained statistical analysis methods which have been adopted by Andrew Kavran in our lab, and Chris juggled many different projects to optimize my protocol and run samples. The MCDB predoctoral class of 2010 including Lavan Khandan, Verity Johnson, Emily Pugach, Audrey Audetat, and Natalie Johnson made graduate school fun and I had a blast exploring Boulder and the rest of Colorado with you. I am grateful for my funding from MCDB, Natalie Ahn, and the NIH Creative Training in Molecular Biology Training Grant (5-T32 GM007135).

My thesis committee has provided vital feedback on this project and includes Will Old, Joaquin Espinosa, Dylan Taatjes, Xuedong Liu, and Tin Tin Su.

Pursuing and completing graduate school would not have been possible without the unconditional support of my family. My parents offered constant encouragement and enabled me to follow my own path. My brothers have given me perspective through their own graduate school experiences, and we never miss an opportunity to share a laugh at one another's expense. Finally, my fiancé Kate has been my best friend, my biggest ally, my adventure buddy, and my emotional support. I can't wait to see where this life will take us together.

Thesis Contents

Chapter 1	Introduction	
1.1	Cancer biology, mortality, and treatment.....	1
1.2	Melanoma biology, disease progression, and genetic mutations.....	2
1.3	MAPK pathway upregulation, targeted inhibition, and drug resistance in melanoma.....	7
1.4	Other MAPK pathways and osmotic stress activation of p38 MAPK.....	13
1.5	Phosphoproteomic analysis of molecular responses to MAPK pathway inhibitors.....	16
1.6	Thesis overview.....	18
Chapter 2	Selective phosphoproteome responses to MKK1/2 and ERK1/2 inhibitors in human melanoma cells	
2.1	Abstract.....	20
2.2	Significance of study.....	21
2.3	Introduction.....	21
2.4	Materials and methods.....	24
2.5	Results.....	31
2.6	Discussion.....	73
Chapter 3	Conclusions and future directions	
3.1	Summary and conclusions.....	77
3.2	Future experiments.....	83
Bibliography.....		87

List of Figures

Chapter 1

Figure 1.1: Pathological progression of melanoma.....	4
Figure 1.2: Somatic gene mutation frequency in melanoma.....	6
Figure 1.3: MAPK-ERK signaling cascade, oncogenic activation, and inhibition.....	8
Figure 1.4: Representative kinase inhibitors targeting mutant BRAF V600E/K, MKK1/2, and ERK1/2.....	13
Figure 1.5: ERK, p38, JNK, and ERK5 MAPK signaling cascades.....	14
Figure 1.6: SILAC labeling allows quantification of changes in phosphopeptide levels in response to inhibitor.....	18

Chapter 2

Figure 2.1: SILAC experiment design.....	33
Figure 2.2: Performance of the ERLIC fractionation method.....	34
Figure 2.3: SILAC labeled phosphoproteomics comparison of trametinib and SCH772984.....	36
Figure 2.4: SILAC labeled phosphoproteomics comparison of trametinib and selumetinib (AZD6244).....	39
Figure 2.5: Quantification of phosphorylated p38 MAPK in WM239a cells by Western blotting.....	43
Figure 2.6: <i>In vitro</i> kinase assay measurement of MKK6, MKK3, and MKK3b activity.....	46
Figure 2.7: Effects of MKK1/2 inhibitors on p38 MAPK pathway effectors and signaling.....	47
Figure 2.8: SILAC labeled phosphoproteomics comparison of SCH772984 and GDC0994.....	50
Figure 2.9: Apoptotic responses to MKK1/2 and ERK1/2 inhibitors in WM239a cells.....	53
Figure 2.10: Human phospho-kinase antibody arrays.....	55

Figure 2.11: SILAC labeled phosphoproteomics comparison of SCH772984 and Vertex-11e....	57
Figure 2.12: Counts of phosphosites that change significantly in response to each MKK1/2 and ERK1/2 inhibitor.....	60
Figure 2.13: Subnetworks of proteins containing phosphosites responsive to all four MKK1/2 and ERK1/2 inhibitors.....	62
Figure 2.14: A STRING network of proteins with phosphosites significantly regulated only in response to GDC0994.....	72

List of Tables

Chapter 2

Table 2.1: Comparison of phosphosites identified in each triple-labeled replicate comparing trametinib and SCH772984.....	35
Table 2.2: Comparison of phosphosites uniquely responsive to trametinib or SCH772984.....	37
Table 2.3: Comparison of phosphosites that change uniquely in response to trametinib of selumetinib (AZD6244).....	41
Table 2.4: Comparison of phosphosites uniquely responsive to SCH772984 and GDC0994.....	51
Table 2.5: Comparison of phosphosites identified in each triple-labeled SILAC replicate comparing SCH772984 and GDC0994.....	52
Table 2.6: Comparison of unique SCH772984 and Vertex-11e significant phosphosites.....	58
Table 2.7: Phosphosites significantly regulated by all inhibitors (trametinib, selumetinib (AZD6244), SCH772984, GDC0994) in SILAC experiments.....	63
Table 2.8: Phosphosites significantly regulated with MKK1/2 inhibitors but not ERK1/2 inhibitors.....	68
Table 2.9: Phosphosites significantly regulated in only one MKK1/2 or ERK1/2 inhibitor.....	71

Appendix

Appendix I. Human Phospho-Kinase Antibody Array.....	84
--	----

Chapter 1

Introduction

1.1 Cancer biology, mortality, and treatment

Cancer is a large group of related diseases characterized by uncontrolled proliferation of abnormal cells, which can include old and damaged cells that evade destruction as well as unnecessary growth of new cells. These abnormal cells can form solid masses in tissues called tumors and malignant tumors can break their normal boundaries and invade surrounding tissues. These cancerous cells can then spread to other tissues and organs, a process known as metastasis, which is responsible for the majority of cancer deaths. In 2016, approximately 1,685,210 new cases of cancer will be diagnosed in the U.S., and about 1 in every 4 deaths per year (595,690 Americans) will be due to cancer, making it the second leading cause of death in the U.S. (American Cancer Society, 2016). Worldwide, over 60% of new cases occur in Africa, Asia, and Central/South America, with 70% of cancer deaths occurring in these regions (Stewart, B. W., Wild, 2014). Consequently, cancer is both a massive financial burden as well as area of financial investment. Medical costs associated with cancer totaled \$74.8 billion in the U.S. in 2013 (American Cancer Society, 2016). To combat this disease, the National Cancer Institute (NCI) received \$5.1 billion in funding for 2016.

Cancer research in public institutions and private businesses (such as pharmaceutical companies) has led to new mechanism-based treatment strategies, which improve patient outcomes and build upon traditional approaches such as surgery, radiation, and cytotoxic chemotherapy. One of these mechanism-based strategies, immunotherapy, uses different approaches to activate the patient's immune system to recognize and attack the cancer. FDA-

approved immunotherapies are now first-line treatments for several cancer types and many more are being evaluated in ongoing clinical trials. Targeted therapies using cell-permeable small molecule inhibitors are a second mechanism-based treatment strategy developed over the past 20 years. These targeted therapeutics are a cornerstone of precision medicine which uses information about a patient's genetic and protein profile to diagnose and treat disease. Cancer is usually caused by genetic changes, often involving accelerated mutational rates. Over time, tumors accumulate a unique combination of mutations leading to disease progression. Some mutations known as driver mutations commonly promote cell survival and/or proliferation by affecting key regulators such as proto-oncogenes, tumor suppressor genes, and DNA repair genes. While some of these mutations are inherited, others are acquired somatic mutations called passenger mutations which in some cases enhance malignancy and in other cases have no effect on cells. Over the last decade, multi-disciplinary projects like The Cancer Genome Atlas (TCGA) have compiled genetic data from over 11,000 patients across 33 different cancer types (Tomczak, Czerwińska, & Wiznerowicz, 2015). These efforts have identified promising novel target genes in many different cancer types that have been used to develop effective targeted therapeutics.

1.2 Melanoma biology, disease progression, and genetic mutations

Skin cancer is the most commonly diagnosed cancer in the U.S. and begins in the epidermis. The epidermis consists of squamous keratinocytes and basal keratinocytes which make up 80% of tissue, melanocytes which produce skin pigments, Langerhans cells which provide immune defense, and neuronal Merkel cells which convey touch sensations. Squamous cell and basal cell carcinomas make up 99% of skin cell diagnoses and can almost always be

cured if treated early. In contrast, melanoma only accounts for 1% of skin cancer diagnoses but is responsible for 75% of skin cancer deaths (American Cancer Society, 2016). In 2012, 232,000 new cases of melanoma were diagnosed with 55,000 estimated deaths (Stewart, B. W., Wild, 2014). Melanoma involves malignant transformation of melanocytes to cancerous cells which typically occurs in the epidermis, but can also form in the eye (primarily uveal melanoma), mucosal tissue (head and neck, female genital tract, and anal/rectal), or unknown primary sites (only metastatic disease diagnosed) (Chang, Karnell, & Menck, 1998). Tumorigenesis is associated with familial history, multiple benign or atypical nevi (moles), previous melanoma, immunosuppression, sun sensitivity, and UV radiation exposure (Miller & Mihm, 2006). Accumulation of inherited genetic changes as well as molecular lesions arising from errors in cell division and DNA damage due to environmental exposures drive the progression of melanoma, from benign nevus to primary melanoma to metastatic melanoma (Figure 1.1). Before the implementation of gene sequencing to identify genetic changes in melanoma, it was common for oncologists to categorize melanoma into four distinct subtypes based on histology. These include nodular melanoma, superficial spreading melanoma, lentigo maligna, acral lentiginous melanoma, and desmoplastic melanoma (Clark, From, Bernardino, & Mihm, 1969; McGovern et al., 1973; Scolyer, Long, & Thompson, 2011). However, the development of large-scale sequencing platforms and drugs that specifically target certain mutation profiles in patients has made genetic alterations a more effective way to categorize disease (Curtin et al., 2005). It is now common for a melanoma diagnosis to include both molecular markers as well as standardized pathological staging measuring thickness and other metrics of the primary tumor, metastatic nodes, and distant metastasis sites (Boland & Gershenwald, 2016). Almost all melanoma tumors diagnosed at early stages can be treated or cured by surgical resection, while

later stage cancer requires more aggressive therapy. Until recently, the chemotherapeutic drug, dacarbazine, and immune stimulating cytokine, interleukin 2 (IL2), were the only approved treatments for melanoma, however both had relatively little effect on overall patient survival (McArthur & Ribas, 2013).

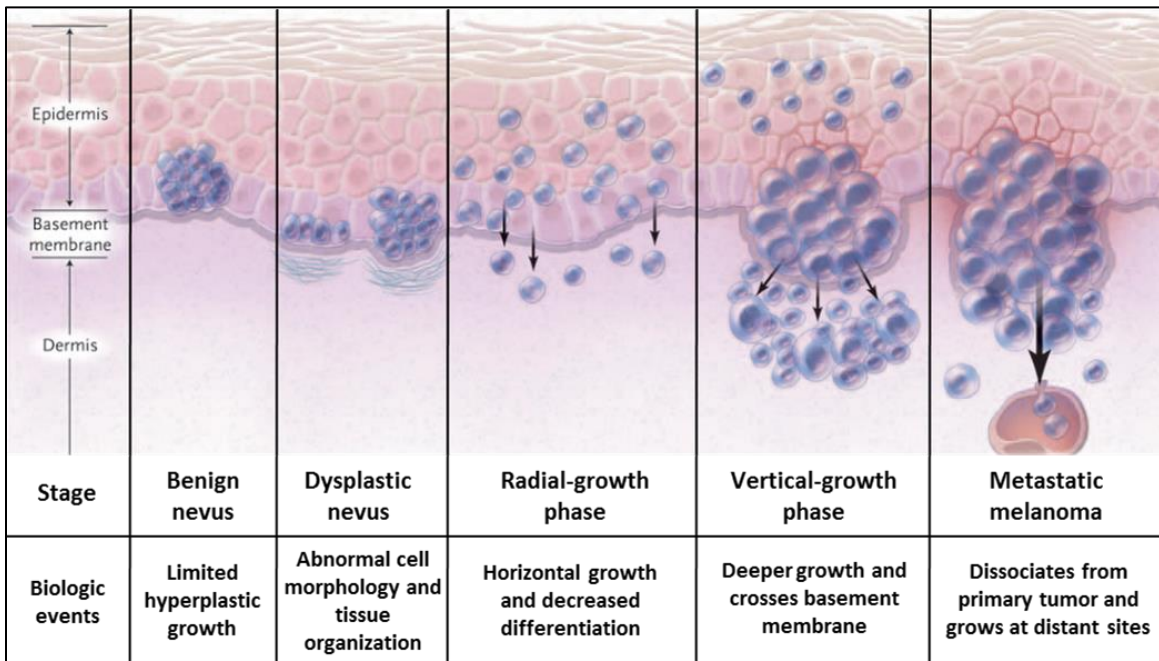


Figure 1.1: Pathological progression of melanoma. Biologic events are often accompanied by molecular lesions including BRAF mutation (benign nevus), CDKN2A and PTEN loss (dysplastic nevus), increased CD1 (radial-growth phase), and changes to cell adhesion in vertical growth phase and metastatic melanoma. Adapted from (Miller & Mihm, 2006).

Melanoma was among the first cancer genomes to be sequenced, along with leukemia (Ley et al., 2008; Mardis et al., 2009), breast cancer (Shah et al., 2009), and small-cell lung cancer (Pleasant, Stephens, et al., 2010), and researchers revealed the dramatic increase in mutation rate of cancerous cells compared to normal cells (Pleasant, Cheetham, et al., 2010). They catalogued all base substitutions, small insertions and deletions (indels), rearrangements, and copy number alterations in a metastatic melanoma cell line and subtracted the mutations found in a lymphoblastoid cell line derived from the same patient to generate a map of somatic

mutations across the genome. In total, 33,345 base substitutions were identified, and the majority of these (~24,000) were verified C>T mutations associated with UV light exposure (Pfeifer, You, & Besaratinia, 2005). Defective DNA repair pathways also contribute to the high mutation rate as seen in other cancers, although melanoma is unique in the high mutational load due to UV mutagenesis (Hodis et al., 2012). A major breakthrough in identifying the molecular alterations associated with malignant melanoma came in a 2002 study, which sequenced the coding sequence and intron-exon junctions of oncogenic candidate gene BRAF in a large human sample set covering a variety of cancers (H. Davies et al., 2002). They found the BRAF kinase mutated in 66% of malignant melanoma with a single amino acid substitution from valine to glutamic acid (V600E) making up the majority of mutations. Additional studies identified amino acid substitutions to arginine (V600R) or lysine (V600K) at lower frequencies (Klein et al., 2013). This BRAF V600 E/K mutation was sufficient to constitutively upregulate downstream signaling in mammalian cells, leading to cell proliferation and independence from upstream activation through the RAS proteins (H. Davies et al., 2002). The success of this study led to increased interest in multi-center projects cataloging the genetic mutations in patients across many cancer types.

A recent interdisciplinary study performed by the TCGA characterized genetic changes across the entire genome in melanoma patients using whole exome sequencing, DNA copy-number profiling, mRNA sequencing, microRNA sequencing, DNA methylation profiling, protein expression profiling, and clinicopathological data on primary and/or metastatic melanomas in 331 patients (Akbari et al., 2015). The whole exome sequencing done on 318 paired tumor and germline normal genomic DNA samples identified BRAF (mutated in 52% of melanoma), NRAS (28% mutated), and NF1 (14% mutated) as the most commonly occurring

driver mutations in melanoma. Gain-of-function mutations at hot spot V600E/K and K601 residues make up 93% of the total mutations in BRAF and occur mutually exclusive to oncogenic NRAS mutations. Mutations also occur in HRAS and KRAS, but at a much lower frequency than NRAS. Loss of function mutations to the tumor suppressor GTPase-activating protein (GAP), NF1, occur mutually exclusive to BRAF V600E/K and K601, but not NRAS mutations. Additional oncogenes and tumor suppressors were mutated in a significant number of the TCGA melanoma patients. These include TP53, ARID2, CDKN2A, PTEN, PPP6C, RAC1, DDX3X, IDH1, MAP2K1, and RB1, many of which were also identified in a separate large-scale comparison of somatic mutations in melanoma across multiple studies, in the COSMIC database (Forbes et al., 2011) (Fig. 1.2). The three top driver mutations, BRAF V600E/K, NRAS, and NF1, all result in activation of the canonical MAPK pathway, which is altered in 91% of TCGA melanoma samples.

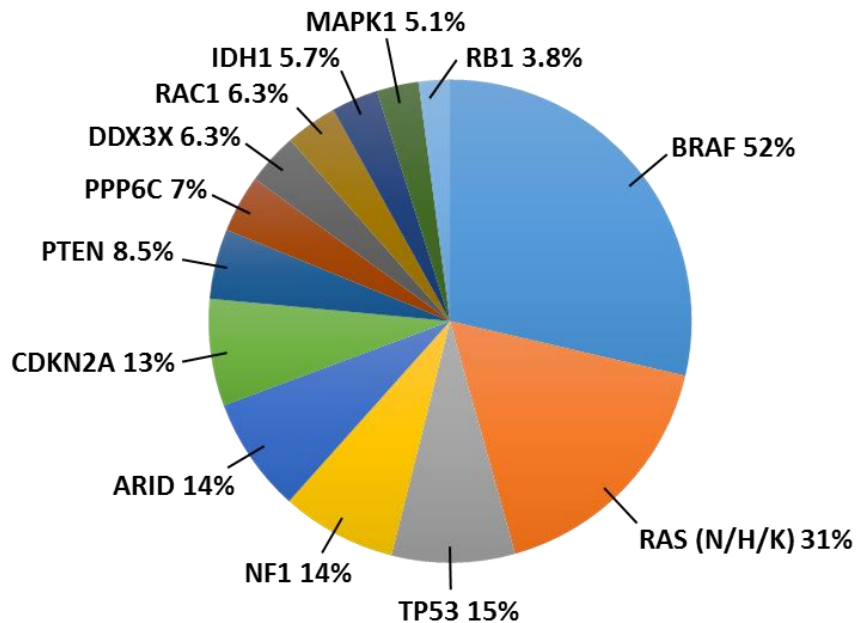


Figure 1.2: Somatic gene mutation frequency in melanoma. Top thirteen significantly mutated genes passing statistical analysis in 331 patients. BRAF, RAS, NF1 are major drivers of disease progression in melanoma. Figure adapted from (Akbari et al., 2015).

1.3 MAPK pathway activation, targeted inhibition, and drug resistance in melanoma

The mitogen-activated protein kinase (MAPK) pathway is a signaling cascade composed of several growth factor receptors, the small GTPase RAS, and downstream kinases, A,B,C-RAF, MKK1/2, and ERK1/2, which elicits a cellular response to extracellular stimuli such as hormones and growth factors through receptor tyrosine kinases (RTKs). The discovery of this pathway in the late 1980s and early 1990s followed a strategy of “working backwards”, similar to characterization of the glycogen phosphorylase kinase signaling cascade by Krebs and Fischer. The strategy started by characterization of kinase activity towards ribosomal protein S6, later shown to represent p90 ribosomal S6 kinase (RSK), in response to cell stimulation with insulin, as well as EGF, PDGF, and phorbol ester (Ahn, 1993). The S6 kinase activity could be activated by a serine/threonine specific kinase which phosphorylated microtubule associated protein-2 (MAP2) or myelin basic protein (MBP). The kinase was later renamed mitogen-activated protein (MAP) kinase, as well as extracellular-signal related kinase (ERK). It integrates upstream signals from different cell stimuli and transmits this message by phosphorylating more than 150 downstream targets in both the nucleus and cytoplasm (Carlson et al., 2011; Yoon & Seger, 2006). Tracking the upstream control of ERK led to the discovery and characterization of the dual specificity MAP kinase kinases (MKK1/2), also known as MAP/ERK kinase (MEK1/2), which phosphorylate ERK1/2 at pThr and pTyr regulatory phosphorylation sites within its activation loop sequence, Thr-Glu-Tyr. MKKs are in turn phosphorylated by upstream serine/threonine kinases named A-RAF, BRAF and CRAF (aka RAF1). The canonical MAPK pathway thus describes a linear cascade starting with the phosphorylation and activation of MKK by A,B or C-RAF, and followed by the phosphorylation and activation of ERK1/2 by MKK1/2 (Katz, Amit, & Yarden, 2007). The pathway is constitutively activated in nearly all cancer types,

with oncogenic BRAF V600E/K mutations prevalent in melanoma, colorectal, thyroid, and ovarian cancers (Burotto, Chiou, Lee, & Kohn, 2014). These cells often depend on this sustained MAPK activation for survival and upregulation of this pathway leads to cell survival, proliferation, and disease progression (Fig. 1.3A,B).

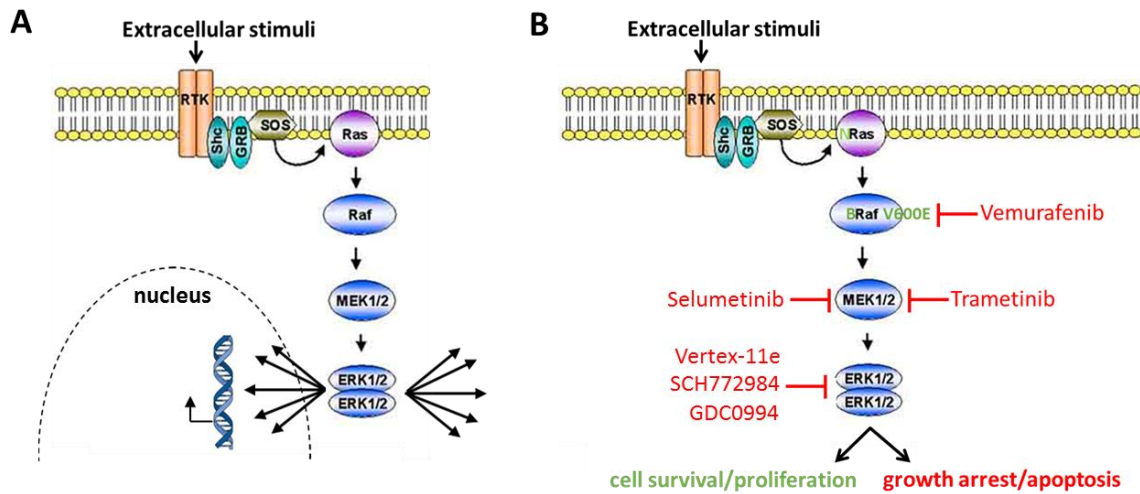


Figure 1.3: MAPK-ERK signaling cascade, oncogenic activation, and inhibition. A, extracellular signals such as growth factors and hormones elicit a downstream response by signaling through the RAF-MKK-ERK kinase cascade. B, 93% of melanoma has activation of the MAPK pathway, primarily through mutations in NRAS (28%) and BRAF V600E/K (52%) leading to cell survival and proliferation. Targeted therapeutics that inhibit the BRAF V600E/K, MEK1/2, and ERK1/2 kinases have been developed to inhibit this pathway in melanoma. Inhibitors characterized in this thesis are listed.

If diagnosed early, primary melanomas can be cured by clinical resection in 80% of cases, but metastatic melanomas are often resistant to traditional chemotherapy and radiotherapy due to the inherently high level of apoptosis resistance in the progenitor melanocyte cells (Gray-Schopfer, Wellbrock, & Marais, 2007). Immunotherapy has emerged as a promising treatment strategy for metastatic melanoma with FDA approval of four drugs in the last five years. Monoclonal antibodies against cytotoxic T-lymphocyte antigen 4 (CTLA-4) (ipilimumab 2011) and programmed cell death protein 1 (PD-1, nivolumab/pembrolizumab 2014) work by blocking CTLA-4 and PD-1 checkpoint inhibitors, thus re-activating the ability of the immune system to

attack cancer cells. A fourth immunotherapy currently used to treat melanoma is the oncolytic viral drug, talimogene laherparepvec (TVEC) which when injected into tumors, causes tumor cell lysis and release of antigens, eliciting an immune response (Franklin, Livingstone, Roesch, Schilling, & Schadendorf, 2016). These immunotherapy drugs are currently used in combination as first-line therapy in metastatic melanoma patients lacking mutant BRAF V600E/K (Coit et al., 2016). While the patient response is generally durable, long-term survival occurs in only ~50% of patients.

Like immunotherapy, the development of drugs that specifically target the MAPK pathway has led to a momentous shift in the treatment of melanoma, by successfully inducing cell death in melanomas containing the BRAF V600E/K mutation. Following the discovery of driver mutations in BRAF V600E/K (H. Davies et al., 2002), several ATP-competitive inhibitors specific for oncogenic BRAF mutated at V600E/K were developed and showed promise in both *in vitro* and animal models (Koo et al., 2002; Weinstein & Joe, 2008), followed by clinical trials. These inhibitors showed dramatic results in patients because they show a significant preference for tumor cells containing the BRAF V600E/K mutation but not cells containing wild type BRAF, allowing effective monotherapy without the toxic effects of targeting BRAF in all tissues. Thus, the FDA has now approved two inhibitors of mutant BRAF V600E/K, vemurafenib (Chapman et al., 2011) in August 2011 and dabrafenib (Hauschild et al., 2012) in May 2013. These are approved for use as single-agent therapies, with several improved “second generation” BRAF V600E/K inhibitors currently in clinical trials (Le, Blomain, Rodeck, & Aplin, 2013; Uehling & Harris, 2015). Other inhibitors target MKK1/2, and Trametinib (aka JTP-74057, GSK1120212) (Gilmartin et al., 2011; Yamaguchi, Kakefuda, Tajima, Sowa, & Sakai, 2011), an allosteric non-ATP competitive inhibitor of MKK1/2, was also approved by the

FDA for monotherapy use in melanomas with mutant BRAF V600E/K, in May 2013. MKK1/2 inhibitor Cobimetinib (Signorelli & Shah Gandhi, 2016) was approved for use in combination with vemurafenib in November 2015.

During dose escalation studies in phase 1 clinical trials for vemurafenib, it was determined that greater than 80% inhibition of phosphorylated ERK1/2 (pERK) was necessary to achieve significant tumor regressions in patients (Bollag et al., 2010). Because this level of pERK inhibition can be difficult to reach with monotherapy targeting the MAPK pathway, clinical trials combining BRAF V600E/K and MKK1/2 inhibitors were conducted with improved patient response compared to BRAF V600E/K inhibitor alone (Flaherty, Infante, et al., 2012; Hartsough, Shao, & Aplin, 2014). The median progression-free survival in the combination group was 9.4 months and 5.8 months in the monotherapy group, and the rate of complete or partial response with combination therapy was 76% with combination and 54% with monotherapy. This led to FDA approval of combination therapies that target both mutant BRAF V600E/K and MKK1/2, including dabrafenib + trametinib (GlaxoSmithKline, January 2014) as well as vemurafenib + cobimetinib (Genentech, November 2015) (Signorelli & Shah Gandhi, 2016; Wu, Nielsen, & Clausen, 2015). Combination therapy using dabrafenib+trametinib or vemurafenib+cobimetinib is currently the preferred first-line therapy in patients with oncogenic mutant BRAF V600E/K (Coit et al., 2016) and have demonstrated very promising results in stage III clinical trials. For the comparison of vemurafenib+cobimetinib and vemurafenib alone, respectively 70% and 50% of patients responded to treatment, with 16% and 11% of patients showing a complete response. The median progression-free survival was respectively 12.2 months and 7.2 months, and the median overall survival was respectively 22.3 months and 17.4

months (Ascierto et al., 2016). Similar responses in clinical trials were seen with the dabrafenib+trametinib combination (Smalley & Sondak, 2015).

Although promising, the tumor regression and progression-free survival of patients typically lasted only one year before resistance to these inhibitors invariably developed, even with combination therapy (Flaherty, Infante, et al., 2012). In both patients and pre-clinical studies of resistance to mono or combination therapy, greater than 70% of cases showed reactivation of the MAPK signaling cascade through a variety of mechanisms (Fedorenko, Gibney, Sondak, & Smalley, 2015). These include genetic causes such as BRAF amplification, MITF amplification, MKK mutations, NRAS mutations, loss of NF1, and PTEN loss leading to increased PI3K pathway activity, as well as non-genetic causes such as BRAF splice-site mutants, activation of the COT kinase, and activation of EGFR (Nazarian et al., 2010; Poulikakos et al., 2011; Shi et al., 2014; Van Allen et al., 2014; Villanueva et al., 2010; Wagle et al., 2014). In addition to the clinical success of MAPK inhibitors, great progress in understanding the underlying cell mechanisms involved in cell death, combination therapy, and resistance has been made in preclinical studies using MAPK inhibitors that failed to obtain FDA approval (Carvajal et al., 2014; Kirkwood et al., 2012; Robert et al., 2013). The MKK1/2 inhibitor selumetinib (*aka* AZD6244) (Yeh et al., 2007) is one such inhibitor used by many labs, including ours, to model MAPK inhibition in preclinical cancer models (B. R. Davies et al., 2007; Ku et al., 2015; Rebecca et al., 2014).

It is clear that targeting the MAPK pathway using combinations of BRAF V600E/K and MKK1/2 inhibitors has failed to overcome resistance mechanisms leading to the re-activation of ERK1/2. For this reason, ERK1/2-specific inhibitors are now being developed, which in preclinical settings show promising ability to overcome acquired resistance (Morris et al., 2013).

Additionally, ERK1/2 inhibitors may build on the success seen in targeting multiple points upstream in the MAPK pathway and disrupt negative feedback loops that potentially lead to MAPK reactivation (Samatar & Poulikakos, 2014). Clinical trials using ERK1/2 inhibitors (Uehling & Harris, 2015) can be found on the clinicaltrials.gov database, and there is encouraging evidence that ERK1/2 inhibition can be used as a second-line clinical therapy following acquired resistance to BRAF V600E/K inhibitors (Krepler et al., 2016). Several ERK1/2 inhibitors with different conformational selectivity are being investigated by our lab (Rudolph, Xiao, Pardi, & Ahn, 2015) including SCH772984 (Morris et al., 2013), Vertex-11e (Aronov et al., 2009), and GDC0994 (Robarge et al., 2014) (Fig. 1.3,1.4). The half-life of each drug is listed in Figure 1.4, and the half-life for ERK1 (68 h) and ERK2 (53 h) was determined by proteomic analysis (Schwanhäusser et al., 2011). Prospective preclinical resistance modeling using chronic dosing of SCH772984 in KRAS mutant HCT-116 cells has shown ERK mutations leading to resistance (Jha et al., 2016), but it remains to be seen if resistance develops in BRAF V600E/K mutant cells or patients.

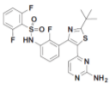
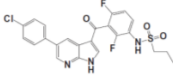
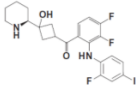
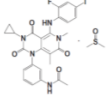
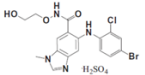
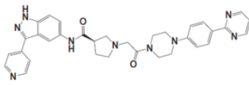
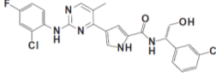
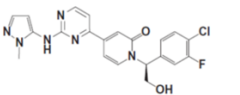
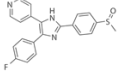
Drug	kinase target	FDA approval	Structure	IC ₅₀	Half-life
Dabrafenib (tafinlar)	BRAF ^{V600E}	approved as mono and combo therapy in V600 mutant melanoma		0.8nM	8 hours
Vemurafenib (Plx4032)	BRAF ^{V600E}	approved as mono and combo therapy in V600 mutant melanoma		31nM	2.1 days
Cobimetinib	MKK1/2	approved as combo therapy in V600 mutant melanoma		4.2nM	2.2 days
Trametinib (mekinist)	MKK1/2	approved as mono and combo therapy in V600 mutant melanoma		1.8nM	4 days
Selumetinib (Azd6244)	MKK1/2	currently in clinical trials		14nM	5-8 hours
Sch772984	ERK1/2	modified form in clinical trials		4nM	
Vertex-11e	ERK1/2	preclinical testing only		<2nM	
Gdc-0994	ERK1/2	currently in clinical trials		1.1nM	1 day
SB203580	p38	currently in clinical trials		40nM	1 day

Figure 1.4: Representative kinase inhibitors targeting mutant BRAF V600E/K, MKK1/2, and ERK1/2. Several inhibitors are approved for use as monotherapy although combination therapies are currently front line treatment in metastatic melanomas with BRAF V600E/K mutations. IC₅₀ values are specific for the targeted kinase.

1.4 Other MAPK pathways and osmotic stress activation of p38 MAPK

In addition to the RAF-MKK-ERK pathway, there are three additional MAPK signaling cascades which also have a three-tiered kinase structure with sequential kinase activation by phosphorylation. In each case, the terminal MAP kinases (MAPKs) transmit the pathway signal to many downstream substrates. These MAPKs are evolutionarily conserved and preferentially phosphorylate serine and threonine residues followed immediately by proline, with specificity also determined by substrate binding to a separate docking domain binding site in the MAP kinase (Tanoue & Nishida, 2003). Activation of the MAPKs by dual phosphorylation at Thr and

Tyr residues within the activation loop is catalyzed by specific MAP kinase kinases (MKKs). MKKs are in turn phosphorylated by several MAPK kinase kinases (MKKKs) which are activated in response to many stimuli (Johnson & Lapadat, 2002) (Fig. 1.5). In general, the ERK1/2 pathway is activated by cell stimuli such as cytokines and growth factors, and controls cell proliferation, differentiation, survival, and migration. The p38 MAP kinase and c-Jun amino-terminal kinase (JNK) pathways are activated by environmental stress and mediate stress responses by regulating transcription. The ERK5 pathway responds to growth factors as well as cellular stress and is the least well characterized (Drew, Burow, & Beckman, 2012).

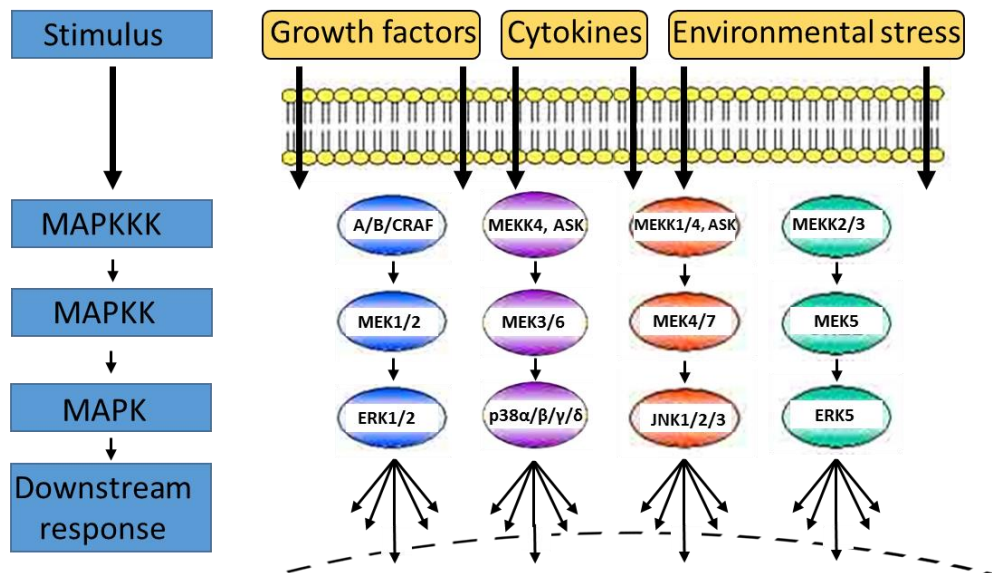


Figure 1.5: ERK, p38, JNK, and ERK5 MAPK signaling cascades. The four mitogen-activated protein kinase signaling cascades regulate many physiological processes through phosphorylation of substrates downstream of MAPKs and respond to a variety of extracellular stimuli. Figure adapted from (Roberts & Der, 2007)

The serine-threonine kinase, p38 α MAPK, is part of the MKKK-MKK3/6-p38 α / β / γ / δ MAPK signaling pathway which is distinct from RAF-MKK-ERK and MKKK-MKK-JNK pathways. Stimulation of this pathway by cytokines and environmental stress has been shown to result in cell proliferation and cytokine production as well as apoptosis and cell death (Zarubin,

T. & Han, 2005). Although the p38 MAPK pathway is similar in its organization to the ERK pathway, targeted kinase inhibitors directed at mutant BRAF V600E/K or MKK1/2 are very specific for ERK1/2 signaling (Uitdehaag et al., 2014; Yamaguchi et al., 2011). Up to now, they have not been previously shown to target components of the p38 pathway for inhibition. However, a phosphoproteomic screen which I conducted revealed that the MKK1/2 inhibitor, trametinib, specifically inhibits p38 α MAPK phosphorylation. This intriguing result led to biochemical examination of the p38 pathway to validate this result, which I describe in Chapter 2.

The first member of the p38 pathway was identified by four independent groups in 1994 (Freshney et al., 1994; J Han, Lee, Bibbs, & Ulevitch, 1994; Lee et al., n.d.; Rouse et al., 1994). This isoform became known as p38 α (aka MAPK14 or SAPK2a) and is the most well-characterized. Identification of p38 β (MAPK11), p38 γ (MAPK12), and p38 δ (MAPK13) followed shortly thereafter. These four isoforms are 60% identical in the amino acid sequence and 40-45% identical to other MAP-kinases identified (Jiang et al., 1997). Expression of p38 α is high across all cell types tested while the other three isoform levels vary based on cell type (Cuadrado & Nebreda, 2010) and only p38 α and p38 β isoforms respond to the widely used small molecule inhibitor, SB203580 (Goedert, Cuenda, Craxton, Jakes, & Cohen, 1997; Lali, Hunt, Turner, & Foxwell, 2000). All p38 isoforms have a Thr-Gly-Tyr (TGY) phosphorylation motif in their activation loop. Dual phosphorylation of the Thr and Tyr residues in this motif is directly catalyzed by the kinases, MKK3/6, and results in activation (Cohen, 1997). MKK3/6 are activated by a group of MKKKs which include upstream Rho GTPase binding proteins, including MLKs, ASK1, TAK1, MEKK3/4, and Rac1. These are activated by environmental stresses and inflammatory cytokines but not typically by growth factors (Cuenda & Rousseau,

2007). The p38 MAPK pathway, and p38 α in particular, has been shown in some systems to have a role as a tumor suppressor and in other systems to have an oncogenic role, in a variety of cancer models including cultured cells, animals, and patients. Tumor suppressor behavior involves negative regulation of cell cycle progression through checkpoint controls and apoptotic regulation, while oncogenic behavior involves promotion of cell invasion, inflammation, and angiogenesis. Thus, p38 can act as a tumor suppressor or an oncogene, depending on the context of the experiment and variables such as cell type, mutational profile, and method of pathway stimulation or inhibition (Cuenda & Rousseau, 2007; Wagner & Nebreda, 2009). Several clinical trials using p38 inhibitors have been initiated but have been unable to pass phase I due to toxicity, which may be ascribed to p38 inhibition or to off-target effects.

1.5 Phosphoproteomic analysis of molecular responses to MAPK pathway inhibitors

Reversible phosphorylation of substrates are critical post translational modifications (PTMs) that regulate processes downstream of the MAPK pathway. Proteomics has been used to characterize targets of the ERK pathway in many ways, including two dimensional gel electrophoresis (Kosako et al., 2009; Lewis et al., 2000), ERK analog sensitive mutants utilizing a radiolabeled ATP analog (Carlson et al., 2011; Eblen et al., 2003), and -79 Da negative precursor ion MS scanning which identifies phosphopeptides by their loss of PO₃⁻ (Old et al., 2009). However, the overlap of substrate identification between different studies has been poor, likely due to low sampling or variation between cell types (Courcelles et al., 2013). Bottom-up phosphoproteomics using a complex mixture of digested proteins extracted from cells coupled with stable isotope labeling of amino acids in cell culture (SILAC) (Mann, 2006) has emerged as

a powerful technique to quantify changes in phosphorylation on a deeper, more global scale (Galan et al., 2014; Pan, Olsen, Daub, & Mann, 2009).

Our lab previously used a SILAC-based approach to identify shared and unique targets of the BRAF V600E/K inhibitor, vemurafenib, and the MKK1/2 inhibitor, selumetinib (Stuart et al., 2015). A metastatic melanoma cell line was triply labeled with media supplemented with arginine and lysine containing different combinations of isotopic labeling with ^{13}C and ^{15}N (Fig. 1.6). During protein digestion, trypsin preferentially cleaves on the carboxyl side of arginine or lysine, and when the resulting peptides are analyzed on a mass spectrometer, the masses of identical peptides will shift depending on the light/medium/heavy isotopic labeling. This allows for quantification of changes in peptide abundance in a mixtures of lysates from cells under three different treatments. Titanium oxide was used to enrich phosphopeptides from the admixtures, which enabled a direct comparison of changes in protein phosphorylation in response to the BRAF V600E/K and MKK1/2 inhibitors. Notably, very few targets were specific to only one drug, thus the high degree of overlap was consistent with a linear model describing signaling from BRAF to MKK1/2. This result also indicated that BRAF V600E/K and MKK1/2 inhibitors when used in combination lead to an additive effect on phosphoproteins, instead of targets unique to one but not the other drug. This suggested that the clinical success of the drug combination is likely due to additive and more complete inhibition of pERK compared to either drug alone, and not due to synergy between targets uniquely regulated by each drug.

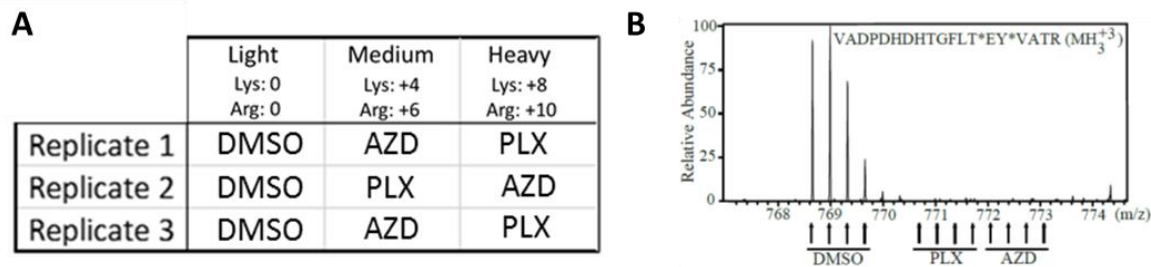


Figure 1.6: SILAC labeling allows quantification of changes in phosphopeptide levels in response to inhibitor. A, label-swapping design of SILAC experiment with triplicate biological replicates, described by Stuart et al., 2015. The labeling code +4/+6/+8/+10 indicates Lys and Arg mass increases in Daltons due to isotopic labeling. Metabolic labeling of cells yields proteins incorporating these labeled amino acids, which generate peptides with increased masses depending on their Lys and Arg composition. All treatments used the metastatic melanoma cell line, WM239a, adding 10 μ M drug for 2 h. AZD=AZD6244 (selumetinib), PLX=PLX4032 (vemurafenib). B, mass spectrum of labeled peptide from ERK2, with dual phosphorylation at the TEY regulatory phosphorylation sites, show a dramatic decrease in response to kinase inhibitor drugs. Adapted from (Stuart et al., 2015).

1.6 Thesis overview

There is a high degree of specificity in the MAPK pathway (Hindley & Kolch, 2002; Matallanas et al., 2011; Roskoski, 2012; Yoon & Seger, 2006), and our lab has used phosphoproteomics to demonstrate a remarkable degree of overlap in molecular changes induced by inhibitors of BRAF V600E/K and MKK1/2 in melanoma cells (Stuart et al., 2015). Using subsaturating concentrations, it was found that inhibitors suppress phosphorylation events in an additive manner, suggesting that the major effects of combination treatment are due to additive effects on signaling responses between inhibitors. The question that is unsolved is: how do molecular responses to ERK1/2 inhibitors compare against those of BRAF V600E/K and MKK1/2 inhibitors? Although a recent study of KRAS mutant colorectal cancer cells reported high overlap between responses to MKK1/2 or ERK1/2 inhibitors (Gnad et al., 2016), the degree of overlap in BRAF V600E/K mutant melanoma cells remains unknown. In Chapter 2, I compare the ERK1/2 inhibitor, SCH772984, which was shown to effectively overcome acquired

resistance to BRAF V600E/K and MKK1/2 inhibitors (Morris et al., 2013), to the FDA-approved MKK1/2 inhibitor, trametinib, in mutant BRAF V600D melanoma cells. Characterizing these inhibitory effects will directly inform the results of ongoing clinical trials using these inhibitors. Afterwards, I compare the phosphoproteomics responses to two MKK1/2 inhibitors, trametinib and selumetinib, and demonstrate a novel off-target of trametinib. Using biochemical assays, I confirm that trametinib inhibition of MKK6 at high doses leads to dephosphorylation of the downstream effector, p38 α MAPK, and speculate that this may help explain the higher drug efficacy that has been observed with trametinib. Finally, I perform a comparative phosphoproteomic screen of three separate ERK1/2 inhibitors (SCH772984, GDC0994, and Vertex-11e) which show different binding properties to ERK2, and compare their specificity with respect to known ERK1/2 substrates, regulatory phosphosites, and molecular pathway enrichment. In Chapter 3, I summarize the significance of this study as well as future directions for a more complete understanding of MAPK inhibition using phosphoproteomics.

Chapter 2

Selective phosphoproteome responses to MKK1/2 and ERK1/2 inhibitors in human melanoma cells

2.1 Abstract

The RAF/MKK/ERK signaling cascade is constitutively activated by oncogenic BRAF V600E/K in melanomas and other cancer types. Although small molecules which inhibit BRAF V600E/K and MKK1/2 have been successful in clinical settings, resistance invariably develops. In preclinical studies, high affinity inhibitors of ERK1/2 block the viability of melanoma cells which are otherwise resistant to BRAF V600E/K and MKK1/2 inhibitors. Thus, ERK1/2 inhibitors are promising as alternative drugs for pathway inhibition. But still unknown is how molecular responses compare between these new ERK1/2 inhibitors and the targeted therapeutics in clinical use. Previously, our lab has shown near complete overlap in the phosphoproteomic changes induced by BRAF V600E/K and MKK1/2 inhibitors. Here, I employ quantitative SILAC-based phosphoproteomics to measure the degree of overlap in molecular responses to the MKK1/2 inhibitor, trametinib, and the ERK1/2 inhibitor, SCH772984, in human metastatic melanoma cells. Biological triplicate experiments reproducibly quantified 8,577 phosphosites, 400 of which were altered significantly in response to either drug. Only 18 phosphosites decreased in response to SCH772984 or trametinib alone. Nevertheless, trametinib shows an ability to block activating phosphorylation sites on p38 α MAPK, which is not shared by the ERK1/2 inhibitor, SCH772984, the MKK1/2 inhibitor, selumetinib, or the BRAF V600E/K inhibitor, vemurafenib. The inhibition can be traced to MKK6, suggesting that MKK6-p38 α signaling is a novel off-target for trametinib. This occurs at concentrations above those achieved in clinical studies but within the range commonly used in preclinical studies. Additionally,

comparison of phosphoproteome changes show a high degree of overlap in responses to the ERK1/2 inhibitors, SCH772984 and GDC0994. Together with previous studies comparing BRAF V600E/K and MKK1/2 inhibitors (Stuart et al. 2015), my findings support linearity in signal transduction through the MAPK pathway, with little evidence for bifurcation in signaling from BRAF V600E/K or MKK1/2 upstream of ERK1/2, and few differences in molecular responses to inhibitors of MKK1/2 and ERK1/2.

2.2 Significance of study

I conducted comparative phosphoproteomics of the ERK1/2 inhibitor, SCH772984, and the MKK1/2 inhibitor, trametinib, in melanoma cells and found almost complete overlap among the phosphosites that significantly changed in response to drug, indicating pathway linearity extends from BRAF V600E/K and MKK1/2 to ERK1/2. Among the small number of unique targets inhibited by trametinib, the canonical TGY activation motif of p38 α is significantly inhibited by trametinib but not other BRAF V600E/K, MKK1/2, or ERK1/2 inhibitors tested. MKK6 is identified as the direct target of trametinib, leading to decreased p38 α activation. Inhibition of p38 α MAPK activation is shown to cooperate with MKK1/2 inhibitors that do not display an off-target effect on this kinase and thus inhibition of p38 α MAPK may augment effects in preclinical studies using trametinib at high concentrations.

2.3 Introduction

The MAPK signaling cascade (RAF-MKK-ERK) is constitutively activated in many cancer types, where sustained activity drives malignancy of melanoma, colorectal, thyroid, and ovarian cancers (Burotto et al., 2014). Upregulation of this pathway leads to cell survival,

proliferation, and disease progression in malignant melanomas, where as many as 50% of cases display activating mutations in BRAF V600E/K, and 20% have mutations in NRAS (Flaherty, Hodi, & Fisher, 2012). Therapeutics that specifically target key protein kinases in this pathway have been successful in clinical as well as preclinical settings. To date, two MKK1/2 inhibitors (trametinib and cobimetinib) and two BRAF V600E/K inhibitors (vemurafenib and dabrafenib) (Signorelli & Shah Gandhi, 2016; Wu et al., 2015) have received FDA approval, as single agent or combination drug therapies. These inhibitors elicit dramatic responses in patients, and combination treatments using BRAF V600E/K and MKK1/2 inhibitors are now frontline therapies for treating metastatic melanomas harboring oncogenic BRAF V600E/K mutations. However, resistance regularly develops through mechanisms that activate MAPK signaling, even in the presence of drug (Van Allen et al., 2014). Development of ERK1/2 inhibitors has emerged as a promising strategy to combat this resistance and several are in early stage clinical trials (Morris et al., 2013). Addition of ERK1/2 inhibitors to the treatment strategy may provide an effective way to extend the average progression-free survival time for patients. Therefore, understanding the molecular responses to ERK1/2 inhibitors and comparing them to clinically used drugs would be important for maximizing their effectiveness.

Previous studies comparing molecular responses to inhibitors of BRAF V600E/K and MKK1/2 by phosphoproteomics overlapped strongly with only a small number of differences (Stuart et al., 2015). This suggests that MAPK pathway signaling at the level of BRAF V600E/K and MKK1/2 works in a predominantly linear manner, with little evidence for targets bifurcating upstream of MKK1/2. Consistent with this finding, mixtures of inhibitors at subsaturating concentrations induced responses that were largely additive (Stuart et al., 2015). This suggested that combinations of BRAF V600E/K and MKK1/2 inhibitors are more effective due to their

additive effects on ERK1/2 inhibition, and that incomplete ERK1/2 inhibition at maximally tolerated doses may limit the efficacy of single drug therapies.

However, an unanswered question is the degree to which promising ERK1/2 inhibitors target the same responses as clinically used MKK1/2 inhibitors. Here I compare phosphorylation responses to ERK1/2 inhibitors SCH772984 (SCH) and GDC0994 (GDC) against the MKK1/2 inhibitor, trametinib (TRA) in human metastatic melanoma cells. The results show strong agreement between phosphorylation responses to SCH772984, GDC0994 and trametinib, revealing pathway linearity at the level of MKK1/2 and ERK1/2. However, trametinib selectively inhibits activating phosphorylation sites in p38 α MAPK, Thr180 and Tyr182. This is due to the ability of trametinib to inhibit MKK6, within a concentration range commonly used in preclinical studies ($K_i = 1 \mu\text{M}$). The MKK1/2 inhibitor, selumetinib, has no effect towards MKK6 or p38 α MAPK, therefore, inhibition by trametinib can be attributed to an off-target effect unique to this compound. All four inhibitors of MKK1/2 and ERK1/2 alter phosphorylation of known MAPK pathway targets, such as S642 on RAF1 (CRAF) which is a negative feedback regulator of MKK activity (Dougherty et al., 2005) and T526 on transcription factor and ERF which controls activity (Sgouras et al., 1995), as well as novel targets. One example is S22 on NCBP1, a known regulatory site targeted by RPS6KB1 downstream of mTOR (Wilson, Wu, & Cerione, 2000), a finding which adds support to the crosstalk model between RAF-MKK-ERK and PI3K signaling networks (Mendoza, Er, & Blenis, 2011). None of the phosphorylation sites that are uniquely altered by any ERK1/2 or MKK1/2 inhibitor are shared with another inhibitor of the same kinase. Taken together, my findings show that MAPK signaling is predominantly linear, with few if any points of bifurcation upstream of ERK1/2. This

establishes a basis for identifying off-target effects induced by future drug candidates developed towards kinases in this pathway.

2.4. Materials and methods

Cell Culture

The metastatic melanoma cell line WM239a was a gift of Dr. Meenhard Herlyn, Wistar Institute, Philadelphia PA. Cells were SILAC-labeled using SILAC RPMI media (Thermo Fisher Scientific 89984) supplemented with heavy, medium, or light isotopically-labeled arginine (40 $\mu\text{g}/\text{mL}$) and lysine (200 $\mu\text{g}/\text{mL}$) (Cambridge Isotope Laboratories), 10% (v/v) dialyzed FBS (Life Technologies 88440), penicillin (100 $\mu\text{g}/\text{mL}$, Gibco), and streptomycin (100 $\mu\text{g}/\text{mL}$, Gibco). Non-SILAC experiments used cells cultured in Gibco RPMI 1640 media (2400-089) and 10% dialyzed FBS, with or without penicillin-streptomycin. Cells were incubated in a humidified chamber maintained at 37°C with 5% CO_2 .

SILAC-labelled phosphopeptide sample preparation

WM239a cells were grown in heavy (H), medium (M) or light (L) SILAC RPMI. Cells in each label were grown in 6 x 15 cm dishes, then then trypsinized, combined, counted, and plated into three dishes at 100% confluence ($\sim 35 \times 10^6$ cells/dish). For each experiment, one dish with cells labeled H, M or L was treated with drug (10 μM) or DMSO carrier for 2 h. Cells in each dish were washed quickly with PBS, then lysed by adding 0.7 mL of 4% (w/v) SDS, 100 mM dithiothreitol, 100 mM Tris pH 7.6 (SDT buffer), and harvested by scraping.

Cell lysates were then sonicated for 30 s with a microtip sonicator and H, M and L samples were combined from each replicate, brought up to 30 mL in urea buffer (8 M urea, 0.1 M Tris pH 8.5) and processed using a modified filter-aided sample preparation (FASP) method

to remove SDS (Wiśniewski, Zougman, Nagaraj, Mann, & Wiśniewski, 2009). The 30 mL sample volume was divided into two Amicon Ultra-15 10K (Millipore) filter units and centrifuged at 4,000 x g for 25 min. Filter-bound samples were washed in 5 mL urea buffer and carbamidomethylated with 5 mL iodoacetamide (50 mM) in urea buffer. After centrifugation and three washes with 5 mL urea buffer, samples were washed with 5 mL ammonium bicarbonate (50 mM) to reduce the urea concentration and incubated with 2% (w/w) sequencing grade modified trypsin (Promega) overnight at 37 °C to digest labeled proteins into peptides. Filter units were centrifuged and washed with 3 mL HPLC grade H₂O. The flow-through was combined for each replicate and acidified to pH 2-3 using 98% formic acid, measured with pH strips.

Oasis HLB sorbent cartridges (150 mg, Waters) were used to desalt samples using 4 mL of 65% (v/v) acetonitrile, 1% (v/v) trifluoroacetic acid (TFA) to elute. TFA was added to bring the final concentration to 2% (v/v), and the protein concentration was determined using the DC protein assay (Bio-Rad). Thirty micrograms of each sample was removed for total protein measurement by mass spectrometry and L-glutamate (Sigma) was added to the remainder to a final concentration of 140 mM. Titanium dioxide beads (5 µm, GL Sciences) were equilibrated with 1 mL washes of eluting buffer 1 [20% (v/v) acetonitrile, 1% (w/v) ammonium hydroxide], wash buffer 1 [65% (v/v) acetonitrile, 0.5% (v/v) TFA], and loading buffer [65% (w/v) acetonitrile, 2% (v/v) TFA, 140 mM glutamic acid]. 20 mg of titanium beads in loading buffer were then added to aliquots of 2 mg protein for each sample, and rotated for 15 min at room temperature to bind phosphopeptides. Sample aliquots with titanium beads were centrifuged and washed with 1 mL loading buffer, 1 mL wash buffer 1, and two times with 1 mL wash buffer 2 [65% (v/v) acetonitrile, 1.0% (v/v) TFA] before being resuspended in 200 µL eluting buffer 1.

This volume was added to C8 stagetips (Proxeon), eluted with a 1 mL syringe followed by 400 μ L of 65% acetonitrile, 1% ammonium hydroxide and lyophilized overnight.

Lyophilized samples enriched for phosphopeptides were resuspended in 65 μ L Buffer A (16.7 mM ammonium formate, 70% acetonitrile, pH 2.2) and sonicated in a water bath for 4 x 30 s pulses before being centrifuged for 1 min at 14,000 x g. The sample was then injected into a 50 μ L sample loop using an Agilent 1100 HPLC with a 100 x 4.6 mm 5 μ m polyWAX LP column (PolyLC) separated using an ERLIC gradient (Zarei, Sprenger, Gretzmeier, & Dengjel, 2013). The gradient was 0-5 min: 100% Buffer A, 5-15 min: increasing linear gradient to 100% Buffer B (16.7 mM ammonium formate, 10% acetonitrile, pH 2.2), 15-20 min increasing linear gradient to 100% Buffer C (1% TFA, 10% acetonitrile), 20-24 min: 100% Buffer C. One minute fractions were collected at a flow rate of 1 mL/min and immediately frozen in liquid nitrogen before being speedvac evaporated and resuspended in 0.1% formic acid, 5% acetonitrile.

Total protein samples (30 μ g) were speedvac evaporated and resuspended in 17 μ L of 1% TFA pH 2.5, 5% (v/v) acetonitrile. High pH reverse-phase fractionation was performed off-line using a Waters M-class Acquity UPLC, loading 15 μ L of each digest onto a hand-packed C18 column (1.8 μ m 120 \AA UChrom C18, 0.5 mm i.d./0.793 mm o.d. X 200 mm) equilibrated in Buffer A (10 mM ammonium formate pH 10) and eluted at 15 μ L/min for 170 min with a linear gradient of increasing Buffer B (10 mM ammonium formate pH 10, 80% acetonitrile). Twelve fractions per replicate were collected.

LC-MS/MS

For SILAC experiments comparing DMSO-trametinib-SCH772984, phosphopeptide fractions were loaded onto a Waters Acquity UPLC M-class Peptide BEH C18 analytical column (1.7 μ m, 130 \AA , 75 μ m i.d., 250 mm). LC-MS/MS was run at 300 nL/min using either a Thermo

nLC100 or a Waters M-class Acquity UPLC. Peptides were eluted from Buffer A (0.1% formic acid in water) into Buffer B (0.1% formic acid, 100% acetonitrile) using a gradient from 3%-85% acetonitrile in 130 min (3% B for 0-5 min, 3%-20% B for 5-105 min, 20%-32% B for 105-125 min, 32%-85% B for 125-126 min, 85% B for 126-130 min). MS/MS was performed on an Orbitrap Fusion mass spectrometer with MS1 120,000 resolution scanning between 380-1500 m/z, 2×10^5 AGC, 50 ms injection time, 20 s dynamic exclusion and data dependent mode top speed on the most intense ions. MS2 was performed using 1.6 m/z isolation with quadrupole, 35% HCD collision energy, 1 μ scan, centroid in ion trap (1.0×10^4 AGC, 35 ms fill time) or orbitrap (30,000 resolution, 5.0×10^4 AGC, 60 ms fill time). Total protein samples were analyzed by MS/MS using the same method and ion trap isolation. For the DMSO-SCH772984-GDC0994 and DMSO-SCH772984-Vertex-11e SILAC experiments, LC-MS/MS analysis was performed using Waters Acquity UPLC and LTQ Orbitrap Velos instrumentation as previously described (Stuart et al., 2015).

Data and statistical analysis

Raw MS files for phosphopeptide and total peptide fractions were searched together using MaxQuant (Cox & Mann, 2008) software and processed with Perseus software as described (Stuart et al., 2015). MaxQuant identifies common contaminants and peptides matching to a target-decoy database containing reversed versions of each peptide in a protein database FASTA file. The DMSO-trametinib-SCH772984 dataset was searched using MaxQuant v1.5.4.2 and further analyzed using Perseus v1.5.4.2. The DMSO-SCH772984-GDC0994 and previously published DMSO-selumetinib-vemurafenib datasets were searched using MaxQuant v1.4.1.2 and further analyzed using Perseus v1.4.1.3. Searches used the Uniprot human proteome

reference (05-11-2016 release for DMSO-trametinib-SCH772984; 08-21-2015 release for DMSO-SCH772984-GDC0994; 01-27-2014 release for DMSO-selumetinib-vemurafenib).

Greater than 1.8 fold changes ($\log_2 \pm 0.840$) was used as significance threshold for SILAC ratios of phosphopeptides, corresponding to $FDR \leq 0.01$ as determined from control replicate experiments of WM239a cells treated with DMSO (Stuart et al., 2015). To identify high-confidence phosphosites and control for variability among replicates, an empirical Bayesian analysis using Bioconductor-Limma software (Ritchie et al., 2015) was used to calculate adjusted p-values controlling the false discovery rate (q-value) (Margolin et al., 2009; Poss et al., 2016). Limma estimated the $\log_2(\text{drug:DMSO})$ ratios of phosphosites from two or three replicates, using phosphosite-wise linear models.

Immunoblotting

After treating cells with DMSO or drug for 2 h, hyperosmotic stress was induced by adding a solution of 5 M NaCl + 0.4 M KCl to a final concentration of 181 mM NaCl and 12.5 mM KCl, yielding media with total osmolality of 500 mOsm/L. Cells were harvested in RIPA lysis buffer supplemented with cOmplete protease inhibitor and Phos-Stop phosphatase inhibitor cocktails (Roche), and lysate protein concentrations were determined using the BioRad DC protein assay. Immunoprecipitation of p38 α MAPK was carried out by incubating 250 μ g cell lysate with 1 μ g anti-p38 α antibody overnight at 4°C, followed by 20 μ L Dynabeads Protein G (Novex) for 1 h at 4°C. Beads were collected magnetically, washed with cold phosphate-buffered saline (PBS) and incubated in Laemmli sample buffer for 10 min at 95°C. All antibodies used were from Cell Signaling Technology and included anti-phospho-p38 α (#9218), anti-p38 α (#4511), anti- β -tubulin (#2146), anti-phospho-ERK1/2 (#4370), anti-MKK6 (#8550), anti-phospho-p90RSK (#9335), anti-BIM (#2819), and anti-cleaved PARP (#5625). Protein samples

were separated on 7.5% or 10% SDS-PAGE and transferred to PVDF membranes (Millipore-SQ), which were incubated with primary antibody overnight at 4°C and secondary antibody for 1 h at room temperature. Pierce ECL2 substrate was used for immunoblot development using X-ray film and/or fluorescence imaging (Typhoon, GE Healthcare).

In vitro kinase assays

Plasmids for expression of Flag-MKK6 and Flag-MKK3 in mammalian cells were generated by Roger Davis' laboratory (Dérijard et al., 1995; Enslen, Brancho, & Davis, 2000; Raingeaud, Whitmarsh, Barrett, Dérijard, & Davis, 1996) and obtained from Addgene: Flag-MKK6 (#13517), Flag-MKK6-S207E/T211E (#13518), Flag-MKK6-K82A (#13519), Flag-MKK3-S189E/T193E (#14670), Flag-MKK3-S189A/T193A (#14669), and Flag-MKK3b-S218E/S222E (#50449). Plasmids were purified using the PureLink HiPure maxiprep kit, and cells were transfected by electroporation using the NEON transfection system both according to manufacturers' protocol (Thermo Fisher Scientific). 1×10^6 cells were transfected with 5 μ g cDNA using 1,200 V x 2 pulses X 20 ms/pulse, then incubated for 72 h, followed by lysis in RIPA buffer. Flag-tagged proteins were purified using anti-Flag M2 affinity gel resin (Sigma-Aldrich) and incubated with 300 μ g lysates overnight at 4°C. Beads were washed in cold Tris-buffered saline (TBS), resuspended in reaction buffer containing 10 mM MgCl₂, 1 mM ATP, 50 mM Tris-HCl pH 7.2, 50 mM NaCl and 1 mM dithiothreitol, and then incubated with DMSO or drug at room temperature for 15 min. Reactions were initiated by adding 1 μ g of unphosphorylated His₆-p38 α MAPK, expressed in *E. coli* and purified by Ni-NTA and MonoQ chromatography as described (Sours, Xiao, & Ahn, 2014). Reactions were incubated for 2 min at 30°C, then quenched by adding Laemmli sample buffer followed by heating for 10 min at 95°C. Proteins were separated by SDS-PAGE followed by immunoblotting for phospho-p38 α MAPK.

Reaction time and kinase levels were chosen within ranges of linear phosphorylation of p38 α MAPK.

The Thermo Fisher Scientific SelectScreen service was used to generate a 10-point dose response curve for trametinib (0, 0.001, 0.003, 0.01, 0.03, 0.1, 0.3, 1, 3, 10 and 30 μ M) against MKK6 activity. The cascade format of this assay uses *in vitro* phosphorylation of inactive p38 γ substrate by MKK6 to then phosphorylate a proprietary fluorophore-conjugated peptide substrate (Z'-LYTE) in the primary reaction. In the secondary reaction, site-specific proteolytic cleavage disrupts the Förster resonance energy transfer (FRET) of donor (coumarin) and acceptor (fluorescein) fluorophores coupled to unphosphorylated Z'LYTE peptide, leading to a decrease in FRET. The emission ratio (coumarin emission 445 nm/fluorescein emission 520 nm) remains high if the Z'LYTE peptide remains unphosphorylated. Maximum and minimum emission ratios were established using a synthetically phosphorylated p38 γ peptide and a control reaction containing no ATP. Inhibition by trametinib was compared to a known inhibitor of MKK6, staurosporine, in a separate 10-point titration activity assay.

Cell viability assay

WM239a cells were seeded into 96-well dishes at 5,000 cells per well and allowed to adhere for 4 h before treating with DMSO or varying concentrations of drug. After 72 h, cellular ATP was quantified using the CellTiter Glo 2.0 Assay (Promega) according to the manufacturer's protocol. Luminescence was recorded using a Biotek Synergy H1 plate reader and curve-fitting was done using Origin software.

Cell death measurements

WM239a cells were seeded into 6 cm dishes at 750,000 cells per dish, and allowed to adhere overnight before treating with DMSO or with 10 μ M selumetinib, Vertex-11e, or

SCH772984. After 48 h, apoptosis and necrosis were quantified using the annexin V-FITC PI assay (Thermo Fisher Scientific) using a FacScan flow cytometer (Beckman Coulter) according to the manufacturer's protocol. Recombinant annexin V conjugated to fluorescein (FITC) binds phosphatidylserine (PS) which translocates to the outer plasma membrane during apoptosis, and marks cells with green fluorescence. Propidium iodide (PI) is a DNA intercalating red-fluorescent molecule that only passes the plasma membrane of cells that have been permeabilized during late-stage cell death. The percentage of total cells staining positive for these markers is compared between drug treatments.

Kinase assays

The Human Phospho-Kinase Array (R & D Systems) was used to profile the relative levels of protein phosphorylation of 43 kinases simultaneously, according to the manufacturer's protocol. Following 4 h treatment with DMSO or 10 μ M drug, cells were harvested in lysis buffer and incubated overnight with a nitrocellulose membrane containing capture antibodies for each phosphorylation site bound to the membrane in duplicate. After washing to remove unbound proteins, the arrays were incubated with a mixture of biotinylated detection antibodies which produce a chemiluminescent reaction when streptavidin-conjugated HRP and substrate are added. The signal produced at each spot corresponds to the amount of phosphorylated protein bound, and was quantified using a Typhoon fluorescence image scanner and ImageQuant software (GE Healthcare).

2.5 Results

I first compared molecular responses to the MKK1/2 inhibitor, trametinib, and the ERK inhibitor, SCH772984, using phosphoproteomics to screen WM239a human metastatic

melanoma cells. Phosphorylation changes were quantified in triple SILAC-labeled cells, treated with DMSO 10 μ M trametinib, or 10 μ M SCH772984 for 2 h followed by cell lysis and trypsinization using a modified FASP protocol, batch enrichment of phosphopeptides with TiO_2 resin, and fractionation by ERLIC chromatography as described previously (Stuart et al., 2015; Wiśniewski et al., 2009; Zarei et al., 2013) (Fig. 2.1A). The WM239a metastatic melanoma cell line harbors a V600D BRAF mutation leading to constitutive upregulation of the MAPK pathway. A two-hour time point allows us to observe downstream effects of kinase inhibition before directed protein degradation of other regulated proteins occurs. This cell line and time point also allow a direct comparison to the previous SILAC phosphoproteomic experiment using MKK1/2 inhibitor AZD6244 published by Scott Stuart in our lab (Stuart et al., 2015). Experiments were conducted in triplicates, varying the isotopic labeling for each condition (Fig. 2.1B). In total, SILAC ratios could be quantified for 12,924 unique phosphosites on 3,851 proteins corresponding to class I phosphosites (localization probability >0.75 , delta score >5). Of these, 8,577 class I phosphosites could be quantified in two or more replicate experiments (Fig. 2.1C). ERLIC fractionation separated phosphopeptides across 24 fractions, allowing a higher number of identifications in complex samples (Fig. 2.2A,B), with the vast majority of phosphopeptides being singly phosphorylated (Fig. 2.2C).

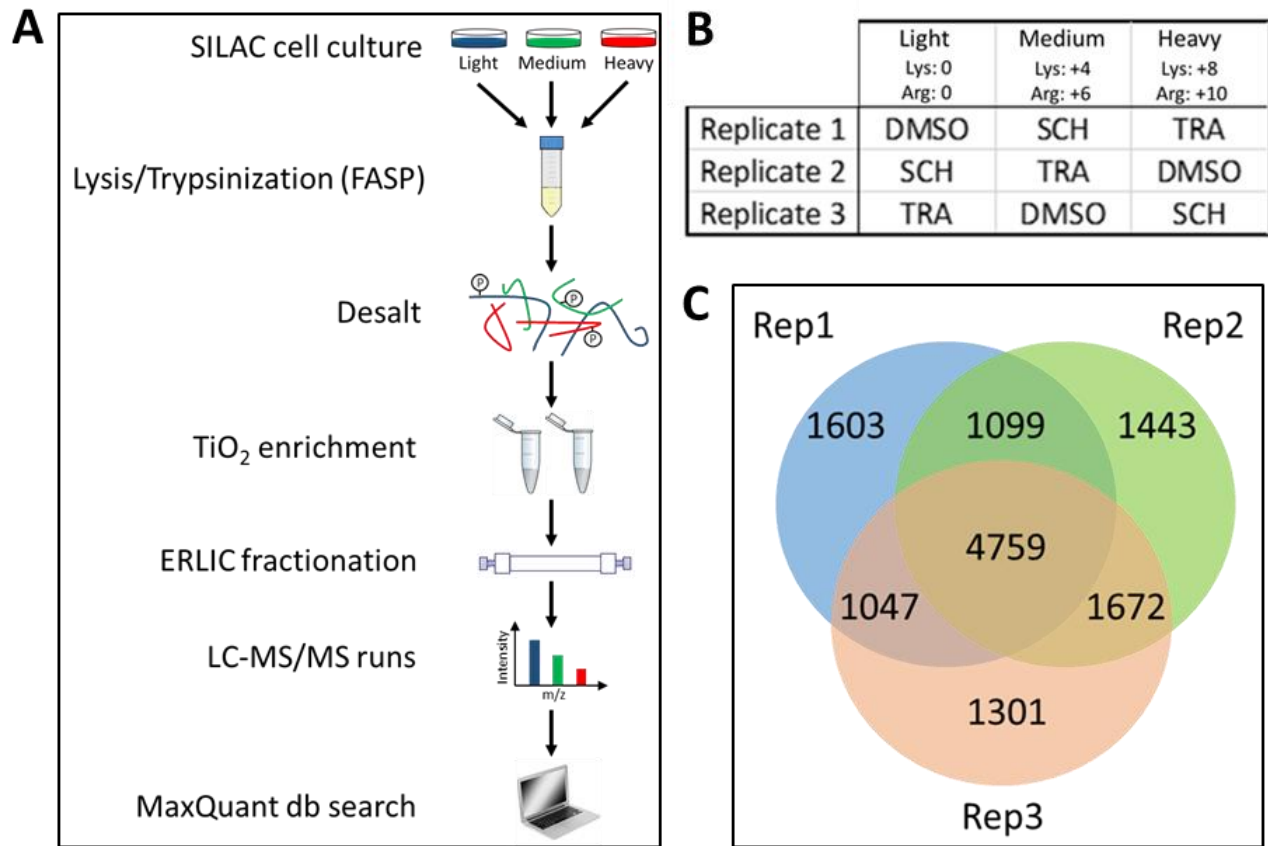


Figure 2.1: SILAC experiment design. A, Experimental workflow and mass spectrum of isotopically labeled peptides. B, Isotope labeling design and label-swap of replicates. WM239a cells were treated 2 h with DMSO or 10 μ M SCH772984 (SCH) or 10 μ M trametinib (TRA). C, Overlap among replicates in 12,924 phosphosites that could be quantified.

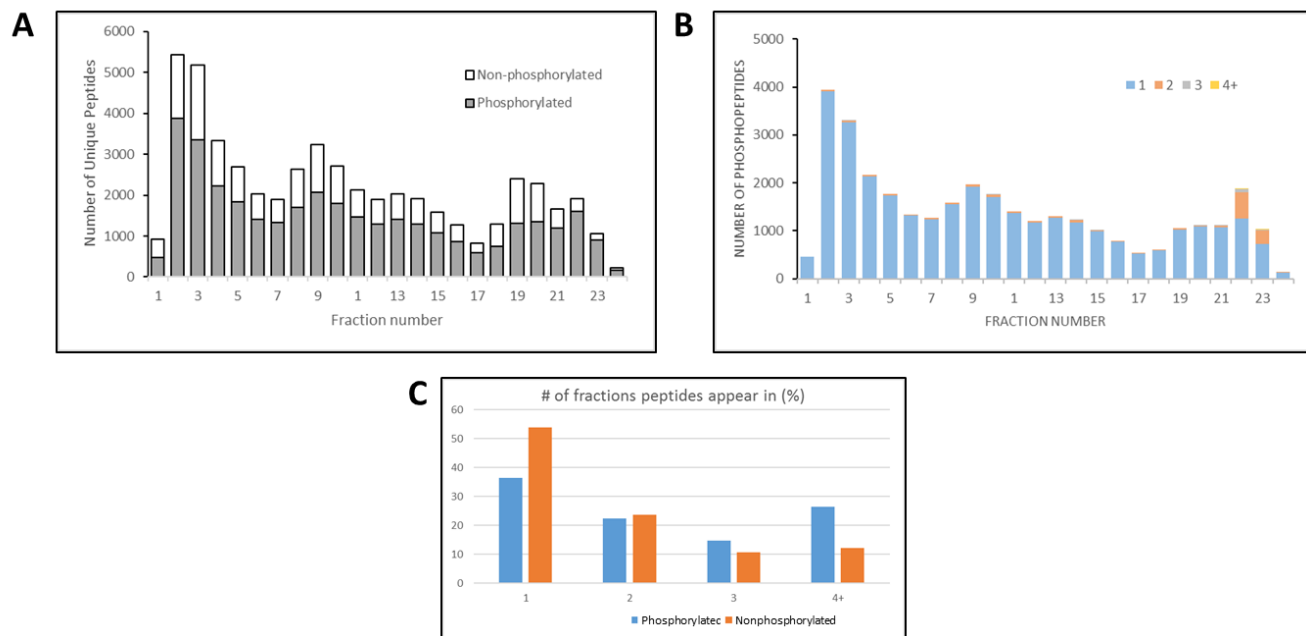


Figure 2.2. Performance of the ERLIC fractionation method. A, Unique phosphorylated and non-phosphorylated peptides in each ERLIC fraction, identified in three replicates. B, Number of singly and multiply-phosphorylated peptides in each fraction identified in three replicates. C, Number of fractions in which each phosphorylated and non-phosphorylated peptide can be identified, among three replicate experiments.

A threshold of 1.8-fold ($\log_2 \pm 0.84$) was used to identify significant changes in phosphosite abundance, based on control experiments of WM239a cells previously reported by our lab (Stuart et al., 2015) (Table 2.1). After filtering with this threshold, 564 class I phosphosites were found to be altered significantly by one or both inhibitors in multiple experiments. As an additional filter for significant changes, an empirical Bayesian analysis using the Limma statistical package was employed to calculate adjusted p-values for each phosphosite (Ritchie et al., 2015). We focused our remaining analysis on the 400 phosphosites that exhibited $\log_2(\text{drug:DMSO ratios})$ less than -0.84 or greater than +0.84, with an adjusted p-value ≤ 0.05 (Fig. 2.3A-C).

Table 2.1. Comparison of phosphosites identified in each triple-labeled replicate comparing trametinib and SCH772984. Number of phosphosites quantified after removing reverse protein database hits and contaminants and expanding the phosphopeptide results to separate phosphosites that were identified in multiply phosphorylated peptides. Ratios were considered significant when $|\log_2 \text{ratio}| \geq \pm 0.84$ determined by empirical Bayes-generated $\log_2(\text{combined ratio})$.

Replicate	Significance	TRA/DMSO	% Total	SCH/DMSO	% Total	SCH/TRA	% Total
1 (8517 sites)	Decreased	447	5.2	490	5.8	149	1.7
	Increased	185	2.2	85	1.0	55	0.6
2 (8989 sites)	Decreased	473	5.3	489	5.4	76	0.8
	Increased	101	1.1	92	1.0	64	0.7
3 (8788 sites)	Decreased	535	6.1	473	5.4	96	1.1
	Increased	104	1.2	139	1.6	181	2.1
Avg (8577 sites)	Decreased	422	4.9	415	4.8	33	0.4
	Increased	43	0.5	73	0.9	33	0.4

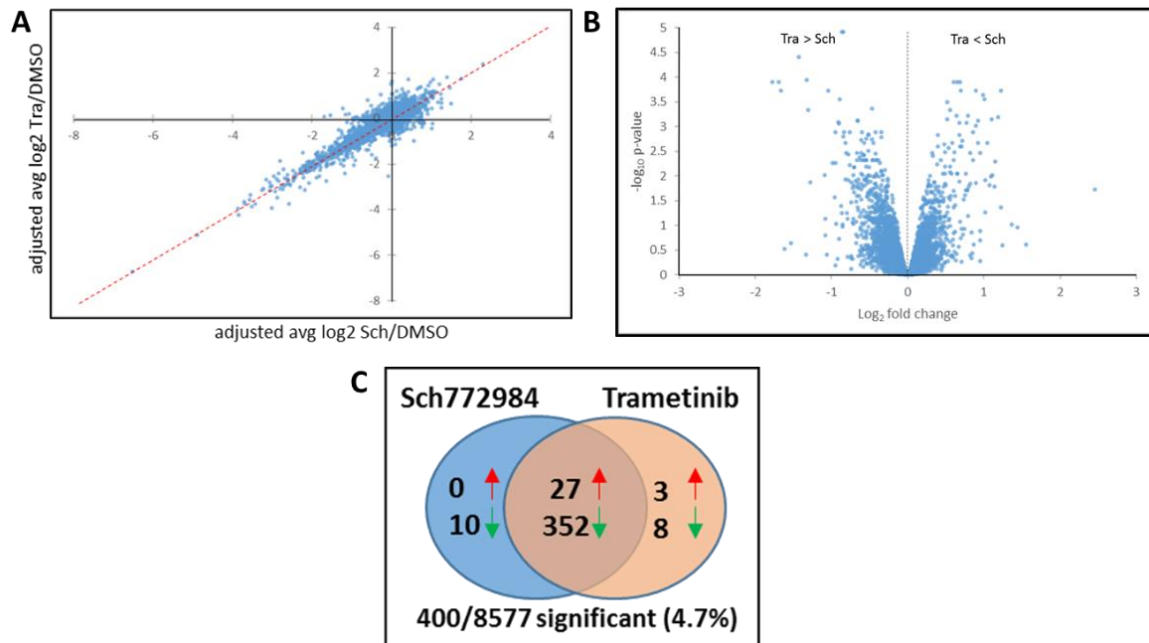


Figure 2.3: SILAC labeled phosphoproteomics comparison of trametinib and SCH772984. A, Log₂-transformed plot showing 8,577 phosphosites changing reproducibly in at least two replicates, in response to drug. B, Volcano plot showing confidence (adjusted p-value) vs fold change in response to SCH772984 or trametinib. Significant changes for phosphosites with $|\log_2(\text{combined ratio})| \geq 0.84$, and adjusted p-value >0.05 . C, Counts of significantly altered phosphosites with $|\log_2(\text{combined ratio})| \geq 0.84$, and adjusted p-value >0.05 .

As expected, the regulatory phosphorylation sites on ERK1 and ERK2, which are the primary substrates of MKK1/2, were among those most significantly inhibited by trametinib. The same sites were also inhibited by SCH772984, reflecting the ability of this molecule to induce disorder in the activation loop of ERK1/2 and interfere with its phosphorylation by MKK1/2 (Chaikuad et al., 2014). We found that the majority of phosphosites responsive to trametinib were similarly responsive to SCH772984 (Fig. 2.3A,C), indicating their regulation downstream of ERK1/2. In contrast, only 11 phosphosites responded to trametinib but not SCH772984, of which 8 decreased and 3 increased with drug (Fig. 2.3C, Table 2.2). The strongest effects unique to trametinib were seen in the regulatory phosphorylation sites in MKK1 and MKK2 (Table 2.2,

gene names MAP2K1, MAP2K2), reflecting interference of the drug-bound MKK1/2 phosphorylation by BRAF V600E/K (Gilmartin et al., 2011). Likewise, only 10 phosphosites responded to SCH772984 but not trametinib, all inhibited by drug (Fig. 2.3C, Table 2.2).

Table 2.2. Comparison of phosphosites uniquely responsive to trametinib or SCH772984. ^a log₂ values of quantified ratios in individual SILAC replicates. ^b Empirical Bayes-generated log₂(combined ratio) and adjusted p-value. [±] Phosphosites above the double line are significantly decreased, and below the double line are significantly increased, in response to drug.

Unique phosphosite changes in response to SCH772984

Uniprot ID	Gene	Position	9 aa window	SCH772984/DMSO ^a			Trametinib/DMSO ^a			SCH/TRA ^b	
				Exp 1	Exp 2	Exp 3	Exp 1	Exp 2	Exp 3	Combined	adj p-value
Q9BXS5	AP1M1	223	LFDNTGRGK		-1.598	-1.815		0.214	-0.002	-1.777	<0.001
Q03252	LMNB2	419	SRATSSSSG	-1.256	-0.981	-1.235	0.376	0.107	0.014	-1.324	<0.001
Q8IXT5	RBM12B	562	FRHSSEDFR	-0.886	-0.957	-0.794	0.346	0.008	-0.194	-0.910	0.001
P38159	RBMX	88	ATKPSFESG	-1.045	-0.973	-0.850	0.044	-0.329	0.114	-0.890	<0.001
Q9NWH9	SLTM	550	KKRISSKSP		-1.094	-0.799		-0.242	0.212	-0.987	0.005
Q9NWH9	SLTM	553	ISSKSPGHM		-1.094	-0.733		-0.242	0.103	-0.945	0.005
Q8IYB3	SRRM1	234	VKEPSVQEA		-0.829	-0.923		0.008	0.075	-0.945	0.001
Q8N1F8	STK11IP	481	APRPSPPQE	-1.297	-0.963		0.579	-0.081		-1.273	0.013
Q8NI27	THOC2	1285	KKEKTPATT	-2.041	-1.231	-1.442	0.192	0.219	0.086	-1.688	<0.001
Q9H3N1	TMX1	270	IRQRSLGPS	-1.447	-1.396	-0.855	0.634	0.424	0.308	-1.662	<0.001

Unique phosphosite changes in response to Trametinib

Uniprot ID	Gene	Position	9 aa window	SCH772984/DMSO ^a			Trametinib/DMSO ^a			SCH/TRA ^b	
				Exp 1	Exp 2	Exp 3	Exp 1	Exp 2	Exp 3	Combined	adj p-value
Q99704	DOK1	269	LRADSHEGE	0.057	-0.223	0.146	-0.849	-1.540	-1.176	1.186	0.001
Q68DA7	FMN1	243	DIPKTPDTD	-0.198	-0.730	-0.606	-1.285	-1.522	-1.933	1.099	0.001
P36507	MAP2K2; MAP2K1	226; 222	SMANSFVGT	-0.334	0.169		-3.471	-1.631		2.451	0.019
Q16539	MAPK14	180	DDEMTGYVA	-0.028	0.080	0.377	-0.958	-1.135	-1.413	1.223	<0.001
Q16539	MAPK14	182	EMTGYVATR	0.004	0.103	0.202	-0.850	-1.183	-0.728	1.012	<0.001
Q86UE4	MTDH	298	SSQISAGEE	-0.095	-0.130	0.117	-0.826	-1.093	-1.042	0.985	<0.001
Q15154	PCM1	93	MSQMSVPEQ	0.000	-0.176	0.750	-0.533	-1.136	-0.958	1.074	0.015
Q5JSZ5	PRRC2B	480	FRQQSIEDK		-0.020	-0.080		-0.775	-1.196	0.947	0.003
Q8TDZ2	MICAL1	1057	ERRLELAL		0.036	-0.177		0.967	1.349	-1.089	0.010
Q9BXB5	OSBPL10	30	SAGSSPSCS	0.416	0.018	0.348	1.494	1.238	1.191	-1.040	<0.001
Q8IY26	PPAPDC2	70	HRRGSFPLA	0.749	0.316	0.122	1.741	1.621	1.852	-1.304	<0.001

I also examined non-TiO₂-enriched proteolytic digests by 2D LC-MS/MS, in order to assess responses to drug at the protein level. Few significant changes were seen in protein abundances after 2 h of drug treatment, and none accounted for any of the phosphorylation sites that changed significantly in response to trametinib or SCH772984. Overall, the results show strong overlap in phosphorylation sites which respond to MKK1/2 and ERK1/2 inhibitors at the level of posttranslational modifications rather than protein synthesis or degradation. Such behavior is similar to our lab's previous phosphoproteomics comparison of the BRAF V600E/K inhibitor, vemurafenib, and the MKK1/2 inhibitor, selumetinib, and reveals linearity in signaling through the MAPK pathway downstream of oncogenic BRAF V600E/K (Stuart et al., 2015). Examples of targets shared by both inhibitors included known ERK1/2 substrates, neuroblast differentiation-associated protein Thr5824 (AHNAK), which has 7 sites significantly decreased and 2 sites significantly increased in response to inhibitor, and cortactin (CTTN), where Ser405 and Ser418, which are known regulatory sites controlling protein degradation and ubiquitination were significantly decreased by inhibitor.

Among the targets that responded only to trametinib were the regulatory phosphorylation sites, T180 and Y182, which control the activity of p38 α MAPK (gene name MAPK14) (Table 2.2). Together with MKK1/2, these were the only phosphorylation sites on protein kinases that differentially responded to only one and not both drugs (Table 2.2). Phosphorylation of both T180 and Y182 in p38 α was decreased by ~2-fold with trametinib [$\log_2(\text{trametinib}/\text{DMSO}) \approx -1.0$], but by less than 8% with SCH772984 [$\log_2(\text{SCH772984}/\text{DMSO}) < +0.1$]. There are four isoforms of p38 MAPKs (α , β , γ , δ) with p38 α MAPK being the most characterized and most consistently expressed across cell types (Cuenda & Rousseau, 2007). RNA-seq analysis showed that the alpha isoform of p38 is the most highly expressed in WM239a cells (Zarubin, T. & Han,

2005, data not shown), and was the only isoform observed in our proteomics dataset. The results suggest that p38 α MAPK is inhibited by trametinib.

In order to examine if inhibition of p38 α phosphorylation is common to other MKK1/2 inhibitors, we compared our trametinib dataset to a previous SILAC dataset examining phosphoproteomics responses to the MKK1/2 inhibitor, selumetinib (AZD6244) (Stuart et al., 2015). In total, 6,495 reproducible phosphosites were quantified in both experiments (Fig. 2.4A,B).

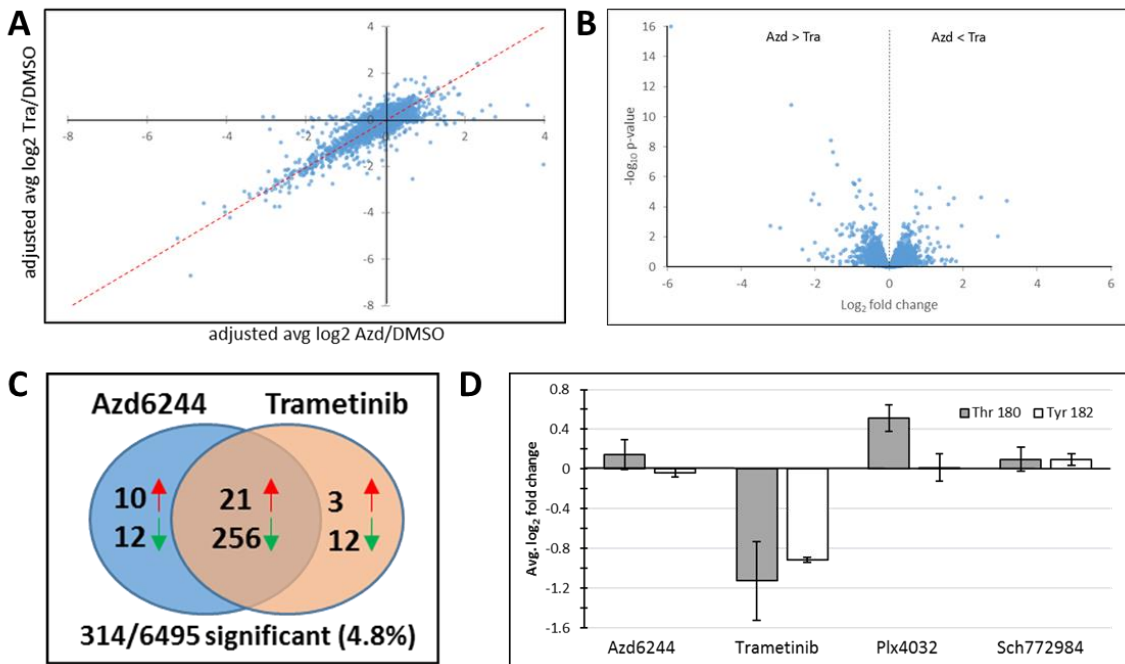


Figure 2.4: SILAC labeled phosphoproteomics comparison of trametinib and selumetinib (AZD6244). A, WM239a cells were treated 2 h with 10 μ M drug, and phosphosite responses were examined in a log₂ transformed plot. The results compared 6,495 phosphosites reproducibly quantified in at least two replicates. B, Volcano plot showing confidence (adjusted p-value) vs fold change in response to trametinib or selumetinib (AZD6244). Significant changes with $|\log_2(\text{combined ratio})| \geq 0.84$, and adjusted p-value >0.05 . C, Counts with significant changes in $|\log_2(\text{combined ratio})| \geq 0.84$, and adjusted p-value >0.05 . D, Log₂(combined ratios) of canonical activation sites on p38 α MAPK, comparing effects of BRAF V600E/K, MKK1/2, and ERK1/2 inhibitors.

Of those phosphorylation sites that could be quantified in each of the two datasets, strong overlap was observed in those responsive to both trametinib and selumetinib (Fig. 2.4A,C). Of these, 256 were significantly inhibited in response to both inhibitors while 12 were uniquely inhibited by trametinib but not selumetinib, and 12 were uniquely inhibited by selumetinib but not trametinib (Fig 2.4C, Table 2.3). Among the phosphosites inhibited by trametinib but not selumetinib, Ser269 on docking protein 1 (DOK1) and Ser298 on metadherin (MTDH) both appear to be novel off-targets of trametinib. In a phosphoproteomics SILAC screen of HeLa cells stimulated with EGF with or without MKK1/2 inhibitor, U0126, both phosphosites were elevated rather than inhibited by U0126. They also detected no change in T180 and Y182 on p38 α MAPK, in response to U0126 (Pan et al., 2009). In the present study, neither T180 nor Y182 in p38 α MAPK changed significantly in response to selumetinib (Fig. 2.4D) and our lab's previous dataset also showed no effect at these two sites, in response to the BRAF V600E/K inhibitor, vemurafenib (Stuart et al., 2015). Thus, the ability of MKK1/2 inhibitor to inhibit p38 α MAPK phosphorylation appears to be specific for trametinib.

Table 2.3. Comparison of phosphosites that change uniquely in response to trametinib or selumetinib (AZD6244). ^a log₂ (ratio) values measured individually in three replicate SILAC experiments. ^b Empirical Bayes-generated log₂(combined ratio) and adjusted p-value. ^c Phosphosites above the double line were significantly decreased, and below the double line were significantly increased, in response to drug.

Unique phosphosite changes in response to Trametinib

Uniprot ID	Gene	Position	9 aa window	Trametinib/DMSO ^a			AZD6244/DMSO ^a			TRA/AZD ^b	
				Exp 1	Exp 2	Exp 3	Exp 1	Exp 2	Exp 3	Combined	adj p-value
P35611	ADD1	12	AVVTSPPT		-0.988	-0.920	-0.473	-0.284	0.559	-0.889	0.037
Q96RKO	CIC	1397	KRKNSTDLD	-2.094	-1.896	-1.788	4.001	3.876	4.094	-5.903	<0.001
Q99704	DOK1	269	LRADSHEGE	-0.849	-1.540	-1.176	0.267	-0.170	-0.424	-1.063	0.001
Q16828	DUSP6	178	SDSSSDIES	-1.276	-1.235	-1.205	0.276	0.381	0.122	-1.581	<0.001
P42566	EPS15	796	NKLDSPDPF	-1.322	-1.230	-1.495	-0.432	-0.441	-0.325	-0.966	<0.001
P05412	JUN	62	SDLLTSPDV	-1.853	-1.770		-0.848	-0.427	-0.402	-1.269	0.007
P17535	JUN; JUND	73; 100	LKLASPELE	-1.755	-1.581	-1.687	-0.836	-0.650	-0.626	-0.936	<0.001
P36507	MAP2K2; MAP2K1	226; 222	SMANSFVGT	-3.471	-1.631		0.578	0.802	0.702	-3.219	0.002
Q16539	MAPK14	180	DDEMTGYVA	-0.958	-1.135	-1.413		0.006	0.304	-1.269	0.002
Q16539	MAPK14	182	EMTGIVATR	-0.850	-1.183	-0.728	-0.091	0.043	-0.063	-0.877	<0.001
Q86UE4	MTDH	298	SSQISAGEE	-0.826	-1.093	-1.042		-0.048	-0.239	-0.870	0.003
P04920	SLC4A2	144	LTQSPVST	-1.251	-0.861	-0.793	1.583		0.663	-2.101	<0.001
Q9BWH2	FUNDC2	151	KIRKSNQIP	1.313	0.975	0.791	0.099	-0.051	0.043	1.024	0.002
Q8IY26	PPAPDC2	70	HRRGSFPLA	1.741	1.621	1.852	-0.004	0.850	1.102	1.064	0.011
O14828	SCAMP3	32	QHRPSRQYA		1.010	0.853	-0.268	-0.038	-0.805	1.305	0.003

Unique phosphosite changes in response to AZD6244

Uniprot ID	Gene	Position	9 aa window	Trametinib/DMSO ^a			AZD6244/DMSO ^a			TRA/AZD ^b	
				Exp 1	Exp 2	Exp 3	Exp 1	Exp 2	Exp 3	Combined	adj p-value
Q09666	AHNAK	210	IRLPSSGSGA	-0.244	-0.522	-0.475	-1.422	-1.316	-1.219	0.878	<0.001
Q68DQ2	CRYBG3	1280	KPCVSPTVG	-0.644	-0.538		-2.396		-2.001	1.597	<0.001
P21333	FLNA	1084	GSAGSPARF	0.066	-0.154	0.325	-1.980	-1.395		1.759	<0.001
Q4GQJ3	LARP7	299	RKRSSSEDA	0.362	-1.093	0.183	-0.792	-1.783	-1.872	1.312	0.022
P10636	MAPT	579	SKIGSTENL		0.146	0.229	-3.982	-1.655		2.942	0.009
P30414	NKTR	1146	VEETSPLGN	0.085	0.129	-0.116	-1.383	-0.956	-1.579	1.358	<0.001
Q16875	PFKFB3	461	MRRNSVTPL	-0.316	-0.353	-0.750	-1.120		-3.068	1.604	0.047
Q14160	SCRIB	1223	NSLESISSI	-0.471	-0.177	-0.569	-2.747	-3.635	-2.355	2.480	<0.001
Q9ULF5	SLC39A10	540	TEESTIGRK	0.374		-0.134		-2.253	-1.517	1.964	0.002
Q8IYB3	SRRM1	756	SVSGSPEPA	0.194	0.127	0.188	-0.560	-0.420	-2.380	1.376	0.043
Q8WVM7	STAG1	1062	DDRMSVNSG	-0.058	0.316		-3.489	-2.651		3.191	<0.001
Q9BRZ2	TRIM56	471	LKSISREPS	0.342	0.325	0.221		-0.709	-0.954	1.093	<0.001
Q09666	AHNAK	5782	HRSNSFSDE	0.171	0.580	0.487	1.378	1.410	1.321	-0.939	<0.001
Q96RKO	CIC	1409	EDPTSPKPK	-0.685	2.195	0.755	2.993	3.729	4.060	-2.946	0.003
Q99543	DNAJC2	49	NASASFQEL	-0.216	-0.154	-0.303	1.148	1.211	1.499	-1.529	<0.001
O60841	EIF5B	186	SSGESGDES		0.180	0.128	1.914	1.577	1.113	-1.327	0.007
O60841	EIF5B	182	SRINSSGES	-0.240		-0.064	2.157	1.587		-1.892	<0.001
Q12789	GTF3C1	1068	TDQGSDEEG	-0.312	0.682	0.282	1.218	1.012	1.710	-1.009	0.003
Q9Y4B5	MTCL1	1417	KEDVTPPLS	0.544		0.760	1.897	2.224	3.836	-2.009	0.022
O43765	SGTA	303	IRSRTPSAS	0.059	-0.595	0.254	0.680	1.046	1.028	-1.000	0.002
O95359	TACC2	2317	NTPASPPRS	1.025	-0.054	0.218	2.644	2.438	2.242	-2.037	<0.001
O60343	TBC1D4	591	GSVDSFERS	0.224	0.237	-0.089	2.618	3.050	2.694	-2.639	<0.001

6495 phosphosites identified in 2 or 3 replicates

Significance	TRA/DMSO	% Total	AZD/DMSO	% Total	TRA/AZD	% Total
Decreased	335	5.2	319	4.9	64	1.0
Increased	51	0.8	64	1.0	47	0.7

Conceivably, phosphosites that were inhibited by trametinib but not selumetinib might reflect the trametinib-specific inhibition of p38 α MAPK. This was examined by searching literature sources for known substrates of p38 signaling (Cuadrado & Nebreda, 2010; Cuenda & Rousseau, 2007; Trempolec, Dave-Coll, & Nebreda, 2013). Of 103 proteins found to be substrates of p38 MAPK, 32 were represented in both trametinib and selumetinib datasets. However, only one protein, c-Jun, showed a phosphorylation site that was inhibited more by trametinib than selumetinib. c-Jun is also known substrate of ERK1/2 as well as JNK, and indeed, a partial inhibition by selumetinib could be observed. Therefore, only p38 α MAPK-Thr180 and Tyr182 were useful as reporters of the selective effect of trametinib on this kinase.

We next carried out biochemical analyses to ask if p38 α MAPK phosphorylation is indeed inhibited by trametinib. Western blots probed with anti-phospho-p38 antibodies showed nearly undetectable basal levels of phosphorylated p38 in whole cell lysates (not shown). These antibodies also could not distinguish different isoforms of p38 MAPK. Therefore, isoform-specific antibodies were used to concentrate p38 α MAPK by immunoprecipitation from cell lysates, followed by Western blotting with the anti-phospho-p38 antibody. The results showed significant inhibition of basal Thr180 and Tyr182 phosphorylation in p38 α MAPK, after treating cells for 2 h with trametinib, but not DMSO or SCH772984 (Fig. 2.5A).

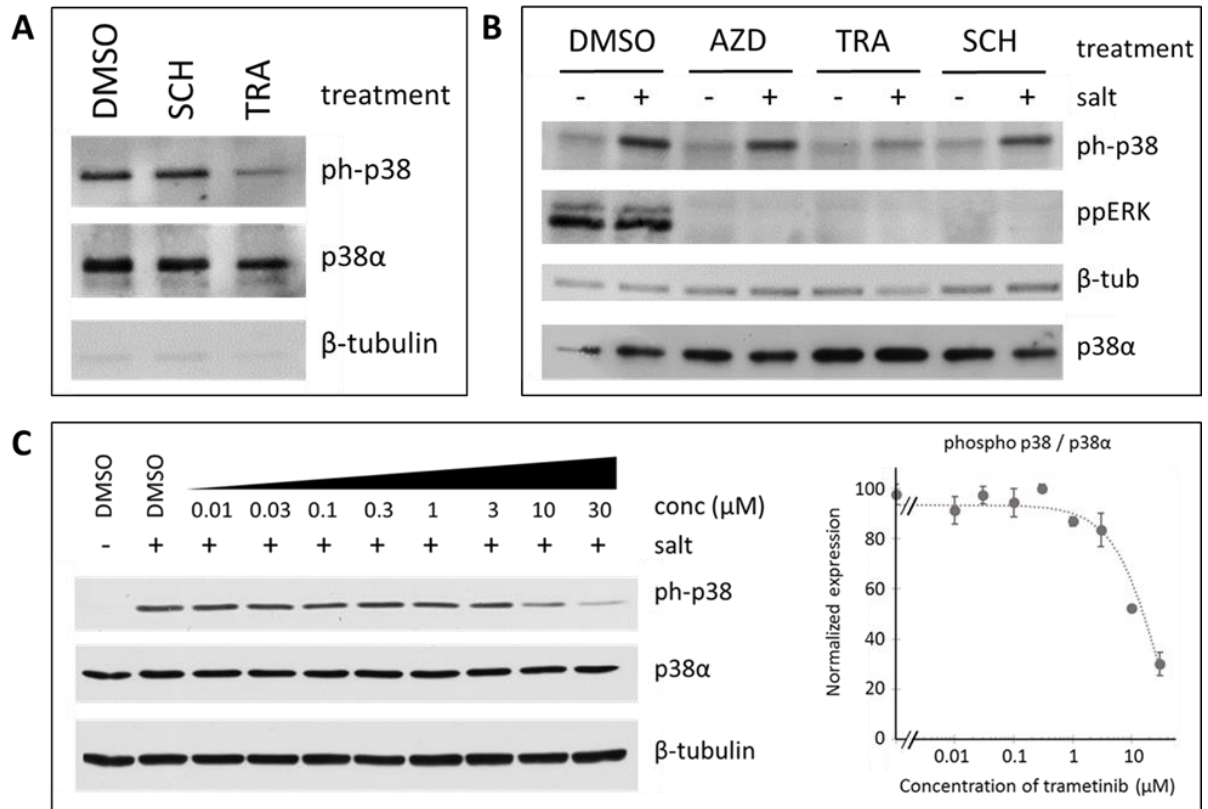


Figure 2.5. Analysis of phosphorylated p38 MAPK in WM239a cells by Western blotting. A, Immunoprecipitation of p38α MAPK following 2 h treatment with DMSO or 10 μM SCH772984 (SCH) or 10 μM trametinib (TRA), followed by Western blotting of phosphorylated p38 MAPK. B, Osmotic stress stimulates p38 phosphorylation. Cells were treated for 30 min with DMSO or 10 μM drug (selumetinib=AZD), then stimulated without or with osmotic stress for 2 h, by raising osmolality of media from 300 mOsm to 500 mOsm. Cells were harvested and lysates examined by Western blotting for phosphorylated p38 MAPK. C, Biological triplicate dose response of trametinib at concentrations 0.01-30 μM (left to right). Cells were treated for 30 min with DMSO or 10 μM drug, then stimulated without or with osmotic stress for 2 h. Cells were harvested and lysates examined by Western blotting for phosphorylated p38 MAPK. Quantification of ph-p38 normalized to p38α using ImageJ quantification on biological triplicate experiments.

Trametinib inhibited the phospho-p38 MAPK signal by approximately 50%, comparable to the estimated decrease quantified by phosphoproteomics (Fig. 2.4D). In order to examine the effect of different MKK1/2 and ERK1/2 inhibitors on p38 α phosphorylation following stress pathway activation, we pretreated cells with selumetinib, trametinib, and SCH772984 for 2 h, and then added NaCl+KCl to induce hyperosmotic stress which has been shown to activate p38 α (Mavrogonatou & Kletsas, 2009, 2012). Salt-stimulation induced a substantial phosphorylated p38 α signal in Western blots of cell lysates, in a manner that was inhibited by trametinib (~50%) but not selumetinib or SCH772984 (Fig. 2.5B). We also carried out a dose response experiment, and observed substantial inhibition of salt-induced p38 phosphorylation at concentrations above 10 μ M trametinib, with estimated IC₅₀ of 10 μ M (Fig. 2.5C). Thus, complementary biochemical strategies using Western blotting and phosphoproteomics confirm that trametinib inhibits p38 α MAPK phosphorylation. Given that the response is unique to trametinib and not observed with SCH772984 or selumetinib, the results suggest a bona-fide off-target effect of trametinib as an inhibitor of p38 α phosphorylation, occurring at ~10 μ M concentrations commonly used in preclinical studies (Yamaguchi et al., 2011) and ~300-fold higher than the maximal plasma concentration observed clinically (36 nM) (Infante et al., 2012).

The specificity of trametinib for MKK1/2 suggested that it might also target MKK3 and/or MKK6, which following hyperosmotic stress are known to phosphorylate and activate p38 α (Zarubin, T. & Han, 2005) (Fig. 2.5B). However, previous reports have shown weak or variable inhibition of MKK3 or MKK6 activity by trametinib. An *in vitro* ELISA assay panel from Yamaguchi et al. 2011, on 99 kinases showed the activity of MKK6 decreased 30% with 10 μ M trametinib, while the target kinase MKK1 decreased 72%. Very few other kinase activity levels changed significantly, indicating high specificity of trametinib including: ERK1 (-14%),

ERK2 (+8%), JNK1 (+4%), JNK2 (-3%), JNK3 (-24%), p38 α (-16%), p38 β (+4%), p38 γ (-3%), p38 δ (+9%). A second study by Uitdehaag et al. 2014 measured the changes in activity of over 300 kinases in response to 1 μ M trametinib using *in vitro* mobility shift assays and reports a 21% increase in MKK6, a 3% decrease in MKK3, a 99% decrease in MKK1, and a 97% decrease in MKK2 activities. Additional kinases measured include: ERK1 (+2%), ERK2 (+4%), JNK1 (+5%), JNK2 (+5%), JNK3 (+2%), p38 α (+4%), p38 β (-2%), p38 γ (-1%), p38 δ (+3%).

Therefore, we tested MKK6 and MKK3b using direct kinase assays of each Flag-tagged kinase expressed in WM239a cells. Flag-MKK6 was expressed as wild-type (wt), constitutively active mutant (S207E/T211E), and catalytically inactive mutant (K82A) forms, each immunopurified from cell lysates using immobilized anti-Flag antibody. Kinases were then preincubated with Mg²⁺-ATP and DMSO, 10 μ M trametinib, or 10 μ M selumetinib, followed by addition of purified unphosphorylated p38 α to initiate *in vitro* kinase assays (Fig. 2.6A). Trametinib inhibited both wt and constitutively active MKK6, leading to significant reduction of the initial rate of p38 α phosphorylation. In contrast, selumetinib had a minimal effect on MKK6 activity. As expected, the MKK6-S207E/T211E mutant exhibited much higher activity than MKK6-wt towards p38 α , although it appeared to be comparably inhibited by trametinib (Fig. 2.6A) (Raingeaud et al., 1996). Similar approaches were used to examine the effects of each drug on a constitutively activated isoform of MKK3, MKK3b-S218E/T222E, which contains a N-terminal recognition domain and has higher specific activity towards p38 α than MKK3-S189E/T193E (Enslin et al., 2000; Jiahui Han, Wang, Jiang, Ulevitch, & Lin, 1997). *In vitro*, MKK3b showed activity towards p38 α MAPK that was too low to observe inhibition by trametinib or selumetinib (Fig. 2.6B).

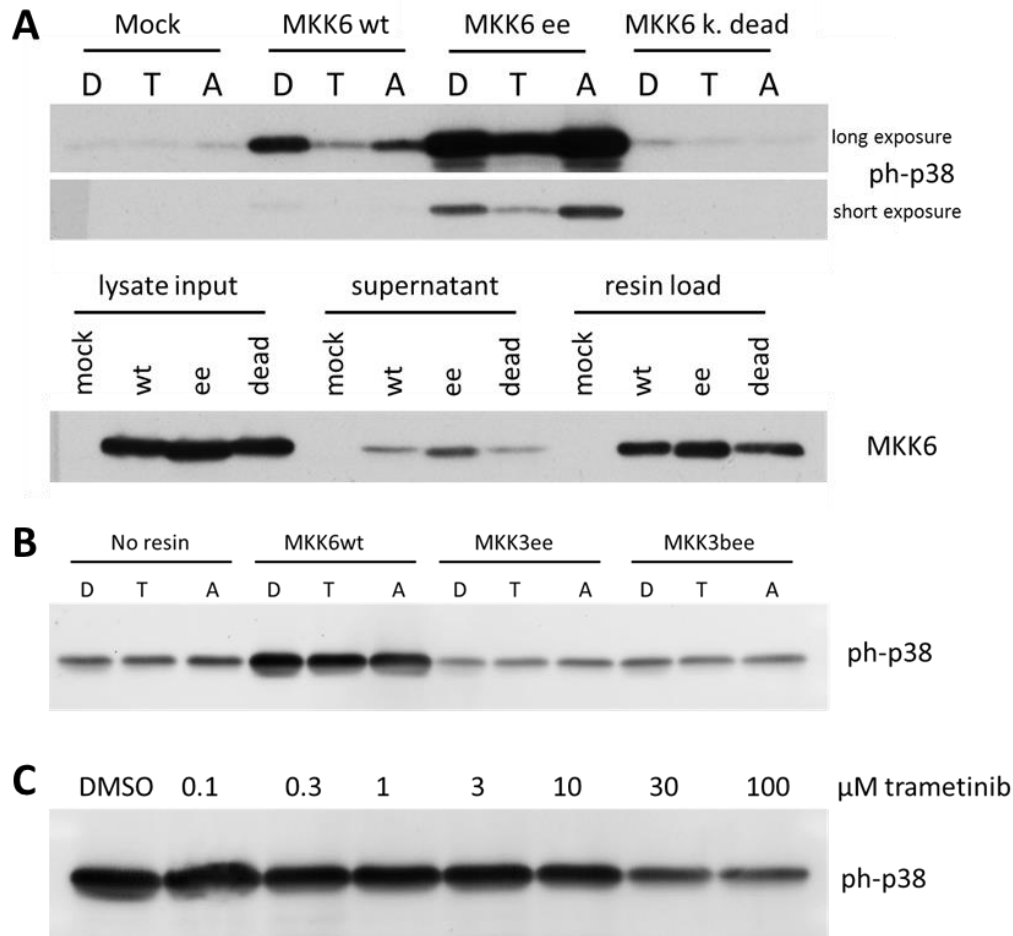


Figure 2.6. *In vitro* kinase assay measurement of MKK6, MKK3 and MKK3b activity. A, Flag-MKK6 was expressed in WM239a cells as wild type (wt), constitutively active (ee), or catalytically inactive (k.dead) mutants, then immunoprecipitated from lysates with immobilized anti-Flag antibody, and incubated for 15 min with DMSO (D), trametinib (T) and selumetinib (AZD6244) (A). *In vitro* kinase activity was measured by phosphorylation of recombinant unphosphorylated p38 α MAPK. As expected, the activity of MKK6ee exceeded that of MKK6wt, but only trametinib inhibited MKK6 activity. B, *In vitro* kinase assays of constitutively active mutants of MKK6 (MKK6ee), MKK3 (MKK3ee) and MKK3b (MKK3bee), measuring phosphorylation of recombinant p38 α by Western blotting with anti-phospho-p38 MAPK. The results show high activity of MKK6ee towards p38 α substrate in a 10 min kinase reaction, but no activity of MKK3ee or MKK3b33 in 10 min reactions, in assays containing DMSO (D). Little effect of trametinib (T, 10 μ M) or selumetinib (AZD6244) (A, 10 μ M), is also seen. Thus, trametinib shows variable reproducibility with respect to MKK6ee inhibition. C, Kinase assays of MKK6ee activity measured by phosphorylation of p38 α MAPK for 2 min, in the presence of varying concentrations of trametinib. The *in vitro* kinase assay reveals an apparent IC₅₀ for trametinib of \geq 10 μ M.

We then measured the dose response for *in vitro* inhibition of MKK6-S207E/T211E by varying concentrations of trametinib. Unexpectedly, the estimated IC₅₀ was greater than 10 μM, for trametinib inhibition of MKK6-S207E/T211E using p38α MAPK as the substrate (Fig. 2.6C). This was surprising, because the sensitivity of MKK6 inhibition *in vitro* was much lower than the IC₅₀ for inhibiting phospho-p38 MAPK in cells (Fig. 2.5C). In order to verify this result, the Scientific Select Screen service contracted with Thermo Corp. was used to generate a 10-point dose response curve of MKK6 inhibition by trametinib (0-30 μM), assayed by coupling its phosphorylation of p38γ MAPK to a proprietary fluorophore-conjugated p38 MAPK peptide substrate (Z'-LYTE) which undergoes changes in Förster resonance energy transfer (FRET) fluorescence signal upon phosphorylation. The results showed that similarly, IC₅₀ > 10 μM for MKK6 inhibition (Fig. 2.7A), comparable to my *in vitro* kinase assay measurements of MKK6 (Fig. 2.6C).

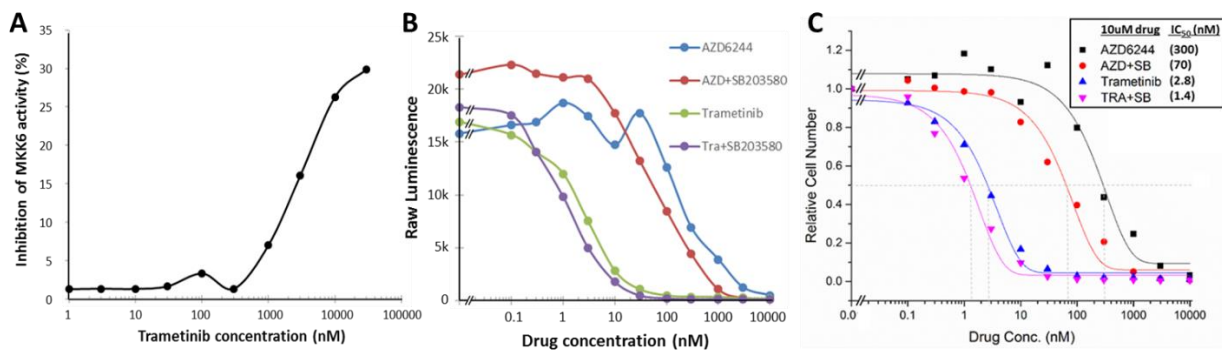


Figure 2.7. Effects of MKK1/2 inhibitors on p38 MAPK pathway effectors and signaling. A, Dose response of MKK6 activity measured by phosphorylation of p38γ MAPK, using FRET-based fluorescence measurements of p38γ MAPK activity using the Thermo SelectScreen assay. The assay shows 30% inhibition at the highest concentration of trametinib (10 μM), indicating IC₅₀ consistent with measurements in 2.6C. C, CellTiter Glo raw intensity values used for C show a slight increase in cell viability with SB203580 alone C, CellTiter Glo viability assay shows that the p38 inhibitor, SB203580 (10 μM) shifts the IC₅₀ for inhibition of cell viability with selumetinib (AZD6244) to 5-fold lower concentrations, but shifts the IC₅₀ with trametinib by less than 2-fold.

Finally, we asked if the ability of trametinib to inhibit p38 α might contribute to its effects on viability or growth of melanoma cells in a manner distinct from MKK1/2 inhibition. To address this, we added the p38 α / β inhibitor, SB203580, to WM239a cells treated with varying concentrations of trametinib or selumetinib, measuring cell viability after 72 h. SB203580 alone had no inhibitory effect on cell viability, and shows a slight increase in cell viability (Fig. 2.7B). However, in combination with selumetinib, it shifted the dose response curve, reducing the IC₅₀ for selumetinib by ~5-fold, from 300 nM in the absence of SB203580 to 60 nM in its presence (Fig. 2.7C). In contrast, SB203580 had minimal effect in combination with trametinib, shifting the IC₅₀ for trametinib by less than 2-fold (Fig. 2.7C). The results are consistent with a model in which inhibiting p38 MAPK augments the ability of the MKK1/2 inhibitor, selumetinib, to suppress cell viability, but has little effect on trametinib due to the latter's off-target interference with p38 α signaling. The results suggested that the off-target effect on MKK6, unique to trametinib, might contribute favorably to the properties of this anti-cancer drug.

Taken together, trametinib inhibits MKK6 *in vitro*, but in a concentration range that may be inconsistent with its ability to inhibit p38 α MAPK in cells. The reason for this inconsistency is currently unknown. On one hand, it may reflect differences between the ability of trametinib to inhibit direct kinase assays *in vitro*, vs its effects on salt-induced pathway activation in cells. For example, the IC₅₀ for p38 MAPK inhibition in cells may be abnormally low, if the compound is sequestered in cells to concentrations exceeding those added to the growth media. On the other hand, MKK3 and MKK6 may not be the relevant target of trametinib in cells, and the compound may target an enzyme located upstream of MKK3 and MKK6 to inhibit p38 MAPK in cells. For example, MEKK3 is a kinase activated by hyperosmotic stress, which functions immediately upstream to directly phosphorylate MKK3 and MKK6. WNK4 is another kinase which can be

directly activated by hyperosmotic stress and serves as an upstream activator of MEKK3 through mechanisms that are not completely elucidated. Further studies are needed to determine if other cellular target(s) of trametinib more fully explain its effects on inhibiting p38 α MAPK. Such studies could conceivably reveal new effectors of salt stress pathway signaling, using the selective off-target response to trametinib as an assay for their identification.

Having identified an intriguing off-target effect specific to trametinib, we next investigated potentially differential responses between two high affinity ERK1/2 inhibitors, SCH772984 ($K_i = 0.12$ nM, (Rudolph et al., 2015)) and GDC0994 ($K_i = 1.1$ nM) (Robarge et al., 2014). To do this, we used a triple SILAC phosphoproteomics screen to compare phosphorylation responses to DMSO, SCH772984 and GDC0994. Triplicate experiments were performed using different combinations of heavy, medium and light isotopically-labeled media. In total, 6,893 class I phosphorylation sites were identified on 2,843 proteins, including 4,436 phosphosites quantified in at least two replicates (Fig. 2.8A-F, Table 2.4).

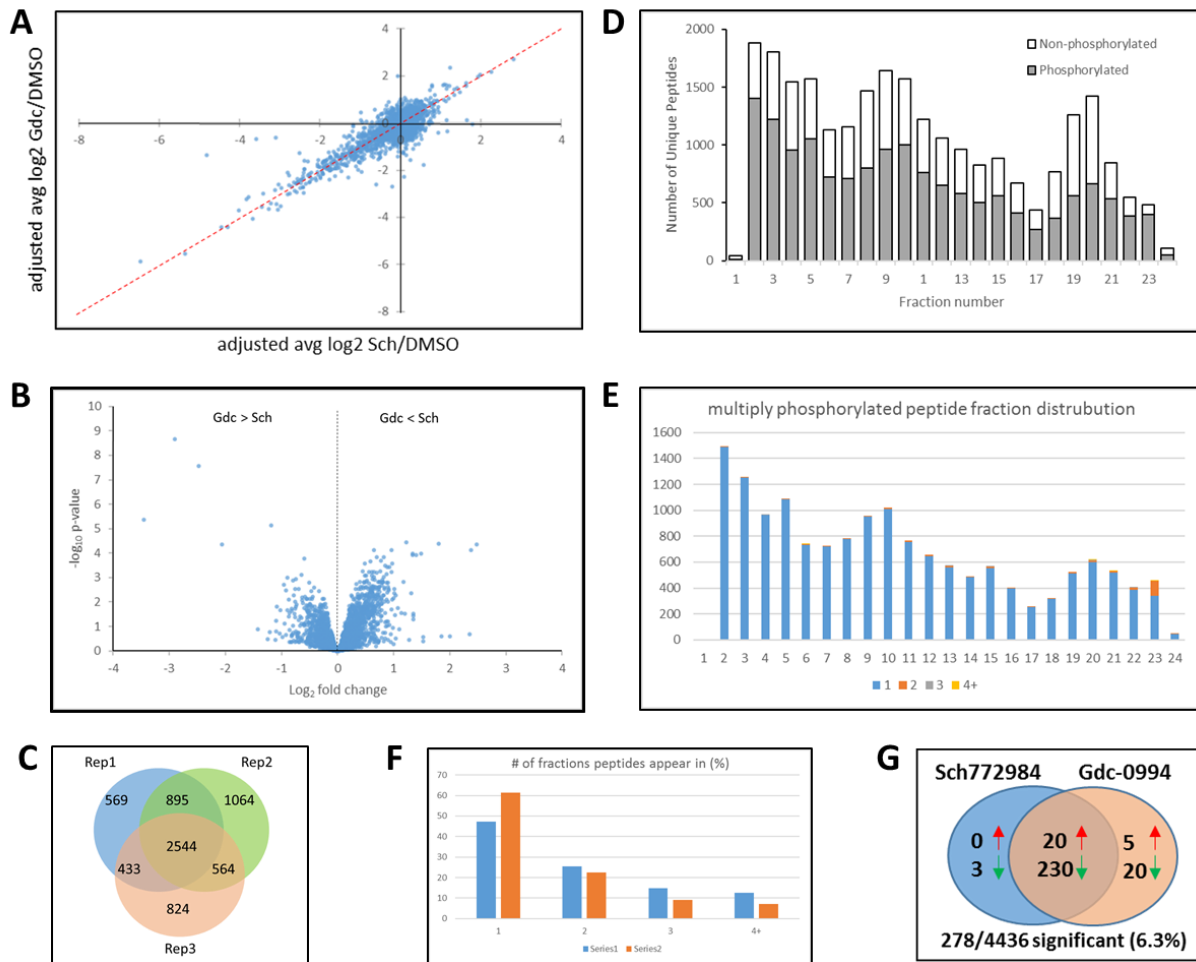


Figure 2.8: SILAC labeled phosphoproteomics comparison of SCH772984 and GDC0994. A, Log₂-transformed plot showing 4,436 phosphosites observed reproducibly in at least two replicates. Strong correlations were seen between phosphosites changing in response to SCH772984 and GDC0994. B, Volcano plot showing confidence (adjusted p-value) vs fold change in response to SCH772984 or GDC0994. C, Overlap among replicates in 6,893 phosphosites quantified across three replicate experiments. D, Numbers of unique phosphorylated and non-phosphorylated peptides identified in each ERLIC fraction among three replicates. E, Number of singly phosphorylated peptides (blue) and multiply phosphorylated peptides (red, grey, yellow) eluting in each ERLIC fraction identified among three replicates. F, Number of ERLIC fractions in which each phosphorylated or non-phosphorylated peptide appear, among three replicates. G, Counts of phosphosites with significant changes, where $|\log_2(\text{combined ratio})| \geq 0.84$, and adjusted p-value > 0.05 .

Table 2.4. Comparison of phosphosites uniquely responsive to SCH772984 and GDC0994. ^a Log₂(ratio) values from individual SILAC replicates. ^b Empirical Bayes-generated log₂(combined ratio) and adjusted p-value. ^c Phosphosites above the double line are significantly decreased, and below the double line are significantly increased, in response to drug.

Unique phosphosite changes in response to SCH772984

Uniprot ID	Gene	Position	9 aa window	SCH772984/DMSO ^a			GDC0994/DMSO ^a			SCH/GDC ^b	
				Exp 1	Exp 2	Exp 3	Exp 1	Exp 2	Exp 3	Combined	adj p-value
P28482	MAPK1	187	FLTEYVATR	-3.206	-3.112	-3.057	-0.659	-0.732	-0.413	-2.470	<0.001
P27361	MAPK3	204	FLTEYVATR	-3.527	-3.640	-3.519	-0.607	-0.835	-0.670	-2.902	<0.001
P38159	RBMX	88	ATKPSFESG	-1.385	-0.920		0.139	-0.336		-1.087	0.015

Unique phosphosite changes in response to GDC0994

Uniprot ID	Gene	Position	9 aa window	SCH772984/DMSO ^a			GDC0994/DMSO ^a			SCH/GDC ^b	
				Exp 1	Exp 2	Exp 3	Exp 1	Exp 2	Exp 3	Combined	adj p-value
Q09666	AHNAK	210	IRLPSGSGA	-0.799	0.048	-0.927	-2.054	-1.150	-1.415	1.002	0.007
Q09666	AHNAK	216	SGAASPTGS	-0.750	0.048	-0.840	-2.014	-1.150	-1.259	0.972	0.008
Q68DQ2	CRYBG3	2902	GGRDTPGAK	0.063		0.015	-1.219		-1.271	1.337	<0.001
Q16555	DPYSL2	509	EVSVTPKTV	-0.070	0.566	0.298	-1.729	-1.751	-1.235	1.804	<0.001
Q14195	DPYSL3	509	DLTTTPKGG	0.287	0.068	-0.026	-1.089	-1.138	-1.721	1.490	<0.001
Q04637	EIF4G1	1209	RKAASLTED	-0.373	-0.427	0.418	-2.905	-3.068	-2.325	2.482	<0.001
P19419	ELK1	196	PPSGSRSTS	-0.257	-0.271	-0.763	-1.317	-1.170	-1.212	0.922	<0.001
Q9H840	GEMIN7	3	MQTPVNI	-0.098	0.305	0.222	-1.164	-1.103	-1.010	1.230	<0.001
Q6Y7W6	GIGYF2	189	GGPTSVGRK		0.414	0.585		-1.225	-0.880	1.307	0.004
Q13098	GPS1	479	QGELTPANS	-0.070	0.265	-0.019	-0.795	-0.493	-2.517	1.353	0.029
P52272	HNRNPM	452	ERMGSPIER		0.076	0.116		-2.153	-2.448	2.384	<0.001
Q659C4	LARP1B	900	VPINSPRRN	0.342	0.292		-1.084	-1.063		1.403	<0.001
Q03252	LMNB2	17	ATPLSPTRL	-0.079	-0.063		-1.988	-0.806		1.349	0.037
Q96L50	LRR1	124	VSTLTPVKT	0.076	0.080		-0.965	-0.668		1.075	0.017
Q9Y608	LRRFIP2	320	TTPLSGNSS	0.385	0.310	0.105	-1.113	-1.175	-1.234	1.142	0.028
O14777	NDC80	69	GSRNSQLGI	-0.199	0.117		-0.680	-0.929		0.870	0.008
Q8NCF5	NFATC2IP	84	GPVASRDNS	0.270	0.137	-0.095	-0.693	-0.814	-1.053	0.961	<0.001
P06748	NPM1	254	KMQASIEKG	0.461	0.491	0.262	-1.010	-0.535	-0.922	1.342	<0.001
Q13131	PRKAA1	382	LVAETPRAR	-0.133	0.135		-1.198	-0.956		0.885	0.004
Q9NX01	TXNL4B	132	LIVQSPIDP	-0.118	0.098		-1.414	-1.123		1.171	0.001
Q09666	AHNAK	4564	VGIDTPDID		0.229	-0.203		0.747	1.266	-1.016	0.022
Q9UHR4	BAIAP2L1	261	TPQASPMIE	0.004	-0.110		1.083	0.733		-0.913	0.003
Q8WUZO	BCL7C	126	SRPVSPAGP	-0.240	-0.412	-0.371	1.074	0.898	0.851	-1.178	<0.001
Q6PKG0	LARP1	766	TIARSLPTT	-0.346	0.393	-0.273	1.641	2.357	2.029	-2.062	<0.001
P19532	TFE3	548	LRAASDLLL	-0.093	0.230		1.098	1.086		-0.959	0.002

Table 2.5. Comparison of phosphosites identified in each triple-labeled SILAC replicate comparing SCH772984 and GDC0994. Number of phosphosites quantified after removing reverse protein database hits and contaminants and expanding the phosphopeptide table to separate phosphosites identified in multiply phosphorylated peptides. Changes were considered significant when their empirical Bayes-generated $|\log_2(\text{combined ratio})| \geq 0.84$.

Experiment	Significance	SCH/DMSO % Total	GDC/DMSO % Total	SCH/GDC % Total
1 (4459 sites)	Decreased	366	8.2	428
	Increased	43	1.0	90
2 (5077 sites)	Decreased	316	6.2	368
	Increased	89	1.8	95
3 (4377 sites)	Decreased	305	7.0	325
	Increased	155	3.5	122
Avg (4436 sites)	Decreased	279	6.3	313
	Increased	34	0.8	52

Of these, 278 phosphosites were significantly responsive to ERK1/2 inhibitors, SCH772984 and GDC0994, the majority of which were inhibited by both compounds and also identified in the trametinib-SCH772984 SILAC experiment. These included known proteins known to be ERK1/2 substrates, such as RAF1, Ets2 repressor factor (ERF), and cortactin (CTTN) (Fig. 2.8G, Table 2.5). Three phosphosites decreased significantly only in response to SCH772984, and 20 phosphosites decreased only in response to GDC0994 (Fig. 2.8G, Table 2.4). Phosphorylation of the RBMX transcription factor was inhibited by SCH772984 and not GDC0994, and also inhibited by only SCH772984 in the trametinib-SCH772984 experiment (Table 2.2). The two remaining phosphorylation sites unique to SCH772984 were part of the canonical TEY activation loop motif on ERK1/2 (Tyr204 on ERK1 and Tyr187 on ERK2). This indicates that while both SCH772984 and GDC0994 inhibit ERK1/2 kinase activity, only SCH772984 also inhibits its phosphorylation by MKK1/2. This finding was validated by Western blotting of whole cell lysates from WM239a cells treated with MKK1/2 and ERK1/2

inhibitors using antibodies specific for the TEY activation motif (Fig. 2.9A). Although ERK1/2 inhibitors GDC0994 and Vertex-11e did not decrease levels of phosphorylated ERK1/2, both were able to reduce phosphorylation of p90RSK (RSK1), an important signaling kinase downstream of ERK1/2, and inhibition of ERK phosphorylation by SCH772984 has previously been shown (Morris et al., 2013). GDC0994 and Vertex-11e also increased levels of the apoptosis markers, BIM and cleaved PARP, after 48 h treatment with 10 μ M inhibitor. An apoptotic response to each inhibitor was confirmed using fluorescence based flow cytometry to quantify recombinant annexin V-FITC bound to apoptotic cells by the externalization of phosphatidylserine, and propidium iodide (PI) staining of cells with permeabilized plasma membranes (Fig. 2.9B). The results demonstrate similar levels of cell death in response to MKK1/2 inhibitor, selumetinib, and ERK1/2 inhibitor, SCH772984, at 48 h, although Vertex-11e is less effective.

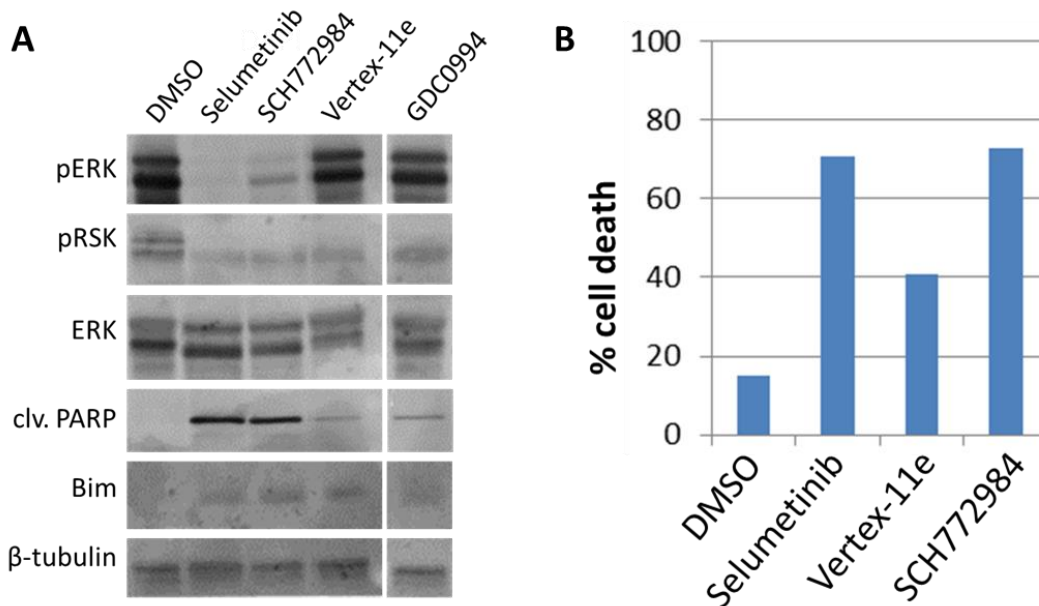


Figure 2.9: Apoptotic responses to MKK1/2 and ERK1/2 inhibitors in WM239a cells. A, Western blots of whole cell lysates harvested 48 h after treatment with 10 μ M of each inhibitor. B, Annexin V-PI flow cytometry assay (Thermo Scientific) measuring apoptosis and cell permeabilization by flow cytometry after 48 h treatment with 10 μ M of each inhibitor.

To explore whether the differences in phosphorylated TEY on ERK1/2 has an effect on other downstream kinase substrates, the Human Phospho-Kinase Array (R & D Systems) was used to simultaneously profile the relative levels of protein phosphorylation of 43 kinases and their substrates. Following 4 h treatment with 10 μ M selumetinib (AZD6244), Vertex-11e, or SCH772984, cell extracts were adsorbed onto membranes that were spotted with capture antibodies for each kinase phosphorylation site, and then incubated overnight. Processing and quantification was similar to a typical Western blotting procedure using a Typhoon fluorescence image scanner and ImageQuant software (GE Healthcare) (Fig. 2.10 A). The results agreed with the individual phospho-ERK1/2 and phospho-RSK Western blots in Fig. 2.9A and were grouped into categories based on response to inhibitor (Fig. 2.10B, Appendix I). As expected, phosphorylation of some protein kinases showed no response to MKK1/2 or ERK1/2 inhibitors (phospho-JNK1/2/3) while others were inhibited by all three inhibitors (phospho-p70 S6 Kinase, phospho-STAT3). The kinases that responded uniquely to certain inhibitors could be divided into those with phosphorylation sites that differed in their responses to MKK1/2 inhibitor, selumetinib (AZD6244), and ERK1/2 inhibitors, SCH772984 and Vertex-11e, and those with phosphorylation sites that responded specifically to Vertex-11e. Interestingly, several kinase phosphorylation sites were increased in response to Vertex-11e, including pTyr sites that suggest potential regulation of Tyrosine kinases and phosphatases. However, we lack certainty that the different responses to MKK1/2 and ERK1/2 inhibitors, and the increases in response to Vertex-11e, were necessarily reproducible between replicate Western blots.

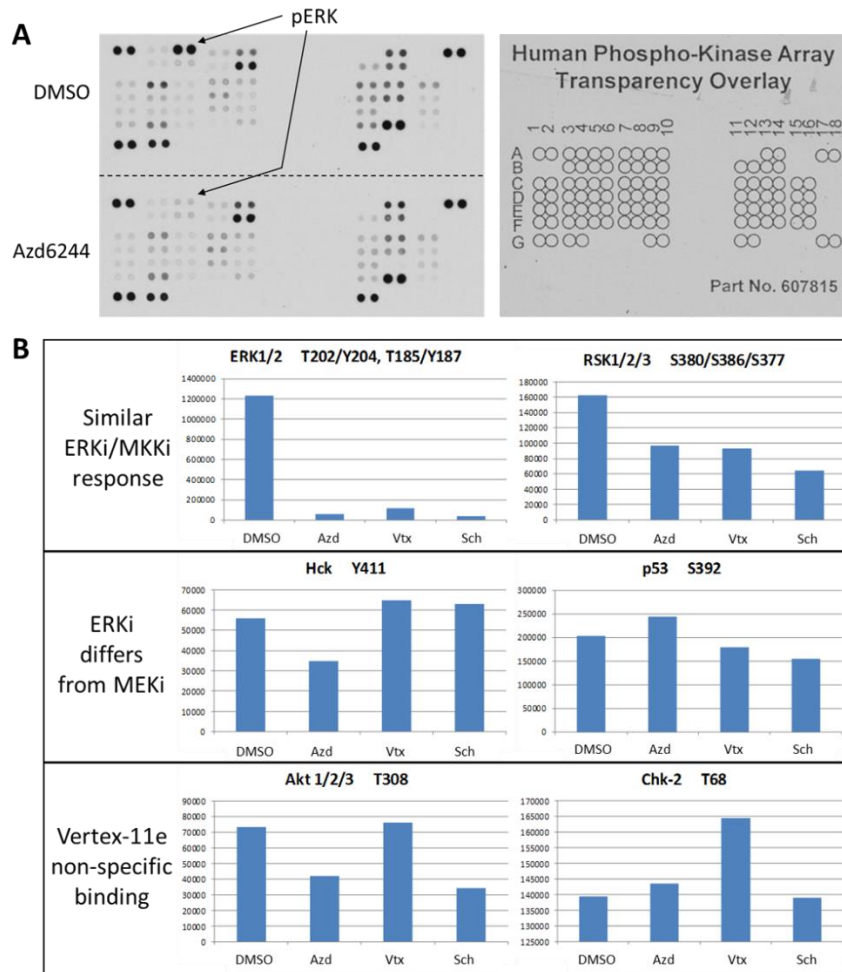


Figure 2.10: Human phospho-kinase antibody array. A, Changes in kinase phosphorylation in response to 10 μ M treatment for 4 h. Decreased levels of pERK with MKK1/2 inhibitor selumetinib (AZD6244 - AZD) compared to DMSO control are indicated. The overlay is used as a key to look up the phosphorylated kinases identified in duplicate spots. B, Quantification of signal, measured as raw intensity of quantified Typhoon membrane scans using ImageQuant. Examples show groups that change in response to MKK1/2 inhibitor (AZD) or ERK1/2 inhibitor (SCH), as well as some that increase in response to Vertex-11e (VTX). Further studies are needed to validate these preliminary findings.

A previous study from our lab identified different binding affinities of Vertex-11e to ERK2 in its inactive, unphosphorylated form ($K_i = 2.5$ nM), and active, phosphorylated form ($K_i = 0.34$ nM) (Rudolph et al., 2015). Corresponding nuclear magnetic resonance (NMR) relaxation experiments further revealed that whereas the unphosphorylated ERK2 is restrained into a single conformer, phosphorylation reduces a thermodynamic barrier for forming a new conformer, allowing equilibrium interconversion between two conformers on a millisecond timescale. Vertex-11e binding shifts the equilibrium of phosphorylated ERK2 entirely to the new conformer. By contrast, unpublished studies show that SCH772984 shifts the equilibrium of phosphorylated ERK2 entirely to the conformer associated with unphosphorylated ERK2. Thus, Vertex-11e and SCH772984 both show properties of conformational selection, but differ in the conformers that they favor. The nature of these conformers is still unknown, however the result suggests that Vertex-11e and SCH772984 favor distinct binding modes. Therefore, I investigated if such differences in binding mode between Vertex-11e and SCH772984 might be reflected by any unique features of each inhibitor with respect to their cellular effects on protein phosphorylation.

Using triple-labeled SILAC phosphoproteomics, I compared phosphorylation responses in cells treated for 2 h with DMSO, 10 μ M Vertex-11e, and 10 μ M SCH772984, following procedures described above. Technical problems with data collection resulted in lower numbers of phosphopeptides than seen before, due to sample contaminants that blocked UPLC runs, such that LC-MS/MS data could be obtained only in ERLIC fractions #5-12. Nevertheless, in total, 2,701 class I phosphorylation sites were identified on 1,617 proteins, including 1,163 phosphosites quantified in at least two replicates (Fig 2.11 A,B, Table 2.6).

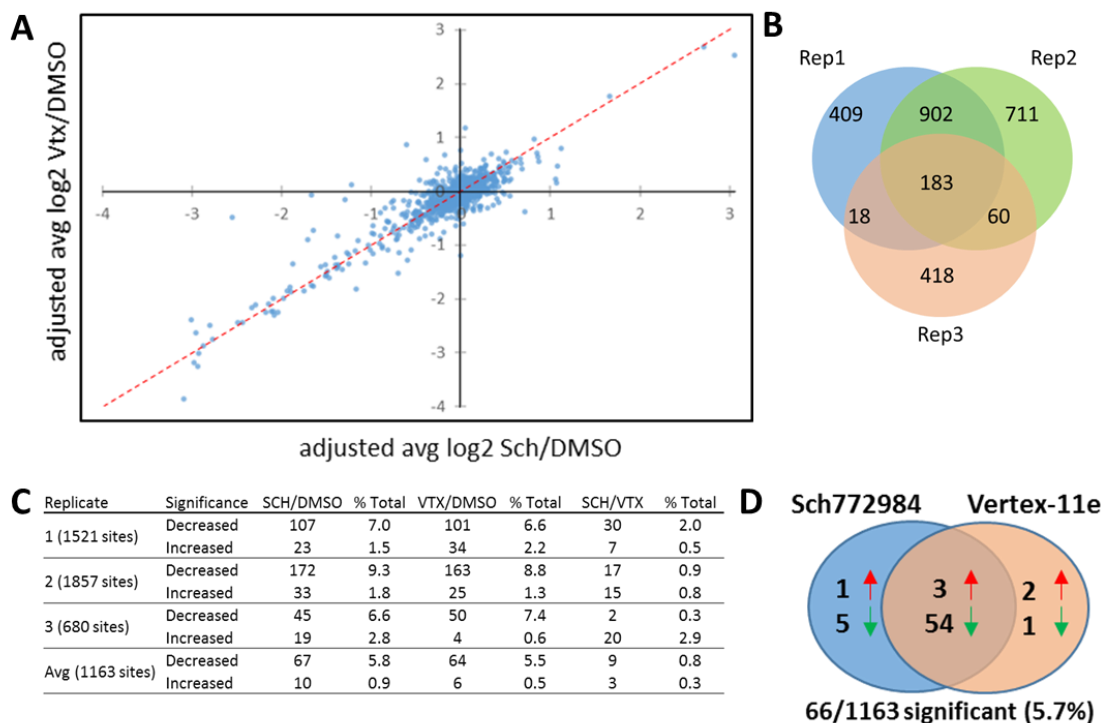


Figure 2.11: SILAC labeled phosphoproteomics comparison of SCH772984 and Vertex-11e. A, Log₂ transformed plot showing 1,163 phosphosites quantified in at least two replicate measurements of responses to treatment with 10 μ M SCH772984 or 10 μ M Vertex-11e each for 2 h. B, Overlap among three replicate experiments quantify 2,701 total phosphosites using SILAC. C, Number and percentages of phosphosites in each replicate showing a significant fold change in response to SCH772984 or Vertex-11e, where $|\log_2(\text{drug/DMSO})| \geq 0.84$. D, Counts of significant changes seen in at least 2 replicates, with $|\log_2(\text{combined ratio})| \geq 0.84$, and adjusted p-value >0.05 .

I found that, like the previous SILAC comparisons, SCH772984 and Vertex-11e had almost complete overlap in the phosphosites that passed the statistical cutoff with adjusted p-value of <0.05 . Only two were uniquely inhibited by SCH772984, and none were unique to Vertex-11e. One of the two unique sites was phospho-Tyr187 on ERK2 (MAPK1), which could be explained by the ability of SCH772984 to block the regulatory phosphorylation of ERK1/2 by MKK1/2. The corresponding site on ERK1 (MAPK3) was also uniquely inhibited, but variations in ratio between replicates yielded an adjusted p-value that was too high to consider. The other site was Ser270 on thioredoxin related transmembrane protein 1 (TMX1), has no

known function (Table 2.6). The results indicated that differences in conformational selection by these ERK1/2 inhibitors were not readily detectable by monitoring downstream drug targets in my experiments. Nevertheless, further phosphoproteomics studies which achieve higher sampling depth might be able to address this important question.

Table 2.6. Comparison of unique SCH7729834 and Vertex-11e significant phosphosites. ^a log₂ values of quantified ratios in individual SILAC replicates. ^b empirical bayes generated log₂ combined ratio and adjusted p-value. ^c phosphosites below double line are significantly increased in response to drug

Unique phosphosite changes in response to SCH772984

Uniprot ID	Gene	Position	9 aa window	SCH772984/DMSO ^a			Vertex-11e/DMSO ^a			SCH/VTX ^b	
				Exp 1	Exp 2	Exp 3	Exp 1	Exp 2	Exp 3	Combined	adj p-value
Q09666	AHNAK	210	IRLPSGSGA	-1.135	-1.449		-0.160	-0.144		-1.140	0.151
P28482	MAPK1	187	FLTEYVATR	-2.745	-2.182	-2.733	-0.740	-0.172	-0.545	-2.068	0.005
P27361	MAPK3	204	FLTEYVATR	-3.061	-1.901	0.031	-0.309	0.213	-2.053	-0.927	0.999
Q9H3N1	TMX1	270	IRQRSLGPS	-1.303	-1.127		0.121	0.121		-1.336	0.049
Q9ULJ3	ZBTB21	411	LRSFSASQS		0.025	-3.360		0.169	-0.312	-1.596	0.999
Q6VY07	PACS1	355	LEHVSREIQI	1.005	1.123		0.622	-0.314		0.909	0.999

Unique phosphosite changes in response to Vertex-11e

Uniprot ID	Gene	Position	9 aa window	SCH772984/DMSO ^a			Vertex-11e/DMSO ^a			SCH/VTX ^b	
				Exp 1	Exp 2	Exp 3	Exp 1	Exp 2	Exp 3	Combined	adj p-value
Q9UJX6	ANAPC2	314	ARPASPEAG	-0.133	0.131		-2.314	-0.074		1.192	0.999
P21359	NF1	2543	GTRKSFDDL	-0.808	-0.412		0.479	1.262		-1.480	0.999
P61247	RPS3A	236	HGEGSSSGK	-0.076	0.166		1.782	0.561		-1.126	0.999

Information from phosphoproteomics comparisons of the two MKK1/2 inhibitors and two ERK1/2 inhibitors can be combined to provide a deeper understanding of pathway specificity. The overlap between significant phosphosite changes with each inhibitor is summarized in Fig 2.12. I highlighted four comparisons of interest. First, I noted 150 phosphosites that were significantly responsive to all four inhibitors. These are candidates for bona fide targets downstream of the BRAF/MKK/ERK signaling pathway. Second, I noted 4 phosphosites that were significantly responsive to both MKK1/2 inhibitors but neither ERK1/2 inhibitor. These are candidates for pathway bifurcation at the level of MKK1/2, upstream of ERK1/2. Third, zero phosphosites were significantly responsive to both ERK1/2 inhibitors but neither MKK1/2 inhibitor. Finally, I noted 48 phosphosites that were responsive to only one inhibitor, and none of the other three. These are candidates for off-target effects of each compound. Vertex-11e was excluded from this analysis because of the limited data collection in the DMSO/Vertex-11e/SCH772984 experiment.

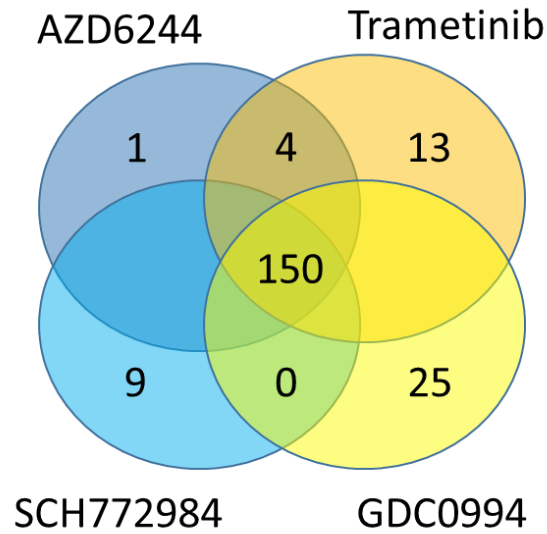


Figure 2.12: Counts of phosphosites that change significantly in response to each MKK1/2 and ERK1/2 inhibitor. Venn diagram summarizing phosphosites identified in each of three SILAC experiments, comparing DMSO-trametinib-SCH772984, DMSO-SCH772984-GDC0994, and DMSO-selumetinib (AZD6244)-vemurafenib, where the $|\log_2(\text{combined ratio})| \geq 0.84$ in at least 2 replicates. In total, 3,382 phosphosites were quantified and comparable across all SILAC experiments. Phosphosites showing significant changes in both SCH772984 treatment experiments were combined. 3,021 phosphosites showed no significant change in response to any inhibitor. Additional overlap remains to be validated.

Phosphosites affected by all four treatments are those most likely to be bona fide targets of the BRAF-MKK1/2-ERK1/2 signaling pathway. I examined these for known and potentially novel targets of signaling. Of the 150 phosphosites that were significantly altered, 141 phosphosites decreased, while 9 increased in response to all inhibitors (Table 2.7). Two-thirds of these phosphosites corresponded to the canonical ERK1/2 substrate recognition motif (Ser/Thr-Pro). Of these, 40 phosphosites were located on proteins known to be ERK1/2 substrates, and 16 of these were known sites for regulation by phosphorylation (Carlson et al., 2011; Hornbeck et al., 2015; Yoon & Seger, 2006). Thus, the majority of phosphosites regulated by all four inhibitors either corresponded to novel MAPK pathway targets, or were uncharacterized with respect to function. This means that MAPK signaling potentially regulates many new processes, and that comparing phosphorylation responses to different small molecules enables the lengthy lists of phosphosites typically generated by these experiments to be filtered in a manner that prioritizes their importance. The subset of genes regulated by all four inhibitors at Ser/Thr-Pro sites (100 phosphosites on 88 genes) was analyzed using STRING software (<http://string-db.org/>) (Szklarczyk et al., 2015), which reports likely gene networks based on different types of interactions reported by literature curation and public datasets. Thirty-one of these genes fell into four subnetworks, including (i) growth factor signaling and transcriptional regulation, (ii) small GTPase signaling, (iii) nuclear pore complex, and (iv) cellular structure, localization and trafficking. Many proteins in these networks were previously identified as ERK1/2 pathway targets in our previous screen (Stuart et al., 2015) including the nucleoporins (Courcelles et al., 2013; Kosako et al., 2009), c-Jun (Pulverer, Kyriakis, Avruch, Nikolakaki, & Woodgett, 1991), and ERF (von Kriegsheim et al., 2009).

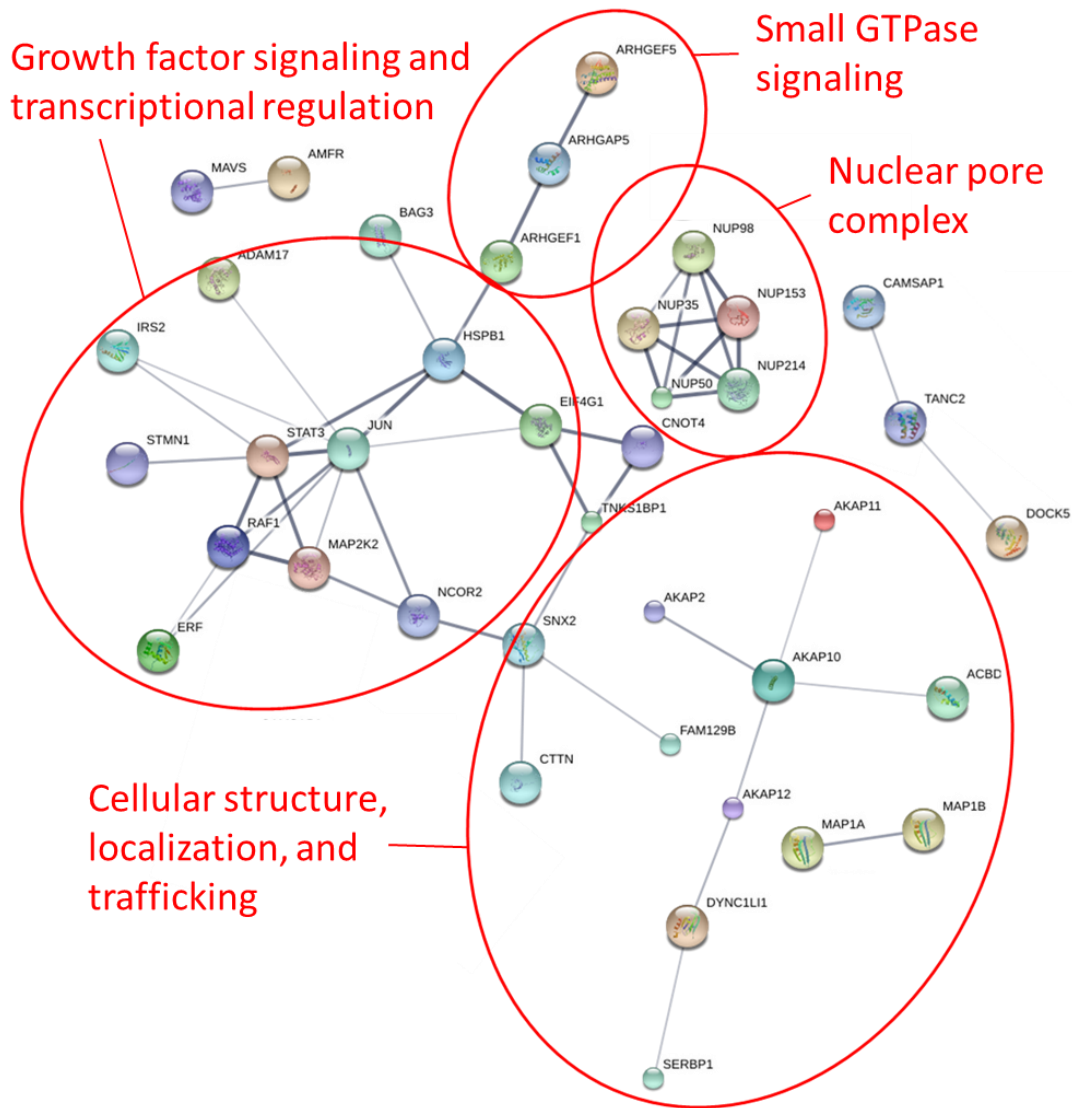


Figure 2.13: Subnetworks of proteins containing phosphosites responsive to all four MKK1/2 and ERK1/2 inhibitors. STRING software was used to examine protein networks among 88 genes containing 100 Ser/Thr-Pro phosphosites significantly regulated by selumetinib (AZD6244), trametinib, SCH772984, and GDC0994. Edges (interactions) between genes nodes (genes) were identified with medium confidence score of 0.7 (Szkarczyk et al., 2015). Color and size of nodes are arbitrary. Disconnected nodes that could not be linked to others are not shown. Edge thickness indicates confidence level of interaction.

Table 2.7. Phosphosites significantly regulated by all inhibitors (trametinib, selumetinib (AZD6244), SCH772984, GDC0994) in SILAC experiments. Log₂ values of quantified ratios in individual SILAC replicates. Empirical bayes generated log₂ combined ratio and adjusted p-value. Phosphosites below double line are significantly increased in response to inhibitor

#	Uniprot ID	Gene	Positio n	Experiment 1			Experiment 2			Experiment 3																																					
				SCH772984/DMSO	Trametinib/DMSO	AZD6244/DMSO	SCH772984/DMSO	GDC0994/DMSO																																							
1	Q2M2I8	AAK1	846	9aa window	Rep 1	Rep 2	Rep 3	Rep 1	Rep 2	Rep 3	Rep 1	Rep 2	Rep 3	Combined	adj p-value																																
2	Q9H3P7	ACBD3	43	QRLPQCTES	-1.935	-1.260	-1.644	<0.001	-2.735	-2.862	-2.752	<0.001	-1.328	<0.001	-1.677	-1.880	<0.001	-1.714	-1.570	-1.640	<0.001																										
3	Q9UUK3	ACIN1	710	LPPSPPGS	-1.273	-1.515	-0.990	-1.266	<0.001	-1.097	-1.511	-1.321	-1.303	<0.001	-1.433	-1.562	-1.548	-1.503	<0.001	-1.045	-1.421	-0.985	-1.156	<0.001	-1.320	-1.474	-1.386	<0.001	-2.17	-1.58	-1.89	0.001	-1.31	-1.92	<0.001	-1.620	-1.285	-1.281	-1.402	<0.001							
4	Q7B536	ADAM17	135	ARRLSQPEs	-0.985	-1.322	-1.352	-1.210	<0.001	-1.360	-1.302	-1.234	-1.309	<0.001	-1.366	-1.288	-1.641	-1.416	<0.001	-1.393	-0.874	-1.156	-1.134	<0.001	-1.393	-0.874	-1.156	-1.134	<0.001	-1.393	-0.874	-1.156	-1.134	<0.001	-1.620	-1.285	-1.281	-1.402	<0.001								
5	Q7WVPS	AHCTF1	732	PAFQTGRSL	-1.169	-1.72	-1.05	-1.49	<0.001	-1.78	-2.29	-1.88	-1.99	<0.001	-1.71	-1.57	-1.48	-1.57	<0.001	-1.839	-1.033	-1.105	-0.966	<0.001	-1.839	-1.033	-1.105	-0.966	<0.001	-1.839	-1.033	-1.105	-0.966	<0.001	-1.620	-1.285	-1.281	-1.402	<0.001								
6	Q09666	AHNAK	135	PRUSDEGV	6.353	-6.692	-6.525	<0.001	-5.923	-7.501	-6.709	<0.001	-6.230	-4.955	-3.147	-4.908	<0.001	-6.230	-4.955	-3.147	-4.908	<0.001	-6.230	-4.955	-3.147	-4.908	<0.001	-6.230	-4.955	-3.147	-4.908	<0.001	-6.027	-5.653	-5.861	<0.001	-4.234	-3.508	-3.339	-3.694	<0.001						
7	Q09666	AHNAK	5110	APIUSPKLE	-3.983	-4.275	-3.296	-3.854	<0.001	-3.979	-4.560	-4.143	-4.224	<0.001	-3.773	-4.104	-3.925	-3.921	<0.001	-3.773	-4.104	-3.925	-3.921	<0.001	-3.773	-4.104	-3.925	-3.921	<0.001	-3.773	-4.104	-3.925	-3.921	<0.001	-3.032	-2.558	-2.803	<0.001	-3.032	-2.558	-2.803	<0.001	-3.019	-2.637	-2.912	-2.867	<0.001
8	Q09666	AHNAK	3426	LNKSPKVK	-2.875	-1.878	-2.407	0.021	-1.792	-3.336	-2.533	0.016	-2.733	-2.566	-2.089	-2.351	<0.001	-2.733	-2.566	-2.089	-2.351	<0.001	-2.733	-2.566	-2.089	-2.351	<0.001	-2.733	-2.566	-2.089	-2.351	<0.001	-2.733	-2.566	-2.089	-2.351	<0.001	-2.733	-2.566	-2.089	-2.351	<0.001	-2.733	-2.566	-2.089	-2.351	<0.001
9	Q09666	AHNAK	2397	LHUSPKAK	-2.893	-2.888	-2.593	-2.844	<0.001	-2.367	-2.601	-2.437	-2.415	<0.001	-2.745	-2.708	-2.220	-2.511	<0.001	-2.745	-2.708	-2.220	-2.511	<0.001	-2.745	-2.708	-2.220	-2.511	<0.001	-2.745	-2.708	-2.220	-2.511	<0.001	-2.745	-2.708	-2.220	-2.511	<0.001	-2.745	-2.708	-2.220	-2.511	<0.001			
10	Q09666	AHNAK	511	LSUSPKLK	-1.592	-1.533	-1.058	-1.389	<0.001	-0.895	-1.178	-1.305	-1.137	<0.001	-1.302	-1.290	-1.087	-1.216	<0.001	-1.302	-1.290	-1.087	-1.216	<0.001	-1.302	-1.290	-1.087	-1.216	<0.001	-1.302	-1.290	-1.087	-1.216	<0.001	-1.302	-1.290	-1.087	-1.216	<0.001	-1.302	-1.290	-1.087	-1.216	<0.001			
11	Q43572	AKAP10	187	AEPVSPSKK	-1.13	-1.11	-1.16	<0.001	-1.07	-0.97	-0.98	<0.001	-0.92	-1.04	-0.97	<0.001	-0.92	-1.04	-0.97	<0.001	-0.92	-1.04	-0.97	<0.001	-0.92	-1.04	-0.97	<0.001	-0.92	-1.04	-0.97	<0.001	-0.92	-1.04	-0.97	<0.001	-0.92	-1.04	-0.97	<0.001	-0.92	-1.04	-0.97	<0.001			
12	Q9UKA4	AKAP11	448	SGLSPSPS	-1.289	-1.279	-1.511	-1.334	<0.001	-1.130	-1.208	-1.283	-1.232	<0.001	-1.167	-1.305	-1.315	-1.267	<0.001	-1.167	-1.305	-1.315	-1.267	<0.001	-1.167	-1.305	-1.315	-1.267	<0.001	-1.167	-1.305	-1.315	-1.267	<0.001	-1.167	-1.305	-1.315	-1.267	<0.001	-1.167	-1.305	-1.315	-1.267	<0.001			
13	Q02952	AKAP12	286	ESPTSPVTS	-1.55	-1.98	-1.00	-1.50	<0.001	-1.23	-2.10	-1.79	-1.71	<0.001	-1.50	-1.58	-1.18	-1.42	<0.001	-1.50	-1.58	-1.18	-1.42	<0.001	-1.50	-1.58	-1.18	-1.42	<0.001	-1.50	-1.58	-1.18	-1.42	<0.001	-1.50	-1.58	-1.18	-1.42	<0.001	-1.50	-1.58	-1.18	-1.42	<0.001			
14	Q9YUW3	AKAP2	748	QSTQSPRTK	-2.875	-3.390	-3.225	-3.083	<0.001	-3.090	-3.162	-3.083	<0.001	-3.035	-2.796	-3.146	-2.991	<0.001	-3.035	-2.796	-3.146	-2.991	<0.001	-3.035	-2.796	-3.146	-2.991	<0.001	-3.035	-2.796	-3.146	-2.991	<0.001	-3.035	-2.796	-3.146	-2.991	<0.001	-3.035	-2.796	-3.146	-2.991	<0.001				
15	Q9YVZ5	AKAP2	152	QVVPSPSST	-1.163	-1.057	-1.316	-1.172	<0.001	-1.373	-1.074	-1.202	-1.224	<0.001	-1.099	-0.822	-1.506	-1.147	<0.001	-1.099	-0.822	-1.506	-1.147	<0.001	-1.099	-0.822	-1.506	-1.147	<0.001	-1.099	-0.822	-1.506	-1.147	<0.001	-1.099	-0.822	-1.506	-1.147	<0.001	-1.099	-0.822	-1.506	-1.147	<0.001			
16	Q9UUV5	AMFR	542	PULSPPLE	-2.651	-2.591	-2.600	<0.001	-2.743	-2.580	-2.682	<0.001	-2.839	-2.692	-2.819	-2.774	<0.001	-2.839	-2.692	-2.819	-2.774	<0.001	-2.839	-2.692	-2.819	-2.774	<0.001	-2.839	-2.692	-2.819	-2.774	<0.001	-2.839	-2.692	-2.819	-2.774	<0.001	-2.839	-2.692	-2.819	-2.774	<0.001					
17	Q9HCE9	ANOR8	641	LEEGSPFMV	-1.503	-1.268	-1.401	<0.001	-1.098	-1.015	-1.040	<0.001	-1.359	-1.177	-1.442	-1.318	<0.001	-1.359	-1.177	-1.442	-1.318	<0.001	-1.359	-1.177	-1.442	-1.318	<0.001	-1.359	-1.177	-1.442	-1.318	<0.001	-1.359	-1.177	-1.442	-1.318	<0.001	-1.359	-1.177	-1.442	-1.318	<0.001					
18	Q14617	AP3D1	658	KHRPSEADE	-1.97	-2.14	-1.83	-1.98	<0.001	-1.86	-1.98	-1.86	-1.94	<0.001	-2.03	-2.15	-1.84	-2.02	<0.001	-2.03	-2.15	-1.84	-2.02	<0.001	-2.03	-2.15	-1.84	-2.02	<0.001	-2.03	-2.15	-1.84	-2.02	<0.001	-2.03	-2.15	-1.84	-2.02	<0.001	-2.03	-2.15	-1.84	-2.02	<0.001			
19	Q13017	ARHGAP5	668	VFLPSPROD	-1.708	-1.881	-1.579	-1.722	<0.001	-1.606	-1.919	-1.953	-1.826	<0.001	-1.794	-1.883	-1.688	-1.775	<0.001	-1.794	-1.883	-1.688	-1.775	<0.001	-1.794	-1.883	-1.688	-1.775	<0.001	-1.794	-1.883	-1.688	-1.775	<0.001	-1.794	-1.883	-1.688	-1.775	<0.001	-1.794	-1.883	-1.688	-1.775	<0.001			
20	Q92888	ARHGFE1	863	SGPSPART	-1.532	-1.204	-1.249	-1.346	<0.001	-1.767	-1.297	-1.383	-1.464	<0.001	-1.081	-1.078	-1.212	-1.122	<0.001	-1.081	-1.078	-1.212	-1.122	<0.001	-1.081	-1.078	-1.212	-1.122	<0.001	-1.081	-1.078	-1.212	-1.122	<0.001	-1.081	-1.078	-1.212	-1.122	<0.001	-1.081	-1.078	-1.212	-1.122	<0.001			
21	Q12774	ARHGFE4	1470	SGDVSPGPR	-1.763	-1.355	-1.540	<0.001	-1.136	-1.680	-1.427	<0.001	-1.110	-1.396	-1.357	-1.310	<0.001	-1.110	-1.396	-1.357	-1.310	<0.001	-1.110	-1.396	-1.357	-1.310	<0.001	-1.110	-1.396	-1.357	-1.310	<0.001	-1.110	-1.396	-1.357	-1.310	<0.001	-1.110	-1.396	-1.357	-1.310	<0.001					
22	Q12774	ARHGFE5	474	PAALSPSLE	-1.983	-0.731	-1.516	-1.388	0.002	-1.678	-1.486	-2.207	-1.713	<0.001	-1.901	-2.487	-2.063	-2.165	<0.001	-1.901	-2.487	-2.063	-2.165	<0.001	-1.901	-2.487	-2.063	-2.165	<0.001	-1.901	-2.487	-2.063	-2.165	<0.001	-1.901	-2.487	-2.063	-2.165	<0.001	-1.901	-2.487	-2.063	-2.165	<0.001			
23	Q12774	ARHGFE5	445	AEELSPAAL	-1.349	-1.940	-1.183	-1.505	<0.001	-1.141	-1.873	-1.592	-1.521	<0.001	-1.139	-1.630	-1.320	-1.334	<0.001	-1.139	-1.630	-1.320	-1.334	<0.001	-1.139	-1.630	-1.320	-1.334	<0.001	-1.139	-1.630	-1.320	-1.334	<0.001	-1.139	-1.630	-1.320	-1.334	<0.001	-1.139	-1.630	-1.320	-1.334	<0.001			
24	Q14155	ATXN1	684	ERKPSDEEF	-1.121	-1.312	-1.399	-1.283	<0.001	-1.209	-1.097	-1.220	-1.169	<0.001	-1.406	-1.702	-1.635	-1.584	<0.001	-1.406	-1.702	-1.635	-1.584	<0.001	-1.406	-1.702	-1.635	-1.584	<0.001	-1.406	-1.702	-1.635	-1.584	<0.001	-1.406	-1.702	-1.635	-1.584	<0.001	-1.406	-1.702	-1.635	-1.584	<0.001			
25	Q04775	ATXN2	284	VRRESEALD	-3.86	-3.09	-3.44	<0.001	-3.70	-3.72	-3.75	<0.001	-4.02	-4.02	-4.08	-4.06	<0.001	-4.02	-4.02	-4.08	-4.06	<0.001	-4.02	-4.02	-4.08	-4.06	<0.001	-4.02	-4.02	-4.08	-4.06	<0.001	-4.02	-4.02	-4.08	-4.06	<0.001	-4.02	-4.02	-4.08	-4.06	<0.001					
26	Q95817	BAG3	377	CPSPSPGCS	-1.45	-1.53	-0.83	-1.29	<0.001	-1.26	-1.31	-0.97	-1.16	<0.001	-1.12	-0.95	-1.03	-1.06	<0.001																												

Table 2.7. Phosphosites significantly regulated by all inhibitors (trametinib, AZD6244, SCH772984, GDC0994) in SILAC experiments. Log₂ values of quantified ratios in individual SILAC replicates. Empirical bayes generated log₂ combined ratio and adjusted p-value. Phosphosites below double line are significantly increased in response to inhibitor

#	Uniprot ID	Gene	Positio n	Experiment 1			Experiment 2			Experiment 3											
				SCH772984/DMSO	Trametinib/DMSO	AZD6244/DMSO	SCH772984/DMSO	GDC0994/DMSO													
51	Q96K07	EHMT2	232	RKLNISGGGL	Rep 1	Rep 2	Rep 3	Rep 1	Rep 2	Rep 3	Rep 1	Rep 2	Rep 3	Combined	adj p-value	log ₂ p-value					
52	Q46837	E1F4G1	1231	LPVYSPGKA	-1.373	-1.454	-1.449	-1.429	-1.226	-1.183	-1.473	-1.290	-1.790	-1.790	-0.001	-1.578	-1.158	-1.255			
53	Q32944	EML3	198	DPVLSPPGK	-2.01	-1.91	-1.79	-1.90	-1.770	-1.652	-1.773	-1.549	-1.777	-1.777	-0.001	-1.78	-1.40	-1.45	-1.60		
54	Q9Y613	EPN1	435	VPAKSPGAF	-1.799	-1.750	-1.773	-1.773	-1.559	-1.421	-1.462	-1.494	-1.444	-1.444	-0.001	-1.669	-1.480	-1.172	-1.444		
55	P50548	ERF	526	GGPIPTPRV	-1.973	-1.976	-1.923	-1.965	-2.158	-2.020	-2.077	-2.074	-2.074	-2.074	-0.001	-1.850	-1.643	-1.776	-1.735		
56	Q86TAL	FAM129B	696	SFAPSPIQH	-1.850	-2.022	-1.683	-1.861	-1.785	-1.283	-1.898	-1.646	-1.646	-1.646	-1.646	-0.001	-1.795	-2.070	-1.821	-1.900	
57	Q86VR2	FAM134C	692	PEASSPPAS	-1.831	-1.603	-1.725	-1.801	-1.792	-1.705	-1.740	-1.740	-1.740	-1.740	-1.740	-0.001	-1.841	-2.066	-1.763	-1.898	
58	Q46046	FAM188B	392	EVLSPVPS	-2.212	-1.268	-2.069	-1.893	-2.472	-1.808	-1.921	-2.023	-2.023	-2.023	-2.023	-0.001	-1.848	-1.749	-1.728	-1.770	
59	Q49327	FASN	7204	LACTPKRED	-0.81	-0.96	-0.95	-0.91	-0.79	-1.06	-1.28	-1.04	-1.04	-1.04	-1.04	-0.001	-1.751	-1.652	-1.336	-1.584	
60	Q9UJ14	GCT7	72	QRVLSSESE	-2.608	-1.875	-2.096	-2.150	-2.145	-2.046	-2.161	-2.161	-2.161	-2.161	-2.161	-0.001	-1.819	-1.13	-1.14	-1.18	
61	Q6Y7W6	G1GYF2	593	RVPFSPGPA	-2.150	-1.749	-1.954	-2.001	-2.129	-1.814	-1.967	-1.967	-1.967	-1.967	-1.967	-1.967	-0.001	-1.274	-2.204	-2.113	-1.863
62	Q6Y7W6	G1GYF2	26	GTSISPLS	-1.336	-1.409	-1.212	-1.314	-1.082	-1.240	-1.333	-1.223	-1.223	-1.223	-1.223	-1.223	-0.001	-1.152	-1.231	-1.193	-1.183
64	Q9UKJ3	GPATCH8	1107	ERKFSVSEE	-1.518	-1.152	-1.322	-1.322	-1.539	-1.438	-1.501	-1.501	-1.501	-1.501	-1.501	-1.501	-0.001	-2.011	-1.802	-1.709	-1.824
65	Q6ZVF9	GRIN3	57	EPLDSPRAA	-0.823	-1.334	-1.224	-1.133	-1.116	-0.916	-1.469	-1.161	-1.161	-1.161	-1.161	-1.161	-1.161	-1.204	-0.932	-1.086	-1.090
66	Q94792	HSPB1	65	AAIESPAVA	-1.70	-0.56	-1.17	-0.916	-0.72	-2.16	-2.40	-2.40	-2.40	-2.40	-2.40	-2.40	-0.001	-1.69	-1.51	-1.56	-1.58
67	Q9Y4H2	IRS2	1203	EPTTSPVOL	-1.313	-1.673	-1.461	-1.461	-1.514	-1.832	-1.706	-1.706	-1.706	-1.706	-1.706	-1.706	-1.706	-1.402	-1.508	-1.448	-1.438
68	Q96572	IWN1	720	RRMNSTGGGQ	-1.238	-1.282	-0.857	-1.117	-0.887	-1.440	-1.778	-1.377	-1.377	-1.377	-1.377	-1.377	-1.377	-1.136	-1.044	-1.017	-1.085
69	P05412	JUN	63	DULTSPDVG	-1.05	-1.42	-1.21	-1.001	-1.93	-2.17	-2.07	-2.07	-2.07	-2.07	-2.07	-2.07	-1.20	-0.65	-0.92	-0.901	
70	Q2L037	KIAA1109	3653	VDAAASGPR	-2.312	-1.141	-2.433	-1.646	-2.095	-0.023	-2.544	-1.521	-1.521	-1.521	-1.521	-1.521	-0.029	-0.020	-2.505	-2.399	-1.708
71	Q6ZJUS	KIAA1211	714	KRHSSTGDS	-1.080	-1.287	-1.569	-1.296	-1.172	-0.788	-1.552	-1.187	-1.187	-1.187	-1.187	-1.187	-1.187	-1.449	-1.428	-1.369	-1.419
72	O14686	KMT2D	2274	EPLLSPPFF	-1.34	-1.34	-1.29	-1.29	-1.26	-1.66	-1.51	-1.51	-1.51	-1.51	-1.51	-1.51	-1.34	-1.39	-1.46	-1.38	
73	P78559	MAP1A	504	SEPQTTPAQ	-2.76	-3.39	-3.07	-3.07	-2.49	-3.08	-2.80	-2.80	-2.80	-2.80	-2.80	-2.80	-0.31	-2.33	-2.94	-1.92	
74	P46821	MAP1B	1797	SPLYSPTFS	-1.58	-1.58	-1.58	-1.58	-1.07	-1.68	-1.38	-1.38	-1.38	-1.38	-1.38	-1.38	-1.77	-1.56	-1.84	-1.74	
75	P11327	MAP2	821	SRLASVSAD	-1.28	-0.87	-1.43	-1.21	-1.07	-1.17	-1.37	-1.32	-1.32	-1.32	-1.32	-1.32	-0.89	-0.88	-0.87	-0.89	
76	P36507	MAP2K2	295	PHLSPPRRP	-1.43	-1.64	-1.39	-1.48	-1.25	-1.61	-1.61	-1.49	-1.49	-1.49	-1.49	-1.49	-1.38	-1.44	-1.49	-1.44	
77	P36507	MAP2K2	293	GEPHSISPR	-1.65	-1.64	-0.99	-1.11	-1.77	-1.59	-1.23	-1.55	-1.55	-1.55	-1.55	-1.55	-0.98	-0.83	-1.60	-1.13	
78	P29966	MARCKS	155	EAGASPVKE	-1.55	-1.95	-1.87	-1.77	-1.60	-1.64	-1.85	-1.75	-1.75	-1.75	-1.75	-1.75	-1.30	-1.61	-1.81	-1.60	
79	P43243	MATR3	188	FRDSDDDR	-1.27	-0.92	-1.42	-1.19	-1.00	-0.91	-1.11	-1.07	-1.07	-1.07	-1.07	-1.07	-0.89	-1.00	-0.96	-0.96	
80	Q72434	MAVS	222	RGPVSPSVS	-1.470	-1.635	-1.482	-1.535	-1.622	-1.593	-1.812	-1.673	-1.673	-1.673	-1.673	-1.673	-1.529	-1.794	-1.499	-1.609	
81	Q7RTP6	MICAL3	685	RRKTSQSEE	-2.148	-2.200	-2.041	-2.120	-2.232	-2.085	-2.129	-2.158	-2.158	-2.158	-2.158	-2.320	-2.642	-2.299	-2.478		
82	Q8YV33	MICAL2	712	GRPLSPAINV	-1.678	-2.297	-2.278	-2.117	-2.136	-2.371	-2.545	-2.315	-2.315	-2.315	-2.315	-2.315	-1.883	-1.913	-1.727	-1.846	
83	Q8YV33	MICAL2	726	ETVTSPPVIL	-2.362	-2.213	-2.311	-2.311	-3.045	-3.058	-3.028	-3.028	-3.028	-3.028	-3.028	-3.015	-2.560	-3.020	-2.863		
84	Q6WCQ1	MRIP	619	EVDKSPGIP	-0.901	-1.112	-1.121	-1.059	-0.926	-0.947	-1.000	-0.943	-0.943	-0.943	-0.943	-0.933	-0.909	-1.052	-0.975		
85	Q86UE4	MTDH	494	LKTISSDOP	-1.149	-1.724	-0.998	-1.266	-0.694	-1.517	-1.662	-1.315	-1.315	-1.315	-1.315	-1.331	-0.624	-1.226	-1.069		
86	Q9Y217	MTMR8	561	VHPFSPLNK	-1.327	-1.647	-1.025	-1.337	-1.261	-1.494	-1.245	-1.330	-1.330	-1.330	-1.330	-1.283	-1.009	-1.085	-1.127		
87	O75592	MYCBP2	3467	RRVNSGDTE	-1.78	-1.71	-2.19	-1.91	-1.56	-1.25	-1.91	-1.56	-1.56	-1.56	-1.56	-1.16	-1.48	-1.49	-1.40		
88	Q09161	NCBP1	22	RRKTSQANE	-3.79	-4.02	-3.68	-3.86	-3.71	-4.07	-4.20	-3.96	-3.96	-3.96	-3.96	-3.75	-3.89	-4.53	-4.04		
89	P16333	NOX1	85	KRFPVSDPE	-1.27	-1.16	-1.72	-1.38	-1.34	-0.86	-1.13	-1.11	-1.11	-1.11	-1.11	-1.52	-1.43	-1.67	-1.55		
90	Q60524	NEMF	831	KKLPSDSDG	-1.62	-1.82	-1.72	-2.001	-1.82	-1.86	-1.84	-1.84	-1.84	-1.84	-1.91	-1.98	-1.84	-1.89			
91	Q12968	NFATC3	344	TRKTSDDQA	-2.708	-2.726	-2.723	-2.723	-2.289	-2.187	-2.232	-2.232	-2.232	-2.232	-2.232	-2.232	-2.232	-2.232	-2.232		
92	P46087	NOF2	58	RRLGSVEAP	-1.72	-2.02	-1.87	-2.001	-1.50	-1.85	-1.68	-1.68	-1.68	-1.68	-1.68	-1.21	-1.26	-1.23	-1.24		
93	O00567	NOP56	563	KRFSNKEP	-1.73	-1.87	-1.81	-2.001	-1.82	-1.76	-1.78	-1.78	-1.78	-1.78	-1.64	-1.69	-1.76	-1.73			
94	R49790	NUP153	338	SLNLSPIQR	-1.33	-1.43	-1.37	-1.34	-1.47	-1.57	-1.69	-1.61	-1.61	-1.61	-1.80	-1.85	-1.97	-1.87			
95	Q8VHF5	NUP153	48	PAPVTPQPR	-2.040	-1.158	-1.505	-2.001	-1.286	-1.153	-1.314	-1.314	-1.314	-1.314	-1.600	-1.426	-1.294	-1.450			
96	Q9UKW7	NUP50	621	AETQSPSLF	-0.989	-0.856	-0.930	-0.901	-1.234	-1.125	-1.172	-1.172	-1.172	-1.172	-1.011	-1.040	-0.931	-0.999			
97	P52948	NUP98	223	ENLASPEY	-1.26	-1.47	-1.39	-2.001	-1.33	-1.24	-1.37	-1.42	-1.42	-1.42	-1.31	-1.42	-1.37	-1.37			
98	Q8VX93	PALD1	893	ARIASDEE1	-2.622	-3.176	-2.696	-2.812	-2.785	-3.265	-3.113	-3.074	-3.074	-3.074	-3.552	-3.489	-3.701	-3.550			
99	Q84880	PHF14	835	GRKFSVPE	-2.50	-2.66	-2.63	-2.59	-2.75	-2.78	-3.06	-2.87	-2.87	-2.87	-2.63	-2.60	-2.59	-2.61			
100	Q16513	PKN2	583	PRASSLGEI	-1.010	-0.817	-1.244	-1.012	-1.270	-0.810	-1.290	-1.134	-1.134	-1.134	-1.134	-1.156	-1.237	-1.432	-1.283		

Table 2.7. Phosphosites significantly regulated by all inhibitors (trametinib, AZD6244, SCH772984, GDC0994) in SILAC experiments. Log₂ values of quantified ratios in individual SILAC replicates. Empirical bayes generated log₂ combined ratio and adjusted p-value. Phosphosites below double line are significantly increased in response to inhibitor

#	Uniprot ID	Gene	Positio n	Experiment 1			Experiment 2			Experiment 3																				
				SCH772984/DMSO	Trametinib/DMSO	AZD6244/DMSO	SCH772984/DMSO	GDC0994/DMSO																						
101	P47172	PLAZG4A	727	PSRCSVSLS	-0.92 -1.77 -1.35	0.002	-0.93 -1.44 -1.18	0.004	-0.99 -0.74 -0.83	-0.84	<0.001	-1.71 -1.03	-1.26	0.002	-1.17 -0.97	-1.18	<0.002													
102	O14874	PROSER2A	507	RRLASTSDI	-4.81 -5.07 -4.63	-4.89	-0.001	-4.71 -5.29 -5.47	-5.10	-0.001	-5.45 -4.96 -5.27	-5.23	<0.001	-6.17 -5.23	-4.72	-5.36	<0.001	-5.42 -5.89 -5.30	-5.55	<0.001										
103	Q86WR7	PROSERF	215	LSPISPFRE	-2.077 -1.665 -1.883	-0.001	-2.028 -1.994 -1.999	-0.001	-1.523 -1.557 -1.130	-1.413	<0.001	-1.688 -1.451 -1.498	-1.555	<0.001	-0.99 -0.85	-0.80	-0.90	<0.001	-0.98 -0.94 -0.83	-0.89	<0.001									
104	P04049	RAF1	642	TLLTSPRAR	-1.17 -1.15 -1.24	-1.18	-0.001	-1.00 -0.98 -1.09	-1.03	-0.001	-1.05 -1.05 -1.07	-1.04	<0.001	-0.99 -0.85	-0.80	-0.90	<0.001	-3.15 -2.94 -3.04	-3.04	<0.001	-3.46 -3.87	-3.66	<0.001							
106	Q7Z534	RAI1	1068	SEPRTPGPP	-2.298 -2.260 -2.288	-2.300	-0.001	-2.213 -2.162 -2.706	-2.342	-0.001	-2.530 -2.316 -2.190	-2.347	<0.001	-2.915 -2.411 -2.479	-2.597	<0.001	-2.796 -2.381 -2.579	-2.590	<0.001	-2.796 -2.381 -2.579	-2.590	<0.001								
107	Q70E73	RAPH1	1154	QVPTSPKSS	-1.053	-0.581	-0.873	0.006	-1.429	-0.806	-1.061	0.002	-0.923 -1.152 -0.606	-0.897	<0.001	-1.283	-0.866	-1.091	0.001	-1.080	-1.168	-1.108	<0.001							
108	Q81Y67	RAVER1	463	AAQLTPPPA	-0.893 -1.182 -1.110	-0.001	-1.135 -1.223 -1.392	-1.221	-0.001	-1.172 -1.493 -1.238	-1.295	<0.001	-1.130 -1.181 -1.107	-1.127	<0.001	-1.399 -1.456 -1.604	-1.498	<0.001	-1.630 -1.243 -1.332	-1.391	<0.001	-1.630 -1.243 -1.332	-1.391	<0.001						
109	Q86071	REPS1	709	RRLUSEDEL	-2.290 -2.135 -1.972	-2.143	-0.001	-1.972 -2.514 -2.468	-2.307	-0.001	-1.891 -1.911 -1.700	-1.818	<0.001	-1.998 -1.717 -1.502	-1.616	<0.001	-2.734 -2.284 -2.424	-2.424	<0.001	-2.734 -2.284 -2.424	-2.424	<0.001								
110	Q9N2J4	SACS	1779	ADLQSPLEF	-1.905 -2.266 -2.083	-0.001	-2.573 -3.096 -2.837	-0.001	-2.281 -2.559 -2.326	-2.402	<0.001	-2.281 -2.559 -2.326	-2.402	<0.001	-1.766 -1.753 -2.029	-1.833	<0.001	-1.607 -1.618 -2.062	-1.778	<0.001	-1.607 -1.618 -2.062	-1.778	<0.001							
111	Q9N2J4	SACS	4264	STPTSPTEF	-1.714	-1.917	-1.807	-0.001	-2.245	-2.264	-2.264	-0.001	-1.677 -0.093 -1.781	-1.829	<0.001	-1.83 -0.76 -1.18	-1.429	<0.001	-1.78 -0.82 -1.32	-1.28	<0.001	-1.78 -0.82 -1.32	-1.28	<0.001						
112	Q43290	SART1	448	RRLVSEVEE	-1.34 -1.55 -0.95	-1.27	-0.001	-1.17 -1.78 -1.58	-1.52	-0.001	-2.05 -1.77 -1.80	-1.83	<0.001	-1.83 -0.76 -1.18	-1.429	<0.001	-1.56 -1.68 -1.64	-1.62	<0.001	-2.34 -2.04 -2.36	-2.25	<0.001	-2.34 -2.04 -2.36	-2.25	<0.001					
113	Q15027	SEC16A	1786	QPLASPARV	-1.64 -1.81 -1.73	-1.74	-0.001	-1.40 -1.54 -1.50	-1.47	-0.001	-1.46 -1.55 -1.46	-1.47	-0.001	-1.63 -1.68 -1.64	-1.62	<0.001	-2.085 -1.697 -1.745	-1.850	<0.001	-1.833 -1.540 -1.468	-1.606	<0.001	-1.833 -1.540 -1.468	-1.606	<0.001					
114	Q48634	SERPBP1	234	ELTESPKY1	-2.278 -2.332 -1.658	-2.082	-0.001	-1.856 -2.149 -1.644	-1.891	-0.001	-1.633 -1.683 -1.843	-1.787	<0.001	-2.382 -2.517 -2.319	-2.363	<0.001	-2.085 -1.697 -1.745	-1.850	<0.001	-1.734 -1.734 -1.872	-1.785	<0.001	-1.734 -1.734 -1.872	-1.785	<0.001					
115	Q72333	SETX	1366	RRLSDGDES	-2.298 -1.621 -2.270	-2.066	-0.001	-2.409 -2.147 -2.303	-2.283	-0.001	-1.755 -1.952 -2.044	-1.930	<0.001	-1.703 -1.816 -2.011	-1.838	<0.001	-2.462 -2.192 -2.315	-2.304	<0.001	-2.394 -2.079 -2.098	-2.209	<0.001	-2.394 -2.079 -2.098	-2.209	<0.001					
116	Q86V55	SGK223	745	AELSLSPEF	-1.710 -1.898 -1.803	-0.001	-1.542 -1.865 -1.705	-0.001	-1.878	-2.364	-2.211	-0.001	-2.048 -2.448 -2.206	-2.194	<0.001	-2.462 -2.192 -2.315	-2.304	<0.001	-2.394 -2.079 -2.098	-2.209	<0.001	-2.394 -2.079 -2.098	-2.209	<0.001						
117	Q9P2F8	SIPAL12	1461	MPLDPSLVE	-2.310	-2.493	-2.312	-0.001	-1.32	-1.24	-1.21	-1.26	-0.001	-1.40 -1.28 -1.44	-1.36	-0.001	-1.45 -1.33 -1.05	-1.29	<0.001	-1.30 -1.32 -0.78	-1.12	<0.001	-1.30 -1.32 -0.78	-1.12	<0.001					
118	Q48637	SUC20A2	268	QEAESPVK	-1.56	-1.63	-1.42	-1.53	-0.001	-2.08 -2.30 -2.18	-0.001	-1.61 -2.17 -1.75	-2.20	-0.001	-2.49 -2.36 -1.96	-2.29	-0.001	-2.43 -2.44 -1.93	-2.22	<0.001	-2.05 -2.40 -1.90	-2.10	<0.001	-2.05 -2.40 -1.90	-2.10	<0.001				
119	Q19634	SUC20A2	703	ARIGSDPLA	-2.08 -2.30 -2.18	-0.001	-2.08 -2.44 -2.27	-0.001	-2.10 -2.10 -2.10	-2.08	-0.001	-1.66 -1.67 -2.34	-1.92	-0.001	-2.62	-2.22	-2.40	<0.001	-2.37	-1.48	-1.95	<0.001	-2.37	-1.48	-1.95	<0.001				
120	Q60749	SIX2	104	VTPVTPITL	-2.38	-2.70	-2.55	-0.001	-2.77	-3.10	-2.93	-0.001	-2.76 -3.04 -1.57	-2.42	<0.001	-2.61	-2.61	-2.45	-2.55	<0.001	-2.54	-2.47	-2.41	-2.48	<0.001	-2.54	-2.47	-2.41	-2.48	<0.001
121	P40783	STAT3	727	DLPMSPTRL	-1.31	-1.67	-1.49	-0.001	-1.23	-1.12	-1.18	-0.001	-1.37 -1.48 -1.33	-1.39	-0.001	-1.26 -1.51 -1.63	-1.49	<0.001	-1.58 -1.35 -1.49	-1.49	<0.001	-1.58 -1.35 -1.49	-1.49	<0.001	-1.58 -1.35 -1.49	-1.49	<0.001			
122	Q94804	STK10	952	PNPSTPSKA	-2.20	-2.85	-1.82	-2.17	-0.001	-1.61 -2.17 -1.75	-2.20	-0.001	-2.49 -2.36 -1.96	-2.29	-0.001	-2.43 -2.44 -1.93	-2.22	<0.001	-2.35 -2.53 -2.64	-2.49	<0.001	-2.35 -2.53 -2.64	-2.49	<0.001	-2.35 -2.53 -2.64	-2.49	<0.001			
123	Q16949	STMN1	25	EULSPRSK	-1.65	-1.35	-1.49	-1.48	-0.001	-1.72 -1.58 -1.53	-1.63	-0.001	-1.73 -1.72 -1.84	-1.76	-0.001	-1.64 -1.60 -1.46	-1.58	<0.001	-2.13 -2.15 -1.52	-1.92	<0.001	-2.13 -2.15 -1.52	-1.92	<0.001	-2.13 -2.15 -1.52	-1.92	<0.001			
124	Q9VY20	SUGT1	285	GDVFTPKQF	-1.538 -1.523 -1.458	-1.509	-0.001	-1.650 -1.674 -1.507	-1.608	-0.001	-1.642 -1.299 -1.502	-1.476	-0.001	-1.775 -1.315 -1.424	-1.300	<0.001	-1.68 -1.68 -1.71	-1.71	<0.001	-2.68 -2.270 -1.782	-2.311	<0.001	-2.68 -2.270 -1.782	-2.311	<0.001					
125	Q95425	SVIL	547	VTRTSLDSF	-0.89	-1.51	-1.18	-0.017	-0.46	-1.60	-1.06	0.024	-1.02 -0.86 -0.88	-0.92	0.007	-1.23 -1.74 -1.50	-0.001	-2.62	-2.22	-2.40	<0.001	-2.37	-1.48	-1.95	<0.001	-2.37	-1.48	-1.95	<0.001	
126	Q95359	TACC2	2317	NTPASPPRS	-2.35	-1.99	-2.19	-0.001	-2.10 -2.10 -2.10	-2.08	-0.001	-1.66 -1.67 -2.34	-1.92	-0.001	-1.66	-1.67	-2.34	-1.92	-0.001	-2.62	-2.22	-2.40	<0.001	-2.62	-2.22	-2.40	<0.001			
127	Q95359	TACC2	2321	SPRSPAPF	-2.35	-1.99	-2.19	-0.001	-2.10 -2.10 -2.10	-2.08	-0.001	-1.66 -1.67 -2.34	-1.92	-0.001	-1.66	-1.67	-2.34	-1.92	-0.001	-2.62	-2.22	-2.40	<0.001	-2.62	-2.22	-2.40	<0.001			
128	Q13769	THOCS	328	RRRPTLGVQ	-2.653 -2.764 -2.268	-2.589	-0.001	-3.568 -3.597 -4.127	-3.736	-0.001	-2.937 -2.882 -2.132	-2.659	<0.001	-2.761 -2.874	-2.809	<0.001	-2.027 -2.179	-2.112	<0.001	-2.027 -2.179	-2.112	<0.001	-2.027 -2.179	-2.112	<0.001					
129	Q12893	TMEM115	320	AKVDSPIPS	-2.712 -2.607 -2.534	-2.618	-0.001	-2.357 -2.388 -2.624	-2.456	-0.001	-2.513 -2.345 -2.296	-2.417	<0.001	-2.638 -2.533 -2.198	-2.475	<0.001	-2.598 -2.848 -2.241	-2.544	<0.001	-2.598 -2.848 -2.241	-2.544	<0.001	-2.598 -2.848 -2.241	-2.544	<0.001					
130	Q86703	TMEM85B	162	QPLSPPEPQ	-1.198 -1.207 -1.794	-1.394	-0.001	-1.558 -1.049 -1.501	-1.375	-0.001	-1.401 -1.381 -1.398	-1.395	-0.001	-1.079 -1.057 -1.984	-1.352	<0.001	-1.332 -0.959 -2.014	-1.457	<0.001	-1.332 -0.959 -2.014	-1.457	<0.001	-1.332 -0.959 -2.014	-1.457	<0.001					
131	Q96002	TMEM85B	131	PPPLTPPAR	-2.822 -3.418 -2.800	-3.043	-0.001	-2.637 -3.230 -3.205	-2.994	-0.001	-3.063 -3.035 -2.903	-2.997	-0.001	-2.866	-2.766	-2.746	<0.001	-2.955	-2.862	-2.988	<0.001	-2.955	-2.862	-2.988	<0.001					
132	Q96104	TRIM47	588	GIPASPIDP	-3.189 -2.569 -2.880	-0.001	-3.005 -3.952 -3.478	-0.001	-2.803 -3.159 -3.087	-3.016	-0.001	-1.003 -1.090 -1.081	-1.038	<0.001	-1.147 -1.133 -1.354	-1.212	<0.001	-1.400 -1.326 -1.370	-1.365	<0.001	-1.400 -1.326 -1.370	-1.365	<0.001	-1.400 -1.326 -1.370	-1.365	<0.001				
133	Q13625	TP53BP2	556	RVLSPSP1P	-0.955 -1.010 -1.109	-1.025	-0.001	-0.807 -1.084 -1.244	-1.045	-0.001	-1.010 -1.138 -0.921	-1.029	-0.001	-2.865 -2.347 -2.485	-2.356	<0.001	-2.632 -2.635 -2.628	-2.647	<0.001	-2.632 -2.635 -2.628	-2.647	<0.001	-2.632 -2.635 -2.628	-2.647	<0.001					
134	Q8VVT3	TRAPP2C	182	QMVVSPFSG	-2.484 -2.406 -2.451	-0.001	-2.470 -2.612 -2.540	-0.001	-3.005 -3.952 -3.478	-0.001	-2.803 -3.159 -3.087	-3.016	-0.001	-1.147 -1.133 -1.354	-1.212	<0.001	-1.400 -1.326 -1.370	-1.365	<0.001	-1.400 -1.326 -1.370	-1.365	<0.001	-1.400 -1.326 -1.370	-1.365	<0.001					
135	Q96104	TRIM47	588	GIPASPIDP	-3.189 -2.569 -2.880	-0.001	-3.005 -3.952 -3.478	-0.001	-2.803 -3.159 -3.087	-3.016	-0.001	-1.003 -1.090 -1.081	-1.038	<0.001	-1.147 -1.133 -1.354	-1.212	<0.001	-1.400 -1.326 -1.370	-1.365	<0.001	-1.400 -1.326 -1.370	-1.365	<0.001	-1.400 -1.326 -1.370	-1.365	<0.001				
136	Q9V3Q8	TSC22D4	279	LVMKSPDPF	-2.344 -3.160 -2.773	-2.737	-0.001	-2.589 -3.117 -3.512	-3.095	-0.001	-2.803 -2.247 -2.869	-2.646	-0.001	-2.607 -2.497 -2.511	-2.549	<0.001	-2.445 -2.7													

My comparison of SILAC datasets allowed me to identify phosphosites that were significantly responsive to the MKK1/2 inhibitors (trametinib and selumetinib) but not ERK1/2 inhibitors (SCH772984 and GDC0994), or vice versa. Only four phosphosites were differentially regulated by one set of inhibitors and not the other (Table 2.8), and all were regulated by MKK1/2 inhibitor, with no sites uniquely regulated by ERK1/2 inhibitors across all three experiments. These sites are intriguing candidates for targets of MKK1/2 which bifurcate upstream of ERK1/2.

These phosphosites included Ser612 in nuclear pore complex protein 98 (NUP98), Thr5824 in giant neuroblast differentiation-associated protein (AHNAK), Ser455 in mitogen activated protein kinase kinase kinase 7 (MAP3K7/TAK1), and Ser893 in DNA double strand break repair G family endonuclease 1 (GEN1). Three of these phosphosites showed significant differences between $\log_2(\text{combined ratio for MKK1/2 inhibitor response})$ vs $\log_2(\text{combined ratio for ERK1/2 inhibitor response})$, using a Student's t-test with p value < 0.05. Thr5824 in AHNAK failed this test (Table 2.8). But the other three phosphosites support the existence of potential branchpoints upstream of ERK1/2, breaking the standard paradigm of linear signaling in the MAPK cascade.

Ser612 in NUP98 has been identified as a target of ERK1/2 inhibition in previous phosphoproteomics experiments (Courcelles et al., 2013; Kosako et al., 2009; Stuart et al., 2015) monitoring responses to MKK1/2 and BRAF V600E/K inhibitors. Six other NUP98 phosphorylation sites identified previously showed similar responses to all four MKK1/2 and ERK1/2 inhibitors, highlighting Ser612 as a particularly interesting site for regulation through a branching pathway. Thr5824 in AHNAK was also identified in previous phosphoproteomic analyses as a site responsive to a MKK1/2 inhibitor but not an ERK1/2 inhibitor (Pan et al., 2009). TAK1 is a MEKK, which is known to phosphorylate and activate MKK3/6 in response to

cytokine signaling, and is also subject to negative feedback inhibition by p38 α through its' binding partner TAB1 (Cheung, Campbell, Nebreda, & Cohen, 2003; Cuadrado & Nebreda, 2010).

Table 2.8. Phosphosites significantly regulated with MKK1/2 inhibitors but not ERK1/2 inhibitors. Log₂ values of quantified ratios in individual SILAC replicates. Empirical bayes generated log₂ combined ratio. Phosphosites significantly inhibited <0.84 are highlighted in green. Phosphosites significantly increased by drug are highlighted in red.

Uniprot ID	Gene	Position	9aa window	p-value	MKK1/2 inhibitors						ERK1/2 inhibitors													
					Trametinib/DMSO Experiment 1			AZD6244/DMSO Experiment 2			SCH772984/DMSO Experiment 1			SCH772984/DMSO Experiment 3			GDC0994/DMSO Experiment 3							
					Rep 1	Rep 2	Rep 3	Combined	Rep 1	Rep 2	Rep 3	Combined	Rep 1	Rep 2	Rep 3	Combined	Rep 1	Rep 2	Rep 3	Combined				
P52948	NUP98	612	SNLFSPVNR	0.027	-1.36	-0.65	-1.01	-1.00	-0.79	-0.87	-0.85	-0.07	-0.48	-0.91	-0.49	-0.69	0.17	1.37	0.75	0.80	0.31	0.36	0.32	
Q09666	AHNAK	5824	LKFGTFGGL	0.136	0.66	0.67	1.22	0.85	0.91	1.15	1.12	1.09	0.32	0.59	0.85	0.58	0.17	1.37	0.75	0.80	-0.55	0.54	1.05	0.32
O43318	MAP3K7	455	GQVSSRSSS	0.004	1.04	0.76	0.82	0.86	0.55	0.70	1.30	0.86	0.16	0.34	0.56	0.37	0.41	0.67	0.38	0.37	0.37	-0.02	0.08	
Q17RS7	GEN1	893	TCLDSPLIPL	0.019	1.24	0.89	1.08	1.08	0.96	1.25	2.02	1.40	0.45	0.25	0.33	-0.20	0.49	-0.17	0.31	-0.28	0.76	1.65	0.67	

Comparison of these datasets can also yield insight about off-target effects of individual compounds, which will most likely be reflected by the phosphosites responding uniquely to one inhibitor, but none of the other three. This was exemplified by the case described above of p38 α MAPK phosphorylation, which appears to be an off-target of only trametinib and none of the other MKK1/2 or ERK1/2 inhibitors.

Table 2.9 describes the phosphosites that can be quantified across all four treatments among three experiments, but change in response to only one drug. In total, 48 phosphosites were identified as significantly altered by only one compound. Eight of these are in proteins previously validated as known components of the RAF-MKK-ERK pathway or downstream targets of pathway signaling (Carlson et al., 2011; Yoon & Seger, 2006). Among these 48 phosphosites, 21 contain the canonical Ser/Thr-Pro motif associated with direct substrates of phosphorylation by ERK1/2. However, none of these were validated by more than one inhibitor, therefore I believe that all 48 phosphosites most likely reflect off-target effects of single compounds. A striking observation was how many phosphosites were targeted only by GDC0994, an ERK1/2 inhibitor which is currently being tested in early stage clinical trials. Twenty-five phosphosites were uniquely responsive to GDC0994, which therefore shows more potential off-targets than the other three drugs combined. The difference was not explained by greater inhibition of ERK1/2 signaling at the 10 μ M concentration used, because GDC0994 shows a similar IC₅₀ for ERK1/2 inhibition as the other inhibitors (Fig. 1.4), and among the 150 phosphosites significantly affected by all four inhibitors, only 33% were most strongly responsive to GDC0994 (Table 2.7). I found no specificity motif among the 25 phosphosites uniquely responsive to GDC0994 that would indicate regulation of a specific set of kinases. In

fact, the range of sequence motifs suggested substrate specificities comparable to the other MKK1/2 and ERK1/2 inhibitors analyzed.

Among the unique GDC0994 off-target candidates were Ser196 on the transcription factor, ELK1. ERK1/2 is known to phosphorylate and activate ELK1, but at a different residue than Ser196, which has no known function (Hornbeck et al., 2015; Stuart et al., 2015). The off-target candidates for GDC0994 were also examined by STRING, which reported a network of genes known to regulate mRNA binding and translational initiation, including the highest ranking target uniquely responsive to GDC0994, eukaryotic translation initiation factor 4 gamma 1 (EIF4G1) (Fig. 2.14). Three additional genes containing phosphosites unique to GDC0994, la ribonucleoprotein domain family member 1 (LARP1), la ribonucleoprotein domain family 1B (LARP1B), and heterogeneous nuclear ribonucleoprotein M (HNRNPM), are among those in the STRING network (Fig. 2.14). These genes are RNA binding proteins, known to function in pre-mRNA processing and specificity of mRNA translation. Further studies are now needed to verify if GDC0994 indeed affects RNA processing or translation in a manner that is independent of MKK1/2-ERK1/2 signaling. Understanding off-targets of drug candidates may provide useful insight about relative frequencies of off-target effects, at early stages of inhibitor screening.

Table 2.9. Phosphosites significantly regulated in only one MKK1/2 or ERK1/2 inhibitor. Log₂ values of quantified ratios in individual SILAC replicates. Empirical bayes generated log₂ combined ratio and adjusted p-value. Phosphosites significantly inhibited <0.84 are highlighted in green. Phosphosites significantly increased by inhibitor are highlighted in red.

#	Unique to	Uniprot ID	Gene	Position	Experiment 1			Experiment 2			Experiment 3									
					Trametinib/DMSO	Rep 1	Rep 2	Rep 3	Combined adj p-value	Rep 1	Rep 2	Rep 3	Combined adj p-value	Rep 1	Rep 2	Rep 3	Combined adj p-value			
1	AZD06244	QB8924	TRIM56	471	LKSIAREPS	0.342	0.325	0.221	0.236	0.036	-0.165	0.206	0.160	0.127	0.263	-	-	-	0.348	
2	Trametinib	QB9704	DOCK1	269	LRADSHGE	-0.849	-1.540	-1.176	-1.191	<0.001	0.057	-0.223	0.146	-0.004	0.990	-	-	-	-	
3	Trametinib	PA2566	FN1	796	NKLDSPDF	-1.322	-1.230	-1.495	-1.378	<0.001	-0.703	-0.483	-0.760	-0.589	<0.001	-0.432	-0.441	-0.325	-0.412	<0.001
4	Trametinib	QB8047	FN1	243	DIKPTPDIT	-1.285	-1.532	-1.933	-1.595	<0.001	-0.188	-0.730	-0.606	-0.496	0.011	-	-	-	-	-
5	Trametinib	QL6539	MAPK14	180	DDMTGVVA	-0.958	-1.135	-1.413	-1.124	<0.001	0.028	0.080	0.377	0.099	0.993	0.006	0.304	0.145	0.492	-
6	Trametinib	QL6539	MAPK14	182	EMTGYVATR	-0.850	-1.183	-0.728	-0.914	<0.001	0.004	0.103	0.202	0.097	0.542	-0.091	0.043	-0.063	-0.038	0.723
7	Trametinib	QB8JEA	MTDH	298	SSQISAGEE	-0.826	-1.093	-1.042	-1.004	<0.001	-0.095	-0.130	0.117	-0.019	0.920	-0.048	-0.239	-0.134	0.397	
8	Trametinib	QL1514	POM1	93	MSQMSVPEQ	-0.533	-1.136	-0.958	-0.879	0.010	0.000	-0.176	0.750	0.195	0.993	-0.275	-0.101	0.253	-0.046	0.870
9	Trametinib	Q5125	PRIIC2B	480	FRQQSEDEK	-0.775	-1.196	-0.991	-0.901	<0.001	-0.020	-0.420	-0.044	0.830	1.583	0.663	1.176	<0.001	-	-
10	Trametinib	PO4920	SIC4A2	144	LTQSPVST	-1.251	-0.861	-0.793	-0.973	<0.001	-0.942	-0.420	-0.803	-0.717	0.001	0.099	-0.051	0.043	-0.008	0.974
11	Trametinib	QB8WH2	FUNDC2	151	KIRKSNQIP	1.313	0.975	0.791	1.016	<0.001	0.349	-0.036	0.269	0.204	0.223	0.099	-0.051	0.043	-0.008	0.974
12	Trametinib	QB8TDD	MICAL1	1057	ERRLSLAL	0.967	1.349	1.068	1.068	0.002	0.036	-0.177	-0.001	0.999	-0.234	0.428	-	-	-	-
13	Trametinib	QB8VB5	OSBP1L0	30	SAGSSPSCS	1.494	1.238	1.191	1.304	<0.001	0.416	0.018	0.348	0.264	0.057	-	-	-	-	-
14	Trametinib	Q1482B	SCAMP3	32	QHRFSRQVA	1.010	0.853	0.931	0.931	0.001	0.333	-0.099	0.117	0.571	-	-	-	-	-	-
15	SCH72984	QB8X55	AP1M1	223	LFDNTRGK	0.214	-0.002	0.088	0.528	0.001	-1.598	-1.815	-1.689	<0.001	-	-	-	-	-	-
16	SCH72984	Q03252	LMNB2	419	SRATSSSSG	0.376	0.107	0.014	0.166	0.257	-1.236	-0.981	-1.235	-1.158	<0.001	-	-	-	-	-
17	SCH72984	QB81T5	RBM12B	562	FRHSSEDFR	0.346	0.008	-0.194	0.042	0.842	-0.886	-0.957	-0.794	-0.868	<0.001	-0.190	-0.120	0.001	-0.108	0.339
18	SCH72984	QB8159	RBX1	88	ATKPSFESG	0.044	-0.329	0.114	-0.061	0.681	-1.045	-0.973	-0.850	-0.952	0.001	-0.102	0.024	-0.012	-0.020	0.856
19	SCH72984	QB8WH9	SITM	550	KKRISKSP	-0.242	0.212	0.013	0.968	0.001	-1.094	-0.799	-0.974	-0.001	-0.152	-	-	-	-	-
20	SCH72984	QB8WH9	SITM	553	ISSKSPGHM	-0.242	0.103	-0.019	0.947	0.001	-1.094	-0.733	-0.964	0.001	-0.217	-0.011	-0.178	-0.130	0.161	
21	SCH72984	QB81F8	STK11P	481	APRSPPOE	0.579	-0.081	0.196	0.536	0.001	1.297	-0.963	-1.077	-0.006	-0.911	0.048	0.885	0.016	0.972	
22	SCH72984	QB8N17	THOC2	1285	KKRPATPT	0.192	0.219	0.086	0.141	0.509	-2.041	-1.231	-1.442	-1.547	<0.001	-	-	-	-	-
23	SCH72984	QB83N1	TMX1	270	JRQBSLQPS	0.634	0.424	0.308	0.442	0.039	-1.447	-1.396	-0.855	-1.219	<0.001	-0.003	0.110	0.269	0.098	0.553
24	GDC0994	QB8666	AHNAK	210	IRLPSGSGA	-0.219	-0.209	-0.226	0.033	0.001	-0.579	-0.624	-0.589	-0.001	-0.096	-0.134	-0.096	-0.105	0.307	
25	GDC0994	QB8666	AHNAK	216	SGAASPFGS	-0.298	-0.219	-0.209	0.242	0.023	-0.311	-0.279	-0.624	-0.505	<0.001	-0.019	-0.205	0.107	-0.053	0.956
26	GDC0994	QB8DQ2	CRYBG3	2902	GGROTPGAQ	0.137	-0.290	-0.055	0.789	0.001	0.248	0.012	0.108	0.551	0.165	0.189	0.115	0.155	0.129	
27	GDC0994	QL1655	DPSY12	509	EVSYTPKTV	0.297	-0.023	0.408	0.234	0.055	0.045	-0.010	0.124	0.046	0.768	0.192	0.185	0.214	0.210	0.010
28	GDC0994	QL14195	DPSY13	509	DLITTPGKG	0.336	0.536	0.162	0.333	0.017	0.279	0.142	-0.165	0.096	0.516	0.298	0.163	0.335	0.246	0.009
29	GDC0994	Q04637	EIF4G1	1209	RKAASLTED	0.452	0.201	0.332	0.335	0.103	-0.563	0.030	0.113	-0.146	0.524	0.143	0.099	0.321	0.184	
30	GDC0994	PI8419	EKL1	196	PFSGSRSTS	-0.384	0.048	0.115	-0.086	0.608	-0.433	-0.142	-0.246	-0.261	0.081	0.104	0.121	-0.099	0.042	0.719
31	GDC0994	QB840	GEMIN7	3	MQQTPVNI	0.039	0.337	0.508	0.295	0.041	0.233	0.407	0.180	0.272	0.061	0.123	0.315	0.279	0.238	0.018
32	GDC0994	QB87W6	GIGYF2	189	GGTTSVGRK	0.479	-0.333	-0.234	-0.051	0.916	-0.325	-0.274	0.213	-0.107	0.796	-0.656	0.135	-0.193	-0.258	0.269
33	GDC0994	QL3098	GF51	479	QGLTTPANS	0.010	0.040	-0.135	-0.026	0.802	0.119	0.029	0.051	0.064	0.464	-0.082	0.125	0.259	0.127	0.082
34	GDC0994	P52272	HNR1PM	452	ERMGSGER	-	-	-	-	-	-	-	-	-	-	-	-	-	-	
35	GDC0994	Q655CA	LARP1	900	VPNSPRRN	0.050	0.195	0.098	0.683	0.001	-0.067	-0.389	0.186	0.391	0.078	0.078	0.305	0.179	0.086	0.342
36	GDC0994	QB3252	LMNB2	17	ATPLSPTRL	-0.227	-0.330	-0.261	0.063	0.001	-0.129	-0.402	-0.283	0.051	0.692	0.018	0.018	0.023	0.822	
37	GDC0994	QB9L50	LRR1	124	VSTLTPVKT	0.203	-	-	-	-	-	-	-	-	-	-	-	-	-	
38	GDC0994	QB9608	LRRFP2	320	TPSLGNSS	-0.001	-	-	-	-	0.620	-	-	-	-	-	-	-	-	
39	GDC0994	Q14777	NDOR0	69	GSRNSQLGI	-0.131	-0.123	-0.134	0.469	0.001	-0.042	0.257	0.115	0.547	0.336	0.035	0.239	0.182	0.113	
40	GDC0994	QB8CFS	NFATC2IP	84	GPVASHSDMS	0.261	0.440	0.235	0.318	0.006	0.080	0.043	-0.062	0.014	0.926	0.376	0.145	0.156	0.239	0.006
41	GDC0994	Q6748	NPM1	254	NMQASTKKG	0.070	0.178	0.158	0.186	0.265	0.250	-	-	-	0.119	1.115	1.096	0.777		
42	GDC0994	QL1311	PRKAA1	382	LVAETPAR	-	-	-	-	-	-	-	-	-	-	-	-	-	-	
43	GDC0994	QB8X01	TNXL4B	132	LIVSFPDP	-0.179	-	-	-	-	-0.404	-	-	-	-	-	-	-	-	
44	GDC0994	QB8666	AHNAK	4564	VGIOTPDID	0.279	-0.525	-0.415	-0.219	0.523	-0.391	-0.965	-0.469	-0.135	0.012	-0.134	0.002	0.311	0.264	
45	GDC0994	QB8UR4	BALAP2L1	261	TPQASPMIE	-0.298	0.132	-0.104	0.760	0.001	0.123	-0.292	-0.063	0.867	0.004	-0.110	-0.029	0.917	1.083	
46	GDC0994	QB8WU0	BCL7C	126	SPVSPVAGP	0.133	-0.449	-0.544	-0.267	0.282	-0.001	-0.225	0.168	-0.039	0.911	-0.625	-0.581	-0.546	-0.567	0.001
47	GDC0994	QB8PQ0	LARP1	766	TIARSLPTT	-0.010	-0.047	-0.603	-0.221	1.185	-0.135	-0.017	-0.544	-0.231	1.668	-0.186	0.166	0.062	0.016	0.941
48	GDC0994	PI9532	TFE3	548	LRAASDPLL	-0.456	0.084	-0.194	0.380	0.001	-0.102	0.295	0.104	0.677	0.105	0.012	-0.202	-0.055	0.674	

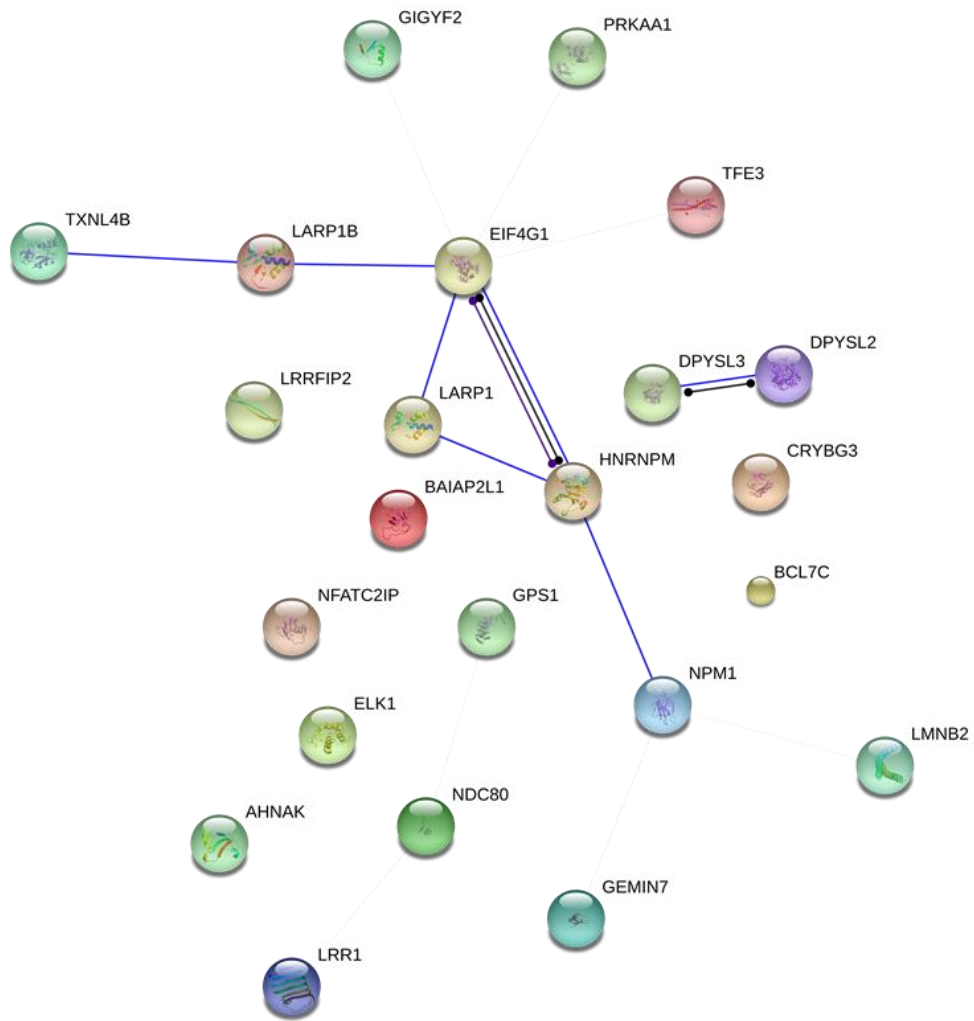


Figure 2.14: A STRING network of proteins with phosphosites significantly regulated only in response to GDC0994. Edges indicate evidence of molecular action such as binding or other reactions, with confidence at the lowest setting (>0.150). Color and size of nodes are arbitrary. Disconnected nodes are not shown.

2.6 Discussion

In summary, I have compared a series of phosphoproteomics experiments to interrogate molecular responses to drugs and drug candidates which inhibit different enzymes in the RAF-MKK-ERK MAPK pathway. From these, I can begin to classify responses to different tiers of the signaling pathway. These can be used to validate known and novel targets of signaling, based on stringent criteria requiring agreement between all four inhibitors. Importantly, the comparison can be used to identify candidates regulated by MKK1/2, which bifurcate upstream of ERK1/2, thus potentially reporting deviations from a linear pathway organization. Finally, compound-specific phosphorylation responses are likely to report off-targets, that can be useful for evaluating specificity of drug candidates.

Previously, our lab found that the BRAF V600E/K inhibitor, vemurafenib, and the MKK1/2 inhibitor, selumetinib, show a very high degree of overlap in their phosphosite responses (Stuart et al., 2015), reinforcing the idea that signaling from BRAF V600E/K to MKK1/2 is remarkably linear. The responses to submaximal concentrations of each inhibitor, singly and in combination, were additive, suggesting that the clinical effectiveness of cotreatment with BRAF V600E/K and MKK1/2 inhibitors in patients is likely due to an additive suppression of ERK1/2 signaling, rather than synergy between unique targets of each treatment individually. With the emergence of ERK1/2 inhibitors as tools to overcome resistance to BRAF V600E/K and MKK1/2 inhibitors, my first aim was to measure overlap in molecular responses to the ERK1/2 inhibitor, SCH772984, and the FDA-approved MKK1/2 inhibitor, trametinib. I found that among the 4.7% of phosphosites which changed significantly in response to either inhibitor, only 5.3% were exclusive to only one inhibitor. This further supports the previous findings of linearity and additivity among inhibitors of the BRAF V600E/K-MKK1/2-ERK1/2

pathway. Several ERK1/2 inhibitors are currently in early stage clinical trials, and may be successful in combination with BRAF V600E/K inhibitors. This is supported by known mechanisms of resistance to the BRAF V600E/K+MKK1/2 inhibitor combination which in the majority of cases lead to the reactivation of ERK1/2.

My next aim was to identify specific targets of MKK1/2 and ERK1/2 inhibitors with known functions. I found that p38 α MAPK phosphorylation sites are novel off-targets of trametinib, but not SCH772984 or GDC0994 in my study, and selumetinib and vemurafenib in our lab's previous study (Stuart et al., 2015). Inhibition of p38 α MAPK phosphorylation occurs at ~10 μ M, concentrations higher than those achieved in plasma during clinical studies. Nevertheless, this concentration range is commonly used in preclinical research studies and should be considered in studies of this drug. Further analysis revealed that MKK6 but not MKK3 can be inhibited *in vitro* by trametinib, and I initially assumed that this explains inhibition of p38 α MAPK downstream. However, unexpectedly, the dose response for MKK6 inhibition was in a concentration range greater than 10 μ M. The results suggest that MKK6 may in fact not be the direct target of trametinib relevant to its cellular inhibition of p38 α MAPK. Further studies are needed to resolve this issue. Meanwhile, I observed that the p38 MAPK inhibitor, SB203580, decreases cell viability when used in combination with selumetinib, but not trametinib. Potentially, an off-target effect of trametinib on p38 α MAPK may beneficially impact the efficacy of this drug in suppressing cell viability, by supplementing effects of RAF-MKK-ERK pathway inhibition.

My final aim was to compare molecular responses between the two different ERK1/2 inhibitors, SCH772984 and GDC0994. Some but not all ERK1/2 inhibitors show properties of conformational selection, based on NMR relaxation studies (Rudolph et al., 2015; Xiao et al.,

2014). While Vertex-11e preferentially binds phosphorylated, active ERK2 in a conformer unique to the active state, unpublished studies show that SCH772984 preferentially binds and locks phosphorylated, active ERK2 in the opposite conformer, characteristic of the inactive, unphosphorylated state. In contrast, GDC0994 binds the phosphorylated, active ERK2 in a manner which allows equilibrium interconversion between conformers, comparable to the apoenzyme, and favoring the new conformer characteristic of the active state (Y. Xiao, J. Rudolph and N. Ahn, unpublished). Thus, SCH772984 favors the inactive conformer, while GDC0994 interconverts but favors the active conformer. It is not yet clear whether conformational selection to shift the equilibrium towards one or the other conformers affects the specificity of inhibition of downstream substrates, or whether one conformer is more important than the other. Conceivably, the molecular responses to SCH772984 and GDC0994 might reflect these differences.

The majority of significantly affected phosphosites responded to both drugs, suggesting that inhibition of ERK1/2 is nearly complete at the 10 μ M concentrations tested. Among the phosphosites uniquely responsive to one but not both ERK1/2 inhibitors, 25 phosphosites changed only in response to GDC0994 and 3 changed only in response to SCH772984. The 25 phosphosites that changed in response to GDC0994 alone included five proteins which are known downstream substrates of ERK1/2, LARP1, ELK1, AHNAK, GIGYF2, and LMNB2. STRING analysis of this gene subset (i.e., significantly inhibited by GDC0994 but not SCH772984) identified a network which included EIF4G1, LARP1, LARP1B, and HNRNPM, all of which are involved in regulating RNA processing and translation. Thus, they are interesting targets which may potentially be useful to ask whether the different conformers that predominate upon binding GDC0994 vs SCH772984 might account for these differences in

target specificity, and whether these phosphoproteins may be markers of the conformational selective binding. Further studies are needed to address this intriguing question.

Chapter 3

Conclusions and future directions

3.1. Summary and conclusions

In this thesis I describe the overlap and specificity of MKK1/2 and ERK1/2 inhibitor targets in WM239a melanoma cells. Using phosphoproteomics, these changes were profiled across three experiments using the MKK1/2 inhibitor trametinib, and ERK1/2 inhibitors SCH772984, GDC0994, and Vertex-11e. These datasets, combined with a previously published study by our lab profiling the phosphoproteomic changes in response to the BRAF V600E/K inhibitor, vemurafenib, and the MKK1/2 inhibitor, selumetinib, constitute a unique resource for probing known and novel processes regulated by targeted MAPK inhibitor therapy in melanoma.

MKK1/2 and ERK1/2 inhibitor comparison by phosphoproteomics

Trametinib is a MKK1/2 inhibitor approved for clinical use as monotherapy or combination therapy with the BRAF V600E/K inhibitor, vemurafenib, in patients with metastatic melanoma. Previously, our lab demonstrated a high degree of overlap between inhibitors, suggesting that beneficial results observed in patients treated with combination therapies are most likely due to additive effects on the inhibition of downstream signaling targets. Preclinical studies established trametinib as a potent, selective inhibitor of MKK1/2 using *in vitro* kinase assays on 100 potential kinase targets (Yamaguchi et al., 2011). Although the prior studies showed few off-target effects of trametinib on other protein kinases, the regulation of downstream effectors such as transcription factors remained unknown. My SILAC-based phosphoproteomics study of responses to trametinib and SCH772984 identified 12,924 phosphosites affected by drug treatment, 8,577 of which were reproducibly quantified in multiple

replicate experiments. Overall, I observed significant changes to approximately 5% of all phosphosites identified, and very few targets specific for only one inhibitor. This indicates a high degree of pathway linearity in the MAPK signaling cascade upstream of ERK1/2, and further supports the additive model of vertical targeting in combination therapies.

Inhibition of novel off-target p38 α by trametinib

Among the small subset of targets uniquely affected by only one inhibitor, the canonical activation sites Thr180 and Tyr182 on p38 α MAPK were significantly inhibited by trametinib but not SCH772984. Intriguingly, Ser796 on the epidermal growth factor receptor pathway substrate 15 (EPS15), which has previously been shown to respond to p38 MAPK inhibition (SB203580) but not MKK1/2 inhibition (U0126) or JNK inhibition (SP600125) in HeLa cells (Zhou et al., 2014), was also inhibited by trametinib, but not SCH772984 (Table 2.9). These findings, showing significant changes in the phosphorylation of p38 α MAPK, as well as a known substrate specifically targeted by p38 MAPK, provide evidence that trametinib effects on p38 α may regulate cellular processes not associated with the RAF-MKK-ERK pathway. To determine if p38 α inhibition is shared among MKK1/2 inhibitors, I compared my datasets to previous SILAC datasets examining phosphoproteomics responses to the MKK1/2 inhibitor, selumetinib (Stuart et al., 2015) (Table 2.3), and again found that inhibition of Thr180 and Tyr182 is unique to trametinib.

Biochemical assays suggested that this unique inhibition of p38 α MAPK phosphorylation by trametinib may be explained by its ability to inhibit MKK6, a kinase upstream of p38 α MAPK. Supporting this hypothesis, MKK6 was identified as a direct target of trametinib but not selumetinib, leading to decreased p38 α MAPK phosphorylation *in vitro*. Arguing against this

hypothesis, trametinib inhibited MKK6 with IC₅₀ 10-fold higher than its inhibition of p38 α MAPK in cells. Therefore, the jury is still out as to whether MKK6 is the direct target of trametinib in cells explaining its effect on p38 α MAPK. No crystal structures of trametinib-bound MKK1/2 are available and the canonical activation motifs differ. MKK1 is activated by dual phosphorylation at S218 and S222 while MKK6 is activated at S207 and T211. These activation sites, as well as the HRD and DFG motifs important for catalytic activity, overlap using NCBI BLAST protein sequence alignment, and there is a 38% sequence identity between MKK1 and MKK6. Nevertheless, cells treated with the p38 α inhibitor, SB203580 + trametinib show small decreases in viability compared to trametinib alone. However, SB203580 + selumetinib (which does not inhibit p38 α) show larger decreases in cell viability compared to selumetinib alone. The findings suggest that p38 α inhibition functionally reduces cell viability of melanoma cells. Taken together, this evidence supports p38 α MAPK as a previously uncharacterized off-target effect of trametinib, which may enhance the beneficial cellular response to this drug. In any case, although this effect is only observed at drug concentrations ~300-fold higher than clinical dosing in patients, preclinical studies often use trametinib concentrations of 10 μ M or higher. Therefore, off-target effects on p38 α MAPK must be considered in studies of trametinib.

Comparing ERK1/2 inhibitors using phosphoproteomics

ERK1/2 inhibitors are emerging as a promising strategy to build on the success seen in targeting multiple points upstream in the MAPK pathway, and to combat the development of resistance to targeted BRAF V600E/K and MKK1/2 inhibitors that are commonly seen in patients. Many of these resistance mechanisms involve re-activation of ERK1/2, and preclinical

studies have shown that inhibitors targeting ERK1/2 are able to overcome resistance to BRAF V600E/K and MKK1/2 inhibitors (Morris et al., 2013). Our lab has previously published evidence that ERK1/2 inhibitors show differences in conformational selectivity upon binding ERK2 (Rudolph et al., 2015). Therefore, I performed phosphoproteomic SILAC experiments comparing ERK1/2 inhibitors, in order to determine if these conformational selection preferences were accompanied by differences in downstream phosphorylation events. In one experiment, the ERK1/2 inhibitor SCH772984 was compared to Vertex-11e, which is structurally related to Vertex-745 currently undergoing clinical trials. A triple labeled SILAC screen (DMSO-SCH772984-Vertex-11e) identified 2,701 phosphosites, 1,163 of which were reproducibly quantified in two or more replicate experiments. Like the previous comparisons, the phosphosites regulated by SCH772984 and Vertex-11e showed almost complete overlap, indicating that different ERK conformational binding characteristics had little to no effect on downstream drug targets. The second screen compared SCH772984 to GDC0994, which is currently in clinical trials (DMSO-SCH772984-GDC0994). I identified 6,893 phosphosites in total, and among the 4,436 phosphosites quantified in two or three replicates, 25 were significantly regulated by GDC0994 and not SCH772984 while only 3 were unique to SCH772984 (Fig. 2.8G, Table 2.4). These unique targets were also unaffected by treatment with other MKK1/2 and ERK1/2 inhibitors (Table 2.9). Potentially, the targets unique to GDC0994 may reflect the distinct conformational selection by this compound, compared to SCH772984. This finding is relevant to current and future clinical trials involving GDC0994, and requires further studies to correlate the effects across many different compounds. Among the novel off-targets, a group of genes regulating protein translation mRNA binding and initiation was identified using STRING protein interaction mapping and included EIF4G1, LARP1, LARP1B, and HNRNPM (Fig. 2.14).

Coordinated regulation of this group of genes might reflect selective regulation of mRNA processing and/or translation, and further studies are needed to investigate this possibility.

Combined phosphoproteomics MAPK inhibitor datasets provide an unparalleled resource for discovery of off target effects

With the completion of my thesis work, our lab has now generated SILAC-based phosphoproteomics data in a single melanoma cell line, WM239a, treated with the BRAF V600E/K inhibitor vemurafenib, the MKK1/2 inhibitors selumetinib and trametinib, and the ERK1/2 inhibitors SCH772984, GDC0994, and Vertex-11e. Comparing the cellular response to inhibitors targeting different levels of the MAPK pathway will lead to a better understanding of the network of signaling responses to MAPK inhibition and interactions with other pathways.

Table 2.7 lists 150 phosphosite targets significantly regulated by all MAPK inhibitors tested and reveals both known and novel targets. Nine of these sites significantly increase phosphorylation in response to inhibitor, and may indicate changes in feedback inhibition or reductions in phosphatase activity. In order to determine potential direct targets, I have compiled information from several sources. First, ERK1/2 is known to preferentially phosphorylate proline driven Ser and Thr residues with a sequence (S/T)P or PX(S/T)P motif. Phosphosites with these motifs underwent further validating by identifying proteins with the ERK binding d-domain and DEF domains. DEF domains were identified manually 6-20 residues C-terminal of the phosphorylated residue (Cargnello & Roux, 2011) and d-domains were identified using a large-scale d-domain profiling study (Zeke et al., 2015) and ScanSite3 high confidence identification (Obenauer, Cantley, & Yaffe, 2003), and mapped to protein sequences to determine the distance from the identified phosphorylated residue. Next, known ERK substrates and phosphorylated

residues were compiled from (Carlson et al., 2011; Yoon & Seger, 2006) and ERK interactors were identified from (von Kriegsheim et al., 2009). Finally, the phosphosite plus database (Hornbeck et al., 2015) downloads for phosphosites with known kinase regulation and protein regulatory function indicate sites that are known to be directly regulated by ERK. These different sources of information allow us to locate likely direct ERK target phosphosites and identify potential novel substrates of ERK.

My findings support previous work revealing linear pathway organization of RAF-MKK-ERK signaling, by identifying only three phosphosites uniquely regulated by two MKK1/2 inhibitors but not two ERK1/2 inhibitors tested (S893-GEN1, S612-NUP98, and S455-MAP3K7/TAK1, Table 2.8). TAK1 is known to activate MKK3/6 and undergoes negative feedback regulation through p38 α signaling to its binding partner TAB1. It is interesting that both trametinib and selumetinib increase the phosphorylation at this site, yet only trametinib inhibits phosphorylation of downstream p38 α MAPK and the p38 α substrate EPS15. Although p38 MAPK is the primary substrate of MKK3/6 (similar to ERK1/2 and MKK1/2), upstream activation of MKK3/6 by cellular and environmental stress signals is not yet fully understood.

My composite phosphoproteomic dataset is also useful for identifying unique targets that reflect potential off-target effects of individual compounds. I have identified 48 phosphosites that specifically respond to only one MKK1/2 or ERK1/2 inhibitor. These phosphosites are likely off-target effects specific to each compound and are good candidates for follow up analysis, using methods similar to those I used in my investigations of p38 α MAPK inhibition by trametinib. I have now built a database of phosphoproteomics changes in response to BRAF V600E/K, MKK1/2, and ERK1/2 inhibitors across four separate SILAC experiments. This dataset will be a valuable resource for the development of new targeted therapies in melanoma. Future studies

may use this database to quickly profile the targets in common with these MAPK inhibitors, in order to identify shared or off-target effects during drug development and identify potential biomarkers for drug treatment.

3.2 Future experiments

The significance of inhibiting p38 α MAPK activity in melanoma is largely unknown, considering that high concentrations of trametinib only decrease p38 α phosphorylation ~50% in cells. The p38 pathway has been reported to have both oncogenic and tumor suppressive effects depending on both the cell type and the type of pathway stimulation. But there is evidence that p38 signaling protects UV-treated melanoma cells from apoptosis (Ivanov & Ronai, 2000), given that melanoma cells expressing constitutively active MKK6 show decreased basal and UV-induced cell death compared to controls, while a catalytically inactive mutant increased the percentage of cell death in response to UV irradiation. To determine if p38 acts as a pro-survival pathway vs inhibits cell viability under normal conditions, future studies are needed to treat cancer cell lines with p38 α/β inhibitors (e.g. SB203580), or by siRNA knockdowns or gene editing of MKK3, MKK6, p38 α , and p38 β , measuring cell viability using the CellTiter Glo assay and apoptosis using annexin V-PI flow cytometry. These results can then be compared to cells where p38 MAPK signaling is activated by hyperosmotic stress or UV-irradiation. Any differences can be followed up by a phosphoproteomic screen of cells treated in parallel to look for p38-specific targets and manually validate candidate effectors that may contribute to apoptosis or survival.

Appendix I. Human Phospho-Kinase Antibody Array. Changes in kinase phosphorylation in response to 10 μ M treatment for 4 h with MKK1/2 inhibitor selumetinib (AZD) or ERK1/2 inhibitors SCH772984 (SCH) and Vertex-11e (VTX)



Appendix I. Human Phospho-Kinase Antibody Array. Changes in kinase phosphorylation in response to 10 μ M treatment for 4 h with MKK1/2 inhibitor selumetinib (AZD) or ERK1/2 inhibitors SCH772984 (SCH) and Vertex-11e (VTX)



Appendix I. Human Phospho-Kinase Antibody Array. Changes in kinase phosphorylation in response to 10 μ M treatment for 4 h with MKK1/2 inhibitor selumetinib (AZD) or ERK1/2 inhibitors SCH772984 (SCH) and Vertex-11e (VTX)



Bibliography

- Ahn, N. (1993). The MAP kinase cascade. Discovery of a new signal transduction pathway. *Mol. Cell. Biochem.*, *127/128*, 201–209.
- Akbani, R., Akdemir, K. C., Aksoy, B. A., Albert, M., Alty, A., Amin, S. B., ... Zou, L. (2015). Genomic Classification of Cutaneous Melanoma. *Cell*, *161*(7), 1681–1696. <https://doi.org/10.1016/j.cell.2015.05.044>
- American Cancer Society. (2016). Cancer Facts & Figures 2016. *Cancer Facts & Figures 2016*, 1–9. <https://doi.org/10.1097/01.NNR.0000289503.22414.79>
- Aronov, A. M., Tang, Q., Martinez-Botella, G., Bemis, G. W., Cao, J., Chen, G., ... Xie, X. (2009). Structure-guided design of potent and selective pyrimidylpyrrole inhibitors of extracellular signal-regulated kinase (ERK) using conformational control. *Journal of Medicinal Chemistry*, *52*(20), 6362–8. <https://doi.org/10.1021/jm900630q>
- Ascierto, P. A., McArthur, G. A., Dréno, B., Atkinson, V., Liskay, G., Di Giacomo, A. M., ... Larkin, J. (2016). Cobimetinib combined with vemurafenib in advanced BRAF(V600)-mutant melanoma (coBRIM): updated efficacy results from a randomised, double-blind, phase 3 trial. *The Lancet. Oncology*, *17*(9), 1248–60. [https://doi.org/10.1016/S1470-2045\(16\)30122-X](https://doi.org/10.1016/S1470-2045(16)30122-X)
- Boland, G. M., & Gershenwald, J. E. (2016). Principles of Melanoma Staging. *Cancer Treatment and Research*, *167*, 131–48. https://doi.org/10.1007/978-3-319-22539-5_5
- Bollag, G., Hirth, P., Tsai, J., Zhang, J., Ibrahim, P. N., Cho, H., ... Nolop, K. (2010). Clinical efficacy of a RAF inhibitor needs broad target blockade in BRAF-mutant melanoma. *Nature*, *467*(7315), 596–9. <https://doi.org/10.1038/nature09454>
- Burotto, M., Chiou, V. L., Lee, J. M., & Kohn, E. C. (2014). The MAPK pathway across different malignancies: a new perspective. *Cancer*, *120*(22), 3446–3456. <https://doi.org/10.1002/cncr.28864>
- Cargnello, M., & Roux, P. P. (2011). Activation and function of the MAPKs and their substrates, the MAPK-activated protein kinases. *Microbiology and Molecular Biology Reviews* : *MMBR*, *75*(1), 50–83. <https://doi.org/10.1128/MMBR.00031-10>
- Carlson, S. M., Chouinard, C. R., Labadorf, A., Lam, C. J., Schmelzle, K., Fraenkel, E., & White, F. M. (2011). Large-scale discovery of ERK2 substrates identifies ERK-mediated transcriptional regulation by ETV3. *Science Signaling*, *4*(196), rs11. <https://doi.org/10.1126/scisignal.2002010>
- Carvajal, R. D., Sosman, J. A., Quevedo, J. F., Milhem, M. M., Joshua, A. M., Kudchadkar, R. R., ... Schwartz, G. K. (2014). Effect of selumetinib vs chemotherapy on progression-free survival in uveal melanoma: a randomized clinical trial. *JAMA*, *311*(23), 2397–405. <https://doi.org/10.1001/jama.2014.6096>

- Chaikuad, A., Tacconi, E. M. C., Zimmer, J., Liang, Y., Gray, N. S., Tarsounas, M., & Knapp, S. (2014). A unique inhibitor binding site in ERK1/2 is associated with slow binding kinetics. *Nature Chemical Biology*, *10*(10), 853–60. <https://doi.org/10.1038/nchembio.1629>
- Chang, A. E., Karnell, L. H., & Menck, H. R. (1998). The National Cancer Data Base report on cutaneous and noncutaneous melanoma: a summary of 84,836 cases from the past decade. The American College of Surgeons Commission on Cancer and the American Cancer Society. *Cancer*, *83*(8), 1664–78. Retrieved from <http://www.ncbi.nlm.nih.gov/pubmed/9781962>
- Chapman, P. B., Hauschild, A., Robert, C., Haanen, J. B., Ascierto, P., Larkin, J., ... BRIM-3 Study Group. (2011). Improved survival with vemurafenib in melanoma with BRAF V600E mutation. *The New England Journal of Medicine*, *364*(26), 2507–16. <https://doi.org/10.1056/NEJMoa1103782>
- Cheung, P. C. F., Campbell, D. G., Nebreda, A. R., & Cohen, P. (2003). Feedback control of the protein kinase TAK1 by SAPK2a/p38alpha. *The EMBO Journal*, *22*(21), 5793–805. <https://doi.org/10.1093/emboj/cdg552>
- Clark, W. H., From, L., Bernardino, E. A., & Mihm, M. C. (1969). The histogenesis and biologic behavior of primary human malignant melanomas of the skin. *Cancer Research*, *29*(3), 705–27. Retrieved from <http://www.ncbi.nlm.nih.gov/pubmed/5773814>
- Cohen, P. (1997). The search for physiological substrates of MAP and SAP kinases in mammalian cells. *Trends in Cell Biology*, *7*(9), 353–61. [https://doi.org/10.1016/S0962-8924\(97\)01105-7](https://doi.org/10.1016/S0962-8924(97)01105-7)
- Coit, D. G., Thompson, J. A., Algazi, A., Andtbacka, R., Bichakjian, C. K., Carson, W. E., ... Engh, A. (2016). NCCN Guidelines Insights: Melanoma, Version 3.2016. *Journal of the National Comprehensive Cancer Network : JNCCN*, *14*(8), 945–58. Retrieved from <http://www.ncbi.nlm.nih.gov/pubmed/27496110>
- Courcelles, M., Frémin, C., Voisin, L., Lemieux, S., Meloche, S., & Thibault, P. (2013). Phosphoproteome dynamics reveal novel ERK1/2 MAP kinase substrates with broad spectrum of functions. *Molecular Systems Biology*, *9*, 669. <https://doi.org/10.1038/msb.2013.25>
- Cox, J., & Mann, M. (2008). *MaxQuant enables high peptide identification rates, individualized p.p.b.-range mass accuracies and proteome-wide protein quantification*. *Nature biotechnology* (Vol. 26). <https://doi.org/10.1038/nbt.1511>
- Cuadrado, A., & Nebreda, A. R. (2010). Mechanisms and functions of p38 MAPK signalling. *The Biochemical Journal*, *429*, 403–417. <https://doi.org/10.1042/BJ20100323>
- Cuenda, A., & Rousseau, S. (2007). p38 MAP-kinases pathway regulation, function and role in human diseases. *Biochimica et Biophysica Acta (BBA) - Molecular Cell Research*, *1773*(8), 1358–1375. <https://doi.org/10.1016/j.bbamcr.2007.03.010>

- Curtin, J. A., Fridlyand, J., Kageshita, T., Patel, H. N., Busam, K. J., Kutzner, H., ... Bastian, B. C. (2005). Distinct sets of genetic alterations in melanoma. *The New England Journal of Medicine*, 353(20), 2135–47. <https://doi.org/10.1056/NEJMoa050092>
- Davies, B. R., Logie, A., McKay, J. S., Martin, P., Steele, S., Jenkins, R., ... Smith, P. D. (2007). AZD6244 (ARRY-142886), a potent inhibitor of mitogen-activated protein kinase/extracellular signal-regulated kinase 1/2 kinases: mechanism of action in vivo, pharmacokinetic/pharmacodynamic relationship, and potential for combination in preclinical. *Molecular Cancer Therapeutics*, 6(8), 2209–19. <https://doi.org/10.1158/1535-7163.MCT-07-0231>
- Davies, H., Bignell, G. R., Cox, C., Stephens, P., Edkins, S., Clegg, S., ... Futreal, P. A. (2002). Mutations of the BRAF gene in human cancer. *Nature*, 417(6892), 949–54. <https://doi.org/10.1038/nature00766>
- Dérijard, B., Raingeaud, J., Barrett, T., Wu, I. H., Han, J., Ulevitch, R. J., & Davis, R. J. (1995). Independent human MAP-kinase signal transduction pathways defined by MEK and MKK isoforms. *Science (New York, N.Y.)*, 267(5198), 682–5. Retrieved from <http://www.ncbi.nlm.nih.gov/pubmed/7839144>
- Dougherty, M. K., Müller, J., Ritt, D. A., Zhou, M., Zhou, X. Z., Copeland, T. D., ... Morrison, D. K. (2005). Regulation of Raf-1 by direct feedback phosphorylation. *Molecular Cell*, 17(2), 215–24. <https://doi.org/10.1016/j.molcel.2004.11.055>
- Drew, B. A., Burow, M. E., & Beckman, B. S. (2012). MEK5/ERK5 pathway: the first fifteen years. *Biochimica et Biophysica Acta*, 1825(1), 37–48. <https://doi.org/10.1016/j.bbcan.2011.10.002>
- Eblen, S. T., Kumar, N. V., Shah, K., Henderson, M. J., Watts, C. K. W., Shokat, K. M., & Weber, M. J. (2003). Identification of novel ERK2 substrates through use of an engineered kinase and ATP analogs. *The Journal of Biological Chemistry*, 278(17), 14926–35. <https://doi.org/10.1074/jbc.M300485200>
- Enslin, H., Brancho, D. M., & Davis, R. J. (2000). Molecular determinants that mediate selective activation of p38 MAP kinase isoforms. *The EMBO Journal*, 19(6), 1301–1311. <https://doi.org/10.1093/emboj/19.6.1301>
- Fedorenko, I. V., Gibney, G. T., Sondak, V. K., & Smalley, K. S. M. (2015). Beyond BRAF: where next for melanoma therapy? *British Journal of Cancer*, 112(2), 217–26. <https://doi.org/10.1038/bjc.2014.476>
- Flaherty, K. T., Hodi, F. S., & Fisher, D. E. (2012). From genes to drugs: targeted strategies for melanoma. *Nature Reviews Cancer*, 12(5), 349–361. <https://doi.org/10.1038/nrc3218>
- Flaherty, K. T., Infante, J. R., Daud, A., Gonzalez, R., Kefford, R. F., Sosman, J., ... Weber, J. (2012). Combined BRAF and MEK inhibition in melanoma with BRAF V600 mutations. *The New England Journal of Medicine*, 367(18), 1694–703. <https://doi.org/10.1056/NEJMoa1210093>

- Forbes, S. A., Bindal, N., Bamford, S., Cole, C., Kok, C. Y., Beare, D., ... Futreal, P. A. (2011). COSMIC: mining complete cancer genomes in the Catalogue of Somatic Mutations in Cancer. *Nucleic Acids Research*, 39(Database issue), D945-50. <https://doi.org/10.1093/nar/gkq929>
- Franklin, C., Livingstone, E., Roesch, A., Schilling, B., & Schadendorf, D. (2016). Immunotherapy in melanoma: Recent advances and future directions. *European Journal of Surgical Oncology : The Journal of the European Society of Surgical Oncology and the British Association of Surgical Oncology*. <https://doi.org/10.1016/j.ejso.2016.07.145>
- Freshney, N. W., Rawlinson, L., Guesdon, F., Jones, E., Cowley, S., Hsuan, J., & Saklatvala, J. (1994). Interleukin-1 activates a novel protein kinase cascade that results in the phosphorylation of Hsp27. *Cell*, 78(6), 1039–49. Retrieved from <http://www.ncbi.nlm.nih.gov/pubmed/7923354>
- Galan, J. A., Geraghty, K. M., Lavoie, G., Kanshin, E., Tcherkezian, J., Calabrese, V., ... Roux, P. P. (2014). Phosphoproteomic analysis identifies the tumor suppressor PDCD4 as a RSK substrate negatively regulated by 14-3-3. *Proceedings of the National Academy of Sciences of the United States of America*, 111(29), E2918-27. <https://doi.org/10.1073/pnas.1405601111>
- Gilmartin, A. G., Bleam, M. R., Groy, A., Moss, K. G., Minthorn, E. A., Kulkarni, S. G., ... Laquerre, S. G. (2011). GSK1120212 (JTP-74057) is an inhibitor of MEK activity and activation with favorable pharmacokinetic properties for sustained in vivo pathway inhibition. *Clinical Cancer Research*, 17(5), 989–1000. <https://doi.org/10.1158/1078-0432.CCR-10-2200>
- Gnad, F., Doll, S., Song, K., Stokes, M. P., Moffat, J., Liu, B., ... Belvin, M. (2016). Phosphoproteome analysis of the MAPK pathway reveals previously undetected feedback mechanisms. *Proteomics*, 16(14), 1998–2004. <https://doi.org/10.1002/pmic.201600119>
- Goedert, M., Cuenda, A., Craxton, M., Jakes, R., & Cohen, P. (1997). Activation of the novel stress-activated protein kinase SAPK4 by cytokines and cellular stresses is mediated by SKK3 (MKK6); comparison of its substrate specificity with that of other SAP kinases. *The EMBO Journal*, 16(12), 3563–71. <https://doi.org/10.1093/emboj/16.12.3563>
- Gray-Schopfer, V., Wellbrock, C., & Marais, R. (2007). Melanoma biology and new targeted therapy. *Nature*, 445(7130), 851–7. <https://doi.org/10.1038/nature05661>
- Han, J., Lee, J. D., Bibbs, L., & Ulevitch, R. J. (1994). A MAP kinase targeted by endotoxin and hyperosmolarity in mammalian cells. *Science (New York, N.Y.)*, 265(5173), 808–11. Retrieved from <http://www.ncbi.nlm.nih.gov/pubmed/7914033>
- Han, J., Wang, X., Jiang, Y., Ulevitch, R. J., & Lin, S. (1997). Identification and characterization of a predominant isoform of human MKK3. *FEBS Letters*, 403(1), 19–22. [https://doi.org/10.1016/S0014-5793\(97\)00021-5](https://doi.org/10.1016/S0014-5793(97)00021-5)

- Hartsough, E., Shao, Y., & Aplin, A. E. (2014). Resistance to RAF inhibitors revisited. *The Journal of Investigative Dermatology*, *134*(2), 319–25. <https://doi.org/10.1038/jid.2013.358>
- Hauschild, A., Grob, J.-J., Demidov, L. V, Jouary, T., Gutzmer, R., Millward, M., ... Chapman, P. B. (2012). Dabrafenib in BRAF-mutated metastatic melanoma: a multicentre, open-label, phase 3 randomised controlled trial. *Lancet (London, England)*, *380*(9839), 358–65. [https://doi.org/10.1016/S0140-6736\(12\)60868-X](https://doi.org/10.1016/S0140-6736(12)60868-X)
- Hindley, A., & Kolch, W. (2002). Extracellular signal regulated kinase (ERK)/mitogen activated protein kinase (MAPK)-independent functions of Raf kinases. *Journal of Cell Science*, *115*(Pt 8), 1575–81. Retrieved from <http://www.ncbi.nlm.nih.gov/pubmed/11950876>
- Hodis, E., Watson, I. R., Kryukov, G. V, Arold, S. T., Imielinski, M., Theurillat, J.-P., ... Chin, L. (2012). A landscape of driver mutations in melanoma. *Cell*, *150*(2), 251–63. <https://doi.org/10.1016/j.cell.2012.06.024>
- Hornbeck, P. V, Zhang, B., Murray, B., Kornhauser, J. M., Latham, V., & Skrzypek, E. (2015). PhosphoSitePlus, 2014: mutations, PTMs and recalibrations. *Nucleic Acids Research*, *43*(Database issue), D512–20. <https://doi.org/10.1093/nar/gku1267>
- Infante, J. R., Fecher, L. A., Falchook, G. S., Nallapareddy, S., Gordon, M. S., Becerra, C., ... Messersmith, W. A. (2012). Safety, pharmacokinetic, pharmacodynamic, and efficacy data for the oral MEK inhibitor trametinib: A phase 1 dose-escalation trial. *The Lancet Oncology*, *13*(8), 773–781. [https://doi.org/10.1016/S1470-2045\(12\)70270-X](https://doi.org/10.1016/S1470-2045(12)70270-X)
- Ivanov, V. N., & Ronai, Z. (2000). p38 protects human melanoma cells from UV-induced apoptosis through down-regulation of NF-kappaB activity and Fas expression. *Oncogene*, *19*(26), 3003–12. <https://doi.org/10.1038/sj.onc.1203602>
- Jha, S., Morris, E. J., Hruza, A., Mansueto, M. S., Schroeder, G., Arbanas, J., ... Samatar, A. A. (2016). Dissecting Therapeutic Resistance to ERK Inhibition. *Molecular Cancer Therapeutics*, *15*(April), 548–560. <https://doi.org/10.1158/1535-7163.MCT-15-0172>
- Jiang, Y., Gram, H., Zhao, M., New, L., Gu, J., Feng, L., ... Han, J. (1997). Characterization of the structure and function of the fourth member of p38 group mitogen-activated protein kinases, p38delta. *The Journal of Biological Chemistry*, *272*(48), 30122–8. Retrieved from <http://www.ncbi.nlm.nih.gov/pubmed/9374491>
- Johnson, G. L., & Lapadat, R. (2002). Mitogen-activated protein kinase pathways mediated by ERK, JNK, and p38 protein kinases. *Science (New York, N.Y.)*, *298*(5600), 1911–2. <https://doi.org/10.1126/science.1072682>
- Katz, M., Amit, I., & Yarden, Y. (2007). Regulation of MAPKs by growth factors and receptor tyrosine kinases. *Biochimica et Biophysica Acta*, *1773*(8), 1161–76. <https://doi.org/10.1016/j.bbamcr.2007.01.002>

- Kirkwood, J. M., Bastholt, L., Robert, C., Sosman, J., Larkin, J., Hersey, P., ... Dummer, R. (2012). Phase II, open-label, randomized trial of the MEK1/2 inhibitor selumetinib as monotherapy versus temozolomide in patients with advanced melanoma. *Clinical Cancer Research : An Official Journal of the American Association for Cancer Research*, 18(2), 555–67. <https://doi.org/10.1158/1078-0432.CCR-11-1491>
- Klein, O., Clements, A., Menzies, A. M., O'Toole, S., Kefford, R. F., & Long, G. V. (2013). BRAF inhibitor activity in V600R metastatic melanoma. *European Journal of Cancer (Oxford, England : 1990)*, 49(5), 1073–9. <https://doi.org/10.1016/j.ejca.2012.11.004>
- Koo, H.-M., VanBrocklin, M., McWilliams, M. J., Leppla, S. H., Duesbery, N. S., & Vande Woude, G. F. (2002). Apoptosis and melanogenesis in human melanoma cells induced by anthrax lethal factor inactivation of mitogen-activated protein kinase kinase. *Proceedings of the National Academy of Sciences of the United States of America*, 99(5), 3052–7. <https://doi.org/10.1073/pnas.052707699>
- Kosako, H., Yamaguchi, N., Aranami, C., Ushiyama, M., Kose, S., Imamoto, N., ... Hattori, S. (2009). Phosphoproteomics reveals new ERK MAP kinase targets and links ERK to nucleoporin-mediated nuclear transport. *Nature Structural & Molecular Biology*, 16(10), 1026–35. <https://doi.org/10.1038/nsmb.1656>
- Krepler, C., Xiao, M., Sproesser, K., Brafford, P. A., Shannan, B., Beqiri, M., ... Herlyn, M. (2016). Personalized Preclinical Trials in BRAF Inhibitor-Resistant Patient-Derived Xenograft Models Identify Second-Line Combination Therapies. *Clinical Cancer Research : An Official Journal of the American Association for Cancer Research*, 22(7), 1592–602. <https://doi.org/10.1158/1078-0432.CCR-15-1762>
- Ku, B. M., Jho, E. H., Bae, Y.-H., Sun, J.-M., Ahn, J. S., Park, K., & Ahn, M.-J. (2015). BYL719, a selective inhibitor of phosphoinositide 3-Kinase α , enhances the effect of selumetinib (AZD6244, ARRY-142886) in KRAS-mutant non-small cell lung cancer. *Investigational New Drugs*, 33(1), 12–21. <https://doi.org/10.1007/s10637-014-0163-9>
- Lali, F. V., Hunt, A. E., Turner, S. J., & Foxwell, B. M. (2000). The pyridinyl imidazole inhibitor SB203580 blocks phosphoinositide-dependent protein kinase activity, protein kinase B phosphorylation, and retinoblastoma hyperphosphorylation in interleukin-2-stimulated T cells independently of p38 mitogen-activated prot. *The Journal of Biological Chemistry*, 275(10), 7395–402. Retrieved from <http://www.ncbi.nlm.nih.gov/pubmed/10702313>
- Le, K., Blomain, E. S., Rodeck, U., & Aplin, A. E. (2013). Selective RAF inhibitor impairs ERK1/2 phosphorylation and growth in mutant NRAS, vemurafenib-resistant melanoma cells. *Pigment Cell & Melanoma Research*, 26(4), 509–17. <https://doi.org/10.1111/pcmr.12092>
- Lee, J. C., Laydon, J. T., McDonnell, P. C., Gallagher, T. F., Kumar, S., Green, D., ... Landvatter, S. W. (n.d.). A protein kinase involved in the regulation of inflammatory cytokine biosynthesis. *Nature*, 372(6508), 739–46. <https://doi.org/10.1038/372739a0>

- Lewis, T. S., Hunt, J. B., Aveline, L. D., Jonscher, K. R., Louie, D. F., Yeh, J. M., ... Ahn, N. G. (2000). Identification of novel MAP kinase pathway signaling targets by functional proteomics and mass spectrometry. *Molecular Cell*, 6(6), 1343–54. Retrieved from <http://www.ncbi.nlm.nih.gov/pubmed/11163208>
- Ley, T. J., Mardis, E. R., Ding, L., Fulton, B., McLellan, M. D., Chen, K., ... Wilson, R. K. (2008). DNA sequencing of a cytogenetically normal acute myeloid leukaemia genome. *Nature*, 456(7218), 66–72. <https://doi.org/10.1038/nature07485>
- Mann, M. (2006). Functional and quantitative proteomics using SILAC. *Nature Reviews. Molecular Cell Biology*, 7(12), 952–8. <https://doi.org/10.1038/nrm2067>
- Mardis, E. R., Ding, L., Dooling, D. J., Larson, D. E., McLellan, M. D., Chen, K., ... Ley, T. J. (2009). Recurring mutations found by sequencing an acute myeloid leukemia genome. *The New England Journal of Medicine*, 361(11), 1058–66. <https://doi.org/10.1056/NEJMoa0903840>
- Margolin, A. A., Ong, S.-E., Schenone, M., Gould, R., Schreiber, S. L., Carr, S. A., & Golub, T. R. (2009). Empirical Bayes analysis of quantitative proteomics experiments. *PloS One*, 4(10), e7454. <https://doi.org/10.1371/journal.pone.0007454>
- Matallanas, D., Birtwistle, M., Romano, D., Zebisch, A., Rauch, J., von Kriegsheim, A., & Kolch, W. (2011). Raf family kinases: old dogs have learned new tricks. *Genes & Cancer*, 2(3), 232–60. <https://doi.org/10.1177/1947601911407323>
- Mavrogonatou, E., & Kletsas, D. (2009). High osmolality activates the G1 and G2 cell cycle checkpoints and affects the DNA integrity of nucleus pulposus intervertebral disc cells triggering an enhanced DNA repair response. *DNA Repair*, 8(8), 930–943. <https://doi.org/10.1016/j.dnarep.2009.05.005>
- Mavrogonatou, E., & Kletsas, D. (2012). Differential response of nucleus pulposus intervertebral disc cells to high salt, sorbitol, and urea. *Journal of Cellular Physiology*, 227(3), 1179–87. <https://doi.org/10.1002/jcp.22840>
- McArthur, G. A., & Ribas, A. (2013). Targeting oncogenic drivers and the immune system in melanoma. *Journal of Clinical Oncology : Official Journal of the American Society of Clinical Oncology*, 31(4), 499–506. <https://doi.org/10.1200/JCO.2012.45.5568>
- McGovern, V. J., Mihm, M. C., Bailly, C., Booth, J. C., Clark, W. H., Cochran, A. J., ... Milton, G. W. (1973). The classification of malignant melanoma and its histologic reporting. *Cancer*, 32(6), 1446–57. Retrieved from <http://www.ncbi.nlm.nih.gov/pubmed/4757934>
- Mendoza, M. C., Er, E. E., & Blenis, J. (2011). The Ras-ERK and PI3K-mTOR pathways: cross-talk and compensation. *Trends in Biochemical Sciences*, 36(6), 320–328. <https://doi.org/10.1016/j.tibs.2011.03.006>
- Miller, A. J., & Mihm, M. C. (2006). Melanoma. *The New England Journal of Medicine*, 355(1), 51–65. <https://doi.org/10.1056/NEJMra052166>

- Morris, E. J., Jha, S., Restaino, C. R., Dayananth, P., Zhu, H., Cooper, A., ... Samatar, A. A. (2013). Discovery of a novel ERK inhibitor with activity in models of acquired resistance to BRAF and MEK inhibitors. *Cancer Discovery*, 3(7), 742–750. <https://doi.org/10.1158/2159-8290.CD-13-0070>
- Nazarian, R., Shi, H., Wang, Q., Kong, X., Koya, R. C., Lee, H., ... Lo, R. S. (2010). Melanomas acquire resistance to B-RAF(V600E) inhibition by RTK or N-RAS upregulation. *Nature*, 468(7326), 973–7. <https://doi.org/10.1038/nature09626>
- Obenauer, J. C., Cantley, L. C., & Yaffe, M. B. (2003). Scansite 2.0: Proteome-wide prediction of cell signaling interactions using short sequence motifs. *Nucleic Acids Research*, 31(13), 3635–41. Retrieved from <http://www.ncbi.nlm.nih.gov/pubmed/12824383>
- Old, W. M., Shabb, J. B., Houel, S., Wang, H., Coutts, K. L., Yen, C.-Y., ... Ahn, N. G. (2009). Functional proteomics identifies targets of phosphorylation by B-Raf signaling in melanoma. *Molecular Cell*, 34(1), 115–31. <https://doi.org/10.1016/j.molcel.2009.03.007>
- Pan, C., Olsen, J. V., Daub, H., & Mann, M. (2009). Global effects of kinase inhibitors on signaling networks revealed by quantitative phosphoproteomics. *Molecular & Cellular Proteomics : MCP*, 8(12), 2796–808. <https://doi.org/10.1074/mcp.M900285-MCP200>
- Pfeifer, G. P., You, Y.-H., & Besaratinia, A. (2005). Mutations induced by ultraviolet light. *Mutation Research*, 571(1–2), 19–31. <https://doi.org/10.1016/j.mrfmmm.2004.06.057>
- Pleasance, E. D., Cheetham, R. K., Stephens, P. J., McBride, D. J., Humphray, S. J., Greenman, C. D., ... Stratton, M. R. (2010). A comprehensive catalogue of somatic mutations from a human cancer genome. *Nature*, 463(7278), 191–6. <https://doi.org/10.1038/nature08658>
- Pleasance, E. D., Stephens, P. J., O’Meara, S., McBride, D. J., Meynert, A., Jones, D., ... Campbell, P. J. (2010). A small-cell lung cancer genome with complex signatures of tobacco exposure. *Nature*, 463(7278), 184–90. <https://doi.org/10.1038/nature08629>
- Poss, Z. C., Ebmeier, C. C., Odell, A. T., Tangpeerachaikul, A., Lee, T., Pelish, H. E., ... Taatjes, D. J. (2016). Identification of Mediator Kinase Substrates in Human Cells using Cortistatin A and Quantitative Phosphoproteomics. *Cell Reports*, 15(2), 436–450. <https://doi.org/10.1016/j.celrep.2016.03.030>
- Poulikakos, P. I., Persaud, Y., Janakiraman, M., Kong, X., Ng, C., Moriceau, G., ... Solit, D. B. (2011). RAF inhibitor resistance is mediated by dimerization of aberrantly spliced BRAF(V600E). *Nature*, 480(7377), 387–90. <https://doi.org/10.1038/nature10662>
- Pulverer, B. J., Kyriakis, J. M., Avruch, J., Nikolakaki, E., & Woodgett, J. R. (1991). Phosphorylation of c-jun mediated by MAP kinases. *Nature*, 353(6345), 670–4. <https://doi.org/10.1038/353670a0>

- Raingeaud, J., Whitmarsh, A. J., Barrett, T., Dérijard, B., & Davis, R. J. (1996). MKK3- and MKK6-regulated gene expression is mediated by the p38 mitogen-activated protein kinase signal transduction pathway. *Mol Cell Biol*, *16*(3), 1247–1255. <https://doi.org/10.1128/MCB.16.3.1247>
- Rebecca, V. W., Wood, E., Fedorenko, I. V., Paraiso, K. H. T., Haarberg, H. E., Chen, Y., ... Smalley, K. S. M. (2014). Evaluating melanoma drug response and therapeutic escape with quantitative proteomics. *Molecular & Cellular Proteomics : MCP*, *13*(7), 1844–54. <https://doi.org/10.1074/mcp.M113.037424>
- Ritchie, M. E., Phipson, B., Wu, D., Hu, Y., Law, C. W., Shi, W., & Smyth, G. K. (2015). limma powers differential expression analyses for RNA-sequencing and microarray studies. *Nucleic Acids Research*, *43*(7), e47. <https://doi.org/10.1093/nar/gkv007>
- Robarge, K., Schwarz, J., Blake, J., Burkard, M., Chan, J., Chen, H., ... Moffat, J. G. (2014). Abstract DDT02-03: Discovery of GDC-0994, a potent and selective ERK1/2 inhibitor in early clinical development. *Cancer Research*, *74*(19 Supplement), DDT02-03-DDT02-03. <https://doi.org/10.1158/1538-7445.AM2014-DDT02-03>
- Robert, C., Dummer, R., Gutzmer, R., Lorigan, P., Kim, K. B., Nyakas, M., ... Middleton, M. R. (2013). Selumetinib plus dacarbazine versus placebo plus dacarbazine as first-line treatment for BRAF-mutant metastatic melanoma: a phase 2 double-blind randomised study. *The Lancet. Oncology*, *14*(8), 733–40. [https://doi.org/10.1016/S1470-2045\(13\)70237-7](https://doi.org/10.1016/S1470-2045(13)70237-7)
- Roberts, P. J., & Der, C. J. (2007). Targeting the Raf-MEK-ERK mitogen-activated protein kinase cascade for the treatment of cancer. *Oncogene*, *26*(22), 3291–310. <https://doi.org/10.1038/sj.onc.1210422>
- Roskoski, R. (2012). MEK1/2 dual-specificity protein kinases: structure and regulation. *Biochemical and Biophysical Research Communications*, *417*(1), 5–10. <https://doi.org/10.1016/j.bbrc.2011.11.145>
- Rouse, J., Cohen, P., Trigon, S., Morange, M., Alonso-Llamazares, A., Zamanillo, D., ... Nebreda, A. R. (1994). A novel kinase cascade triggered by stress and heat shock that stimulates MAPKAP kinase-2 and phosphorylation of the small heat shock proteins. *Cell*, *78*(6), 1027–37. Retrieved from <http://www.ncbi.nlm.nih.gov/pubmed/7923353>
- Rudolph, J., Xiao, Y., Pardi, A., & Ahn, N. G. (2015). Slow inhibition and conformation selective properties of extracellular signal-regulated kinase 1 and 2 inhibitors. *Biochemistry*, *54*(1), 22–31. <https://doi.org/10.1021/bi501101v>
- Samatar, A. A., & Poulikakos, P. I. (2014). Targeting RAS-ERK signalling in cancer: promises and challenges. *Nature Reviews. Drug Discovery*, *13*(12), 928–42. <https://doi.org/10.1038/nrd4281>
- Schwanhäusser, B., Busse, D., Li, N., Dittmar, G., Schuchhardt, J., Wolf, J., ... Selbach, M. (2011). Global quantification of mammalian gene expression control. *Nature*, *473*(7347), 337–42. <https://doi.org/10.1038/nature10098>

- Scolyer, R. A., Long, G. V, & Thompson, J. F. (2011). Evolving concepts in melanoma classification and their relevance to multidisciplinary melanoma patient care. *Molecular Oncology*, 5(2), 124–36. <https://doi.org/10.1016/j.molonc.2011.03.002>
- Sgouras, D. N., Athanasiou, M. A., Beal, G. J., Fisher, R. J., Blair, D. G., & Mavrothalassitis, G. J. (1995). ERF: an ETS domain protein with strong transcriptional repressor activity, can suppress ets-associated tumorigenesis and is regulated by phosphorylation during cell cycle and mitogenic stimulation. *The EMBO Journal*, 14(19), 4781–93. Retrieved from <http://www.ncbi.nlm.nih.gov/pubmed/7588608>
- Shah, S. P., Morin, R. D., Khattri, J., Prentice, L., Pugh, T., Burleigh, A., ... Aparicio, S. (2009). Mutational evolution in a lobular breast tumour profiled at single nucleotide resolution. *Nature*, 461(7265), 809–13. <https://doi.org/10.1038/nature08489>
- Shi, H., Hugo, W., Kong, X., Hong, A., Koya, R. C., Moriceau, G., ... Lo, R. S. (2014). Acquired resistance and clonal evolution in melanoma during BRAF inhibitor therapy. *Cancer Discovery*, 4(1), 80–93. <https://doi.org/10.1158/2159-8290.CD-13-0642>
- Signorelli, J., & Shah Gandhi, A. (2016). Cobimetinib: A Novel MEK Inhibitor for Metastatic Melanoma. *Annals of Pharmacotherapy*. <https://doi.org/10.1177/1060028016672037>
- Smalley, K. S. M., & Sondak, V. K. (2015). Inhibition of BRAF and MEK in BRAF-mutant melanoma. *Lancet (London, England)*, 386(9992), 410–2. [https://doi.org/10.1016/S0140-6736\(15\)60972-2](https://doi.org/10.1016/S0140-6736(15)60972-2)
- Sours, K. M., Xiao, Y., & Ahn, N. G. (2014). Extracellular-regulated kinase 2 is activated by the enhancement of hinge flexibility. *Journal of Molecular Biology*, 426(9), 1925–35. <https://doi.org/10.1016/j.jmb.2014.02.011>
- Stewart, B. W., Wild, C. P. (2014). World Cancer Report 2014. *World Health Organization*. <https://doi.org/9283204298>
- Stuart, S. a, Houel, S., Lee, T., Wang, N., Old, W. M., & Ahn, N. G. (2015). A Phosphoproteomic Comparison of B-RAFV600E and MKK1/2 Inhibitors in Melanoma Cells. *Molecular & Cellular Proteomics : MCP*, 14(6), 1599–615. <https://doi.org/10.1074/mcp.M114.047233>
- Szklarczyk, D., Franceschini, A., Wyder, S., Forslund, K., Heller, D., Huerta-Cepas, J., ... von Mering, C. (2015). STRING v10: protein-protein interaction networks, integrated over the tree of life. *Nucleic Acids Research*, 43(Database issue), D447-52. <https://doi.org/10.1093/nar/gku1003>
- Tanoue, T., & Nishida, E. (2003). Molecular recognitions in the MAP kinase cascades. *Cellular Signalling*, 15(5), 455–62. Retrieved from <http://www.ncbi.nlm.nih.gov/pubmed/12639708>
- Tomczak, K., Czerwińska, P., & Wiznerowicz, M. (2015). The Cancer Genome Atlas (TCGA): an immeasurable source of knowledge. *Contemporary Oncology (Poznan, Poland)*, 19(1A), A68-77. <https://doi.org/10.5114/wo.2014.47136>

- Trempolec, N., Dave-Coll, N., & Nebreda, A. R. (2013). SnapShot: P38 MAPK substrates. *Cell*, 152(4), 924–924.e1. <https://doi.org/10.1016/j.cell.2013.01.047>
- Uehling, D. E., & Harris, P. A. (2015). Recent progress on MAP kinase pathway inhibitors. *Bioorganic & Medicinal Chemistry Letters*, 25(19), 4047–56. <https://doi.org/10.1016/j.bmcl.2015.07.093>
- Uitdehaag, J. C. M., De Roos, J. A. D. M., Van Doornmalen, A. M., Prinsen, M. B. W., De Man, J., Tanizawa, Y., ... Zaman, G. J. R. (2014). Comparison of the cancer gene targeting and biochemical selectivities of all targeted kinase inhibitors approved for clinical use. *PLoS ONE*, 9(3), 1–13. <https://doi.org/10.1371/journal.pone.0092146>
- Van Allen, E. M., Wagle, N., Sucker, A., Treacy, D. J., Johannessen, C. M., Goetz, E. M., ... Dermatologic Cooperative Oncology Group of Germany (DeCOG). (2014). The genetic landscape of clinical resistance to RAF inhibition in metastatic melanoma. *Cancer Discovery*, 4(1), 94–109. <https://doi.org/10.1158/2159-8290.CD-13-0617>
- Villanueva, J., Vultur, A., Lee, J. T., Somasundaram, R., Fukunaga-Kalabis, M., Cipolla, A. K., ... Herlyn, M. (2010). Acquired resistance to BRAF inhibitors mediated by a RAF kinase switch in melanoma can be overcome by cotargeting MEK and IGF-1R/PI3K. *Cancer Cell*, 18(6), 683–95. <https://doi.org/10.1016/j.ccr.2010.11.023>
- von Kriegsheim, A., Baiocchi, D., Birtwistle, M., Sumpton, D., Bienvenut, W., Morrice, N., ... Kolch, W. (2009). Cell fate decisions are specified by the dynamic ERK interactome. *Nature Cell Biology*, 11(12), 1458–64. <https://doi.org/10.1038/ncb1994>
- Wagle, N., Van Allen, E. M., Treacy, D. J., Frederick, D. T., Cooper, Z. A., Taylor-Weiner, A., ... Garraway, L. A. (2014). MAP kinase pathway alterations in BRAF-mutant melanoma patients with acquired resistance to combined RAF/MEK inhibition. *Cancer Discovery*, 4(1), 61–8. <https://doi.org/10.1158/2159-8290.CD-13-0631>
- Wagner, E. F., & Nebreda, A. R. (2009). Signal integration by JNK and p38 MAPK pathways in cancer development. *Nature Reviews. Cancer*, 9(8), 537–49. <https://doi.org/10.1038/nrc2694>
- Weinstein, I. B., & Joe, A. (2008). Oncogene addiction. *Cancer Research*, 68(9), 3077–80; discussion 3080. <https://doi.org/10.1158/0008-5472.CAN-07-3293>
- Wilson, K. F., Wu, W. J., & Cerione, R. A. (2000). Cdc42 stimulates RNA splicing via the S6 kinase and a novel S6 kinase target, the nuclear cap-binding complex. *The Journal of Biological Chemistry*, 275(48), 37307–10. <https://doi.org/10.1074/jbc.C000482200>
- Wiśniewski, J. R., Zougman, A., Nagaraj, N., Mann, M., & Wiśniewski, J. R. (2009). Universal sample preparation method for proteome analysis. *Nature Methods*, 6(5), 359–62. <https://doi.org/10.1038/nmeth.1322>

- Wu, P., Nielsen, T. E., & Clausen, M. H. (2015). FDA-approved small-molecule kinase inhibitors. *Trends in Pharmacological Sciences*, *36*(7), 422–439. <https://doi.org/10.1016/j.tips.2015.04.005>
- Xiao, Y., Lee, T., Latham, M. P., Warner, L. R., Tanimoto, A., Pardi, A., & Ahn, N. G. (2014). Phosphorylation releases constraints to domain motion in ERK2. *Proceedings of the National Academy of Sciences of the United States of America*, *111*(7), 2506–11. <https://doi.org/10.1073/pnas.1318899111>
- Yamaguchi, T., Kakefuda, R., Tajima, N., Sowa, Y., & Sakai, T. (2011). Antitumor activities of JTP-74057 (GSK1120212), a novel MEK1/2 inhibitor, on colorectal cancer cell lines in vitro and in vivo. *International Journal of Oncology*, *39*(1), 23–31. <https://doi.org/10.3892/ijo.2011.1015>
- Yeh, T. C., Marsh, V., Bernat, B. A., Ballard, J., Colwell, H., Evans, R. J., ... Wallace, E. (2007). Biological characterization of ARRY-142886 (AZD6244), a potent, highly selective mitogen-activated protein kinase kinase 1/2 inhibitor. *Clinical Cancer Research : An Official Journal of the American Association for Cancer Research*, *13*(5), 1576–83. <https://doi.org/10.1158/1078-0432.CCR-06-1150>
- Yoon, S., & Seger, R. (2006). The extracellular signal-regulated kinase: multiple substrates regulate diverse cellular functions. *Growth Factors (Chur, Switzerland)*, *24*(1), 21–44. <https://doi.org/10.1080/02699050500284218>
- Zarei, M., Sprenger, A., Gretzmeier, C., & Dengjel, J. (2013). Rapid combinatorial ERLIC-SCX solid-phase extraction for in-depth phosphoproteome analysis. *Journal of Proteome Research*, *12*(12), 5989–5995. <https://doi.org/10.1021/pr4007969>
- Zarubin, T. & Han, J. (2005). Activation and signaling of the p38 MAP kinase pathway. *Cell Res.*, *15*(1), 11–18. <https://doi.org/10.1038/sj.cr.7290257>
- Zeke, A., Bastys, T., Alexa, A., Garai, Á., Mészáros, B., Kirsch, K., ... Reményi, A. (2015). Systematic discovery of linear binding motifs targeting an ancient protein interaction surface on MAP kinases. *Molecular Systems Biology*, *11*(11), 837. Retrieved from <http://www.ncbi.nlm.nih.gov/pubmed/26538579>
- Zhou, Y., Tanaka, T., Sugiyama, N., Yokoyama, S., Kawasaki, Y., Sakuma, T., ... Sakurai, H. (2014). p38-Mediated phosphorylation of Eps15 endocytic adaptor protein. *FEBS Letters*, *588*(1), 131–7. <https://doi.org/10.1016/j.febslet.2013.11.020>